

AD-A052 685

TEXAS UNIV AT EL PASO DEPT OF ELECTRICAL ENGINEERING
A COMPUTATIONAL METHOD FOR SPECTRAL MOLECULAR ABSORPTION USING --ETC(U)
MAY 77 P C VAN DER WOOD

F/G 4/1

UNCLASSIFIED

NL

1 OF 2
AD
A052 685



AD A 052685

①

A COMPUTATIONAL METHOD FOR
SERIAL MOLECULAR ABSORPTION
USING AN IMPROVED VOICET ALGORITHM

BY

PETER CLARK VAN DERWOOD

AD NO. []
DDC FILE COPY

DDC
RECEIVED
APR 4 1978
B

DISTRIBUTION STATEMENT A
Approved for public release;
Distribution Unlimited

①

⑥

A COMPUTATIONAL METHOD FOR SPECTRAL
MOLECULAR ABSORPTION
USING
AN IMPROVED VOIGT ALGORITHM.

by

⑩

Peter Clark Van Derwood

⑨

Master's THESIS,

ID No. 1
DDC FILE COPY

Presented to the Faculty of the Electrical Engineering

Department of

The University of Texas at El Paso

in Partial Fulfillment

of the Requirements

For the Degree of

MASTER OF SCIENCE

DDC
RECEIVED
APR 4 1978
B

THE UNIVERSITY OF TEXAS AT EL PASO

El Paso, Texas

⑪

May 1977

⑫ 179 p.

DISTRIBUTION STATEMENT A
Approved for public release;
Distribution Unlimited

408 579 mt

A COMPUTATIONAL METHOD FOR SPECTRAL MOLECULAR ABSORPTION

USING

AN IMPROVED VOIGT ALGORITHM

ACCESSION for	
NTIS	White Section <input checked="" type="checkbox"/>
DDC	Buff Section <input type="checkbox"/>
UNANNOUNCED	<input type="checkbox"/>
JUSTIFICATION	
PER LETTER ON FILE	
BY _____	
DISTRIBUTION/AVAILABILITY CODES	
Dist. AVAIL. and/or SPECIAL	
A	

APPROVED BY SUPERVISORY COMMITTEE:

Joseph A. Pincus
CHAIRMAN
Robert E. Bruce
Yiu-cheng Lin

DEAN OF GRADUATE SCHOOL

*Dedicated to My Parents and
to John*

*"Be ye transformed by the
renewing of your mind"*

Romans XII, 2

ACKNOWLEDGEMENTS

I am sincerely grateful and will be forever indebted to Dr. Joseph H. Pierluissi for his encouragement, inspiration and prayers throughout the various stages of this thesis. Without his skillful insistence this dissertation would have never been attempted and less his daily guidance it would have never been consummated. His meticulous fashion and dedicated professionalism have influenced me immeasurably.

To Dr. Richard B. Gomez, Atmospheric Sciences Laboratory, White Sands Missile Range, I express my appreciation for providing the data needed in this thesis and for his clear explanations of technical jargon whenever needed.

Assistance with the formula derivations and computer implementation was provided by Dr. Glenn A. Gibson and Dr. Yu-Cheng Liu. Debugging of the program was with the help of Mr. Paul Weissmann. To all of them I express my genuine thanks.

The draft typing, formatting, and final manuscript were done by Lilia Tapia, Brenda Erks, Millie F. Del Valle, and Julieta Rodriguez with the adept direction and assistance of Beatrice G. Hollander. The figures were excellently drawn by Alejandro Diaz. To them I express my bonafide appreciation for a job well done.

A very special heartfelt thanks goes to my very good friend Michael T. Potter. His astutness, humor, sympathy, and consolation has helped me enjoy every day and given me direction when needed. Also, thanks to Joseph M. Ragusa, my good friend and

neighbor for reviewing the script and offering helpful suggestions.

Finally, to my darling wife, Hiromi, I wish to express my never-ending love and admiration for singly carrying the heavy marital load throughout my studies. Her devotion is truly appreciated.

ABSTRACT

Discussion of the fundamental elements and theory related to atmospheric transmittance is presented. A line-by-line transmission computer program is developed that utilizes the combined Doppler-Lorentz (Voigt) line broadening function. In addition a rapid algorithm to evaluate the Voigt function with a maximum relative error of about one part in 10^4 ^{10,000} is described and a software package that processes the absorption line parameters necessary to calculate transmittance is given. The results of transmittance calculations for seven channels in the fifteen micrometer band, corresponding to the seven High Resolution Infrared Radiation Sounder (HIRS) channels, are furnished and the procedure to compute a band averaged transmission discussed. It is concluded that the Voigt algorithm developed here is an excellent computational procedure and the resulting transmittance program correctly calculates atmospheric transmission.

TABLE OF CONTENTS

	PAGE
ACKNOWLEDGEMENTS	i
ABSTRACT	iii
TABLE OF CONTENTS.	iv
LIST OF FIGURES	vii
LIST OF TABLES	ix
I. INTRODUCTION	1
II. FUNDAMENTALS OF ATMOSPHERIC ABSORPTION	3
2.1 Preface	3
2.2 The Atmosphere	3
2.2.1 Atmospheric Temperature	7
2.2.2 Atmospheric Pressure	9
2.3 Molecular Energy Transitions	11
2.4 Spectral Line Broadening	16
2.4.1 Natural Broadening	16
2.4.2 Doppler Broadening	18
2.4.3 Pressure Broadening	20
2.5 Summary	23
III. TRANSMITTANCE AND VOIGT FUNCTION IN THE FIFTEEN MICROMETER BAND	25
3.1 Preface.	25
3.2 Absorption and Transmittance	25
3.2.1 The Transmittance Differential Equation	30
3.2.2 The Absorption Coefficient $K(\nu, T, P)$	36
3.3 The Voigt Function	37
3.4 The Fifteen Micron Band	42
3.5 Summary	47
IV. COMPUTER ALGORITHMS FOR THE VOIGT PROFILE	51
4.1 Preface	51

Contents	Page
4.2 J. K. Kielkopf's Voigt Algorithm	51
4.3 S. R. Drayson's Voigt Algorithm	58
4.4 Proposed Voigt Algorithm	64
4.5 Comparison of Voigt Algorithms	71
4.5.1 Accuracy Tests	72
4.5.2 Execution Time Tests	80
4.5.3 The Selected Voigt Algorithm	82
V. ABSORPTION LINE PARAMETERS AND UNITS	87
5.1 Preface	87
5.2 Review of Transmittance Equations	87
5.3 The Mixing Ratio and the Combined Extinction Coefficient	90
5.4 Units	99
5.5 The Absorption Line Parameters	104
5.5.1 Derivation of Line Parameters	105
5.5.2 The Line Parameter Data Tape	107
5.6 The DATSET Computer Subroutine	109
VI. THE TRANSMITTANCE PROGRAM	115
6.1 Preface	115
6.2 The Rotational and Vibrational Partition Functions	115
6.3 Euler's Solution of the Transmittance Differential Equation	118
6.4 Transmittance Iteration Technique	120
6.5 Transmittance Program Flowchart and Utilization . .	127
VII. DISCUSSION AND CONCLUSION	132
7.1 Preface	132
7.2 Discussion	132
7.3 Conclusion	132
7.4 Ongoing Research	133
APPENDIX A: Kielkopf's Voigt Algorithm	135
APPENDIX B: Drayson's Voigt Algorithm	137
APPENDIX C: Proposed Voigt Algorithm	140
APPENDIX D: DATSET Subroutine	142

Contents	Page
APPENDIX E: Transmittance Program	145
APPENDIX F: Definition of Variables Used in the Transmittance Program	149
APPENDIX G: Monochromatic Transmittances	152
APPENDIX H: Averaged Transmittance	160
REFERENCES	162

LIST OF FIGURES

FIGURE		PAGE
2.2-1	Variation of Water Vapor	5
2.2-2	Variation of Ozone	6
2.2-3	Atmospheric Nomenclature	8
2.2-4	Variation of Pressure with Altitude.	9
2.3-1	Diagram of Vibrational and Rotational Levels of Two Electronic States of a Molecule	13
2.3-2	Vibrational Modes of CO ₂ and H ₂ O	15
2.4-1	Doppler and Lorentz Line Shapes and Halfwidths	17
3.2-1	Passage of Energy Through a Substance of Length ΔX	26
3.2-2	Solar Zenith Angle θ and Downward Intensity I_{down}	31
3.3-1	Doppler, Lorentz, and Voigt Line Shapes	43
3.4-1	Electromagnetic Spectrum	44
3.4-2	HIRS Filter Responses	46
3.4-3	A Spectral Line That Absorbs in Channel One Although The Center Is Out of the Channel	48
4.3-1	Computational Regions Used By Drayson.	61
4.4-1	Regions Proposed By This Work.	66
4.4-2	Number of Series Terms Required For Convergence	68
4.5-1	Coverage of Proposed Regions By Accuracy Test Two	74
4.5-2	Coverage of Drayson's Regions For Accuracy Test Three	78
6.4-1	A Single Transmittance Calculation Per Channel. Channel Limits Not Adjusted	124

FIGURE		PAGE
6.4-2	A Single Transmittance Calculation Per Channel. Channel Limits Adjusted By BOUND	125
6.4-3	Three Transmittance Calculations Per Channel. Channel Limits Adjusted By BOUND	126
6.5-1	Transmittance Program Flowchart	128
6.5-2	Input Data Format and Number Required	131

LIST OF TABLES

TABLE		PAGE
2.2-1	Composition of the Atmosphere	4
3.4-1	NIMBUS 6 Characteristics	45
4.5-1	Initial Accuracy Tests. Drayson's Value Used as True	73
4.5-2	Results of Accuracy Test Two	76
4.5-3	Deviation of Proposed Method From Drayson's Method Using Drayson's Regions	79
4.5-4	Results of Time Tests Conducted Using Regions and Points Indicated in Fig. 4.5-1 . . .	81
4.5-5	Results of Time Tests Conducted Using 100 Points From Each Region Indicated In Fig. 4.3-1	83
4.5-6	Results of Time Tests Conducted Using Regions and Points Indicated In Fig. 4.5-2	84
4.5-7	Results of Time Tests Conducted Using Ten- Thousand Points and No Regions	85
5.3-1	Mixing Ratio and Molecular Weights of Non- Varying Atmospheric Constituents	94
5.3-2	Density of Atmospheric Absorbers at Standard Temperature and Pressure	95
5.3-3	Mixing Ratio For Water Vapor and Ozone From A Midlatitude Summer Atmosphere	96
5.4-1	Physical Constants Used In This Work	101
5.5-1	Mean Halfwidths and Intensity Minimums Used by McClatchey In Compilation of AFCRL Data Tape	108
5.5-2	Computer Format of Each Spectral Line's Data . . .	110
6.2-1	Rotational and Vibrational Partition Functions . .	116
6.2-2	Regression Coefficients For Quadratic and	

TABLE		PAGE
	Cubic Fit of Vibrational Partition Function	119
6.5-1	Equations Used In Transmittance Program	129

CHAPTER I

INTRODUCTION

The thin film of gas that clings to the surface of the earth performs many functions, and has a correspondingly large number of important properties. To a meteorologist the atmosphere is basically a sink for solar radiation, and its most interesting characteristic is the ability to transform that energy into wind systems and rainfall averages. This phenomenon of radiative transfer through the atmosphere is too complex, in general, for a closed solution. However, if the scope of investigation is narrowed, mathematical models can be developed that are useful. One such application, that of energy transfer theory, is the retrieval of the vertical temperature structure of the atmosphere from remote satellite measurements [Kaplan²³]. This requires not only accurate measurements and a stable mathematical inversion scheme, but also very accurate transmittance functions. This transmittance is easily calculated if atmospheric absorption is known. The most accurate method to predict atmospheric absorption is to add the contribution of each molecular species, line-by-line. These line-by-line calculations are very time consuming even with today's high speed computers. This document is concerned with molecular absorption and the mathematical functions that may reduce the time required for a given line calculation. It is organized into seven chapters as outlined below.

The equations of atmospheric transmittance are reviewed in

Chapter two. Additionally the composition of the atmosphere and some of its optical properties are examined. The constituents of interest and the processes by which they absorb energy are touched upon. The concept of an absorbing line is introduced and the phenomenon of line broadening is discussed.

Chapter three defines atmospheric absorption and transmittance. Then the transmittance differential equation this work is to solve is developed. A relation for the combined effects of Lorentz and Doppler spectral line broadening is obtained, and finally the frequency bands of interest for temperature retrieval from satellite soundings are defined and the molecular absorbers within the band identified.

In Chapter four begins the major contribution of this work. Three methods of evaluating the Voigt function are presented. The results of tests for accuracy and speed conducted for each of the methods are tabulated and discussed.

In Chapter five the data used in transmittance calculations and the units of all equations are covered. Some remarks on the derivation of absorption line parameters are given and the computer software used to handle the data is developed. The units of the data and necessary conversion factors are also presented.

Chapter six ties together the work of the other chapters and presents the end product of this research, the transmittance program.

Finally there is discussion of the results of this work and some conclusions are drawn. Where appropriate the work of a chapter is supported in an appendix.

CHAPTER II

FUNDAMENTALS OF ATMOSPHERIC ABSORPTION

2.1 Preface

This chapter discusses the composition of the atmosphere and molecular energy absorption. The atmosphere is presented first, followed by an outline of molecular energy transitions. Then spectral line broadening is treated and finally the important points of the chapter are summarized.

2.2 The Atmosphere

The gases that compose our atmosphere are listed in Table 2.2-1 [Hudson¹⁸]. Those whose relative proportions are nearly constant up to altitudes in excess of 80 kilometers are called the permanent constituents. The atmosphere contains several other gases, called the variable constituents; their amounts varying with temperature, altitude and location. Chief among them is water vapor, which may constitute as much as 2 percent of a humid atmosphere at sea level. The amount of water vapor decreases rapidly with altitude. Another variable constituent ozone, is seldom observed at sea level. The amount of ozone in the atmosphere increases with altitude to a maximum at about 20 kilometers and then decreases at higher altitudes. Fig. 2.2-1 depicts the variance of water vapor with altitude and season, while Fig. 2.2-2 reflects the correlation for ozone [McClatchey³²].

Constituent	Formula	Percent by Volume
Nitrogen	N ₂	78.1
Oxygen	O ₂	20.9
Argon	Ar	0.934
Carbon Dioxide	CO ₂	0.032
Neon	Ne	1.81 · 10 ⁻³
Helium	He	5.24 · 10 ⁻⁴
Methane	CH ₄	2.0 · 10 ⁻⁴
Krypton	Kr	1.14 · 10 ⁻⁴
Nitrous Oxide	N ₂ O	5.0 · 10 ⁻⁵
Hydrogen	H ₂	5.0 · 10 ⁻⁵
Carbon Monoxide	CO	2.0 · 10 ⁻⁵
Xenon	Xe	9.0 · 10 ⁻⁶
Ozone	O ₃	Varies
Water Vapor	H ₂ O	Varies

TABLE 2.2-1. Composition of the Atmosphere [Hudson¹⁸].

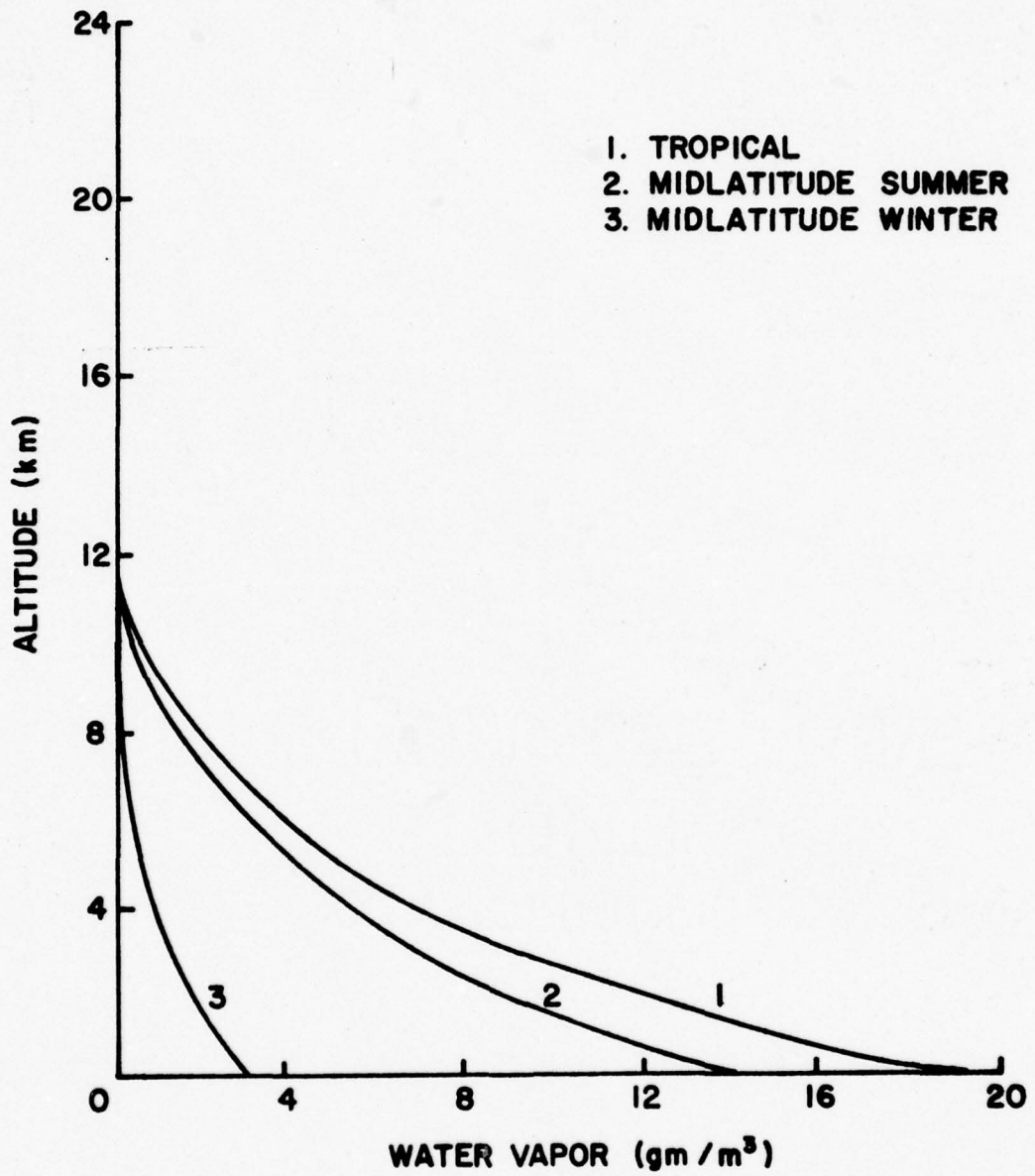


Figure 2.2-1. Variation of Water Vapor [McClatchey³²].

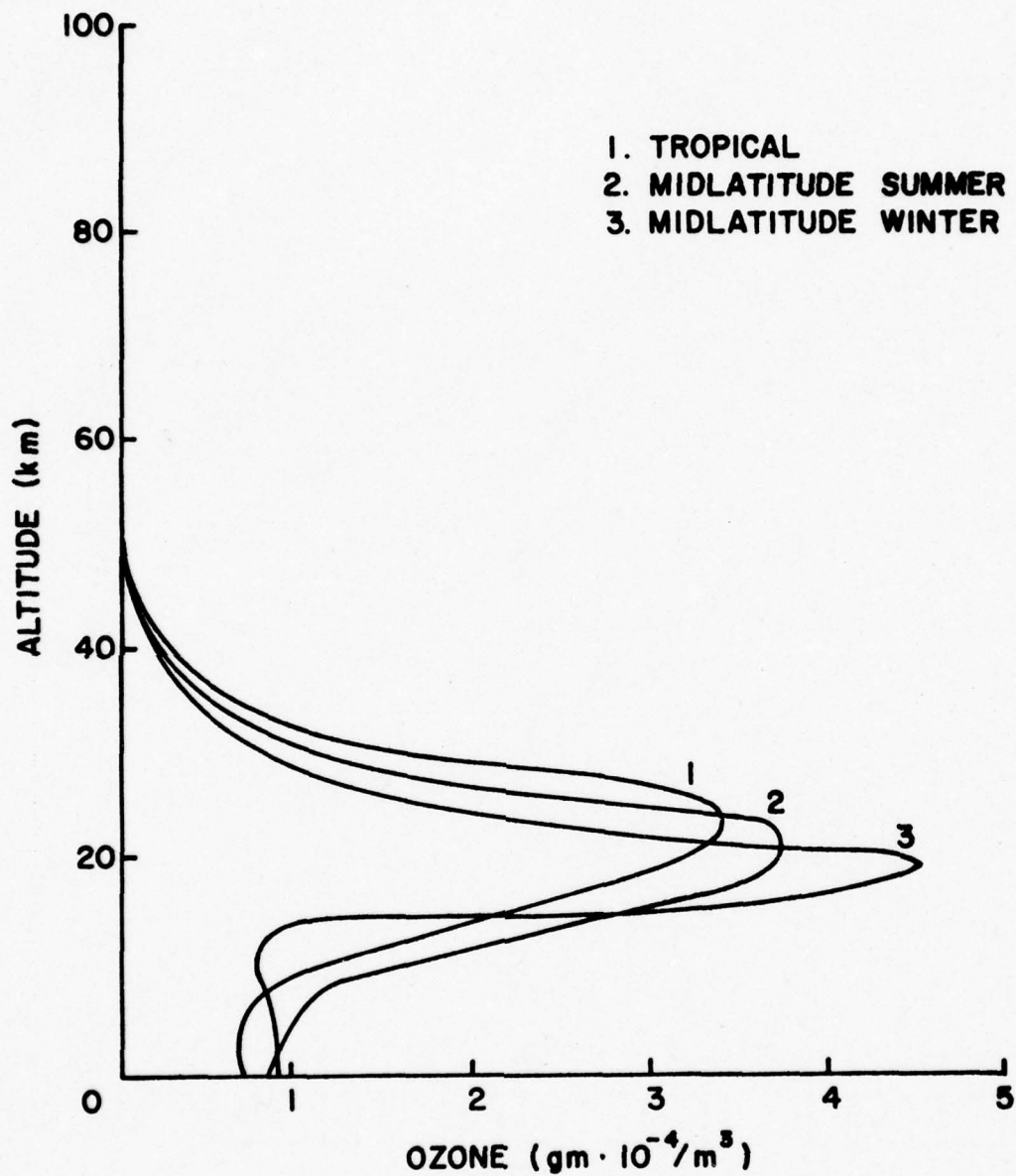


Figure 2.2-2. Variation of Ozone [McClatchey³²].

In addition to the gases listed, the atmosphere may contain a variety of particles that may be of concern. Depending on the nature of the investigation it could be necessary to consider salt from ocean spray, fine dust from the earth's surface, or carbon particles resulting from combustion. Near cities or industrial complexes atmospheric pollutants such as ammonia, hydrogen sulfide, and sulfur dioxide are present in significant amounts.

2.2.1 Atmospheric Temperature

Having considered the composition of the atmosphere we now discuss its thermal properties. The earth's atmosphere is divided into four regions primarily on the basis of temperature gradients, as shown in Fig. 2.2-3. Typically the temperature decreases with altitude (termed a positive lapse rate) in the troposphere passing through a minimum at the tropopause, and then rises with increasing altitude in the stratosphere. A region in which temperature increases with altitude is termed an inversion, or inversion layer. At the stratopause the temperature passes through a more or less well defined maximum, then decreases through the mesosphere to a second minimum at the mesopause. Above the mesopause, in the thermosphere, the kinetic temperature again increases with altitude, reaching a maximum value at a height of several thousand kilometers. Above the thermosphere, and demarcated from it by the thermopause, is essentially an isothermal region, the exosphere. At any particular time or place the true temperature structure may differ appreciably from Fig. 2.2-3, but in

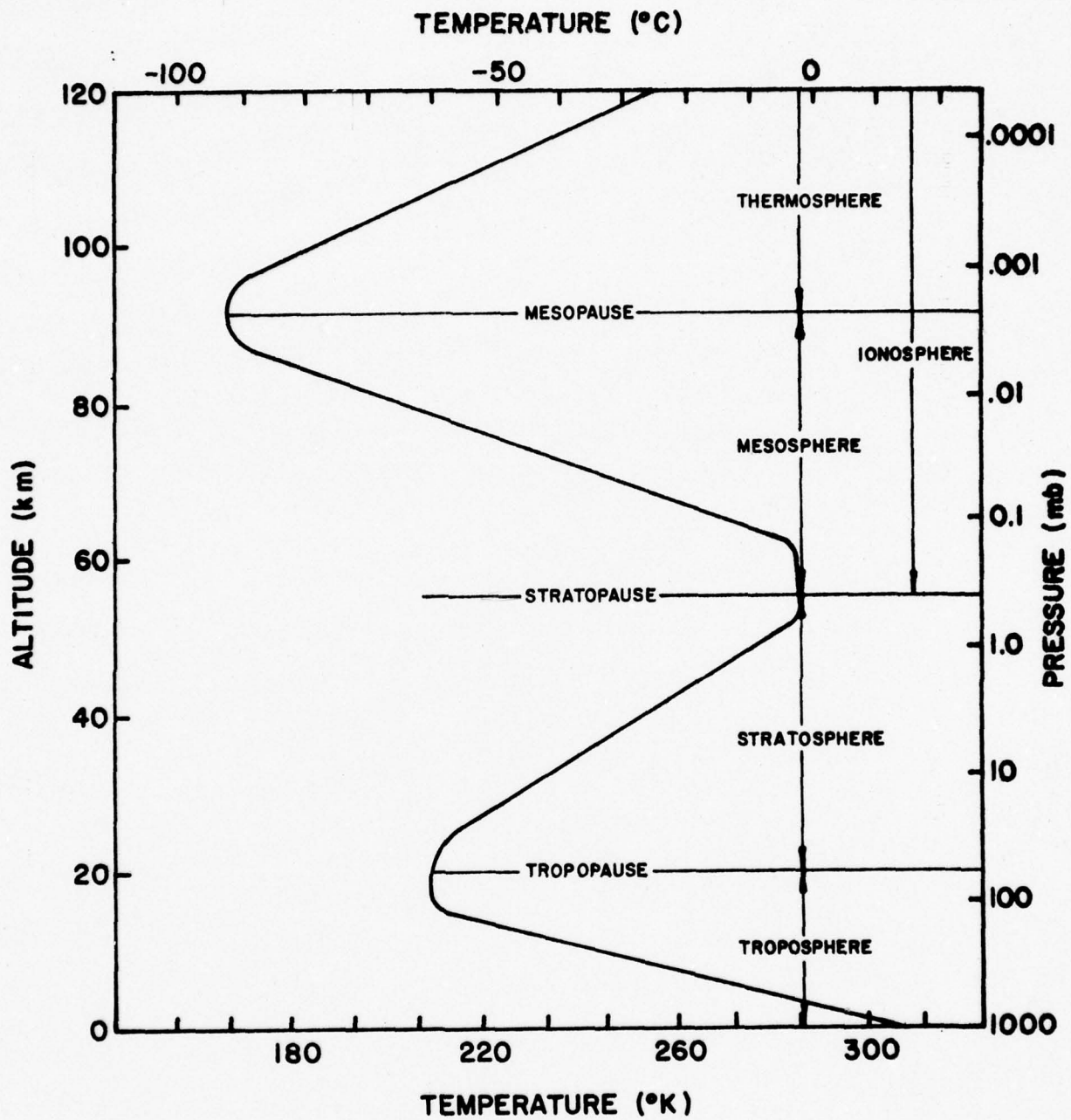


Figure 2.2-3. Atmospheric Nomenclature

(Adapted from [45])

general, the curve shown is at least qualitatively correct [McEwan and Phillips³⁴].

Various regions or layers of the atmosphere have properties which are sufficiently characteristic to justify their being given special names, most notable the ionosphere. The ionosphere itself is divided into three regions according to altitude and electron density.

2.2.2 Atmospheric Pressure

The variation of atmospheric pressure with altitude is governed by the hydrostatic equation, which is derived with the aid of Fig. 2.2-4 [McEwan and Phillips³⁴]. The pressure is P at an altitude Z , and $P - \Delta P$ at altitude $Z + \Delta Z$.

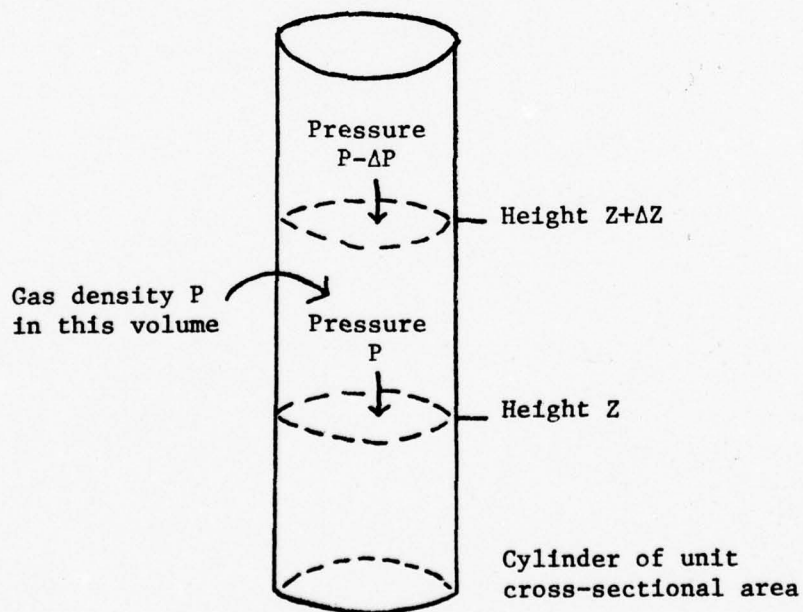


Figure 2.2-4. Variation of Pressure with Altitude.

The difference in pressure is due to the weight of the gas in the column of unit cross-sectional area and length ΔZ . Hence in the limit

$$\frac{dP}{dZ} = -\rho g, \quad (2.2-1)$$

where g is the acceleration due to gravity and ρ is the gas density. For air we use the equation of state for an ideal gas,

$$P = nkT. \quad (2.2-2)$$

Dividing Eq. 2.2-1 by Eq. 2.2-2 yields

$$\frac{dP}{P} = -\frac{\rho g}{nkT} dz = -\frac{dz}{H}, \quad (2.2-3)$$

where $H = \frac{nkT}{\rho g}$, is termed the scale height [Whitten and Poppoff⁵²].

Assuming the scale height to be constant, Eq. 2.2-3 can be integrated to obtain

$$\frac{P}{P_0} = \exp \left[-\frac{Z}{H} \right], \quad (2.2-4)$$

which shows the expected exponential decrease of pressure with height in a region of constant g and T . The left scale of Fig. 2.2-3 depicts the decrease of atmospheric pressure with altitude.

2.3 Molecular Energy Transitions

In first approximation, the energy (E) of an isolated molecule can be presented in the form

$$E = E_{\text{trans}} + E_{\text{vib}} + E_{\text{ro}} + E_{\text{el}} \quad (2.3-1)$$

where E_{trans} is the translational motion, which depends on velocity and may assume any value, E_{el} is the energy of the electrons, and E_{vib} and E_{ro} are the vibrational and rotational energies. The last three terms in Eq. 2.3-1 are quantized [Weidner and Sells⁵⁰] and take discrete values only, the values being specified by one or more quantum numbers. Any combination of quantum numbers defines an energy state or quantum state, or term. Radiation is absorbed or emitted when a transition takes place from one energy state to another. The frequency (ν) of the absorbed or emitted quantum is given by Planck's relation,

$$\Delta E = h\nu, \quad (2.3-2)$$

where h is Planck's constant. Equation 2.3-1 is valid only when the interaction of different molecular motions is disregarded. In general, the energy of a molecule is

$$E = E_{\text{trans}} + E_{\text{vib}} + E_{\text{ro}} + E_{\text{el}} + E_{\text{el-vib}} + E_{\text{el-ro}} + E_{\text{vib-ro}} \quad (2.3-3)$$

where the last three terms represent the interaction [Zuev⁵⁴]. Thus, the most general transition involves simultaneous changes of electronic, vibrational, and rotational energy.

The electronic, vibrational, and rotational energies of a molecule differ in order of magnitude. The energy of an electronic transition is of the order of several electron volts, a vibrational energy transition is reckoned in the tenths or hundredths of an electron volt, and a rotational energy transition is in the thousandths or ten-thousandths of an electron volt. But, since a molecule has electronic, vibrational, and rotational energies, and these energies change simultaneously on emission or absorption, the electronic and vibrational spectra are not evidenced in pure form. Depending on the frequency range of interest we deal either with an electronic-vibrational-rotational molecular spectrum, or with a vibrational-rotational spectrum, or with purely a rotational spectrum. These spectra are referred to as the electronic, vibrational, and rotational spectra [Goody¹⁵], respectively.

Each electron state has a corresponding grid of vibrational energy levels characterized by certain values of the vibrational quantum number v . Each vibrational level has a corresponding series of rotational levels, characterized by a rotational quantum number j .

In Fig. 2.3-1 it is easily seen why electronic and vibrational transitions of a molecule cannot be observed in pure form. For each electronic transition of a molecule the vibrational and rotational energies change simultaneously. The entire aggregate of electronic transitions gives rise to the electronic-vibrational-rotational spectrum, whose line strengths are determined by the energy-level distributions of the molecules and by the probabilities of the corresponding transitions.

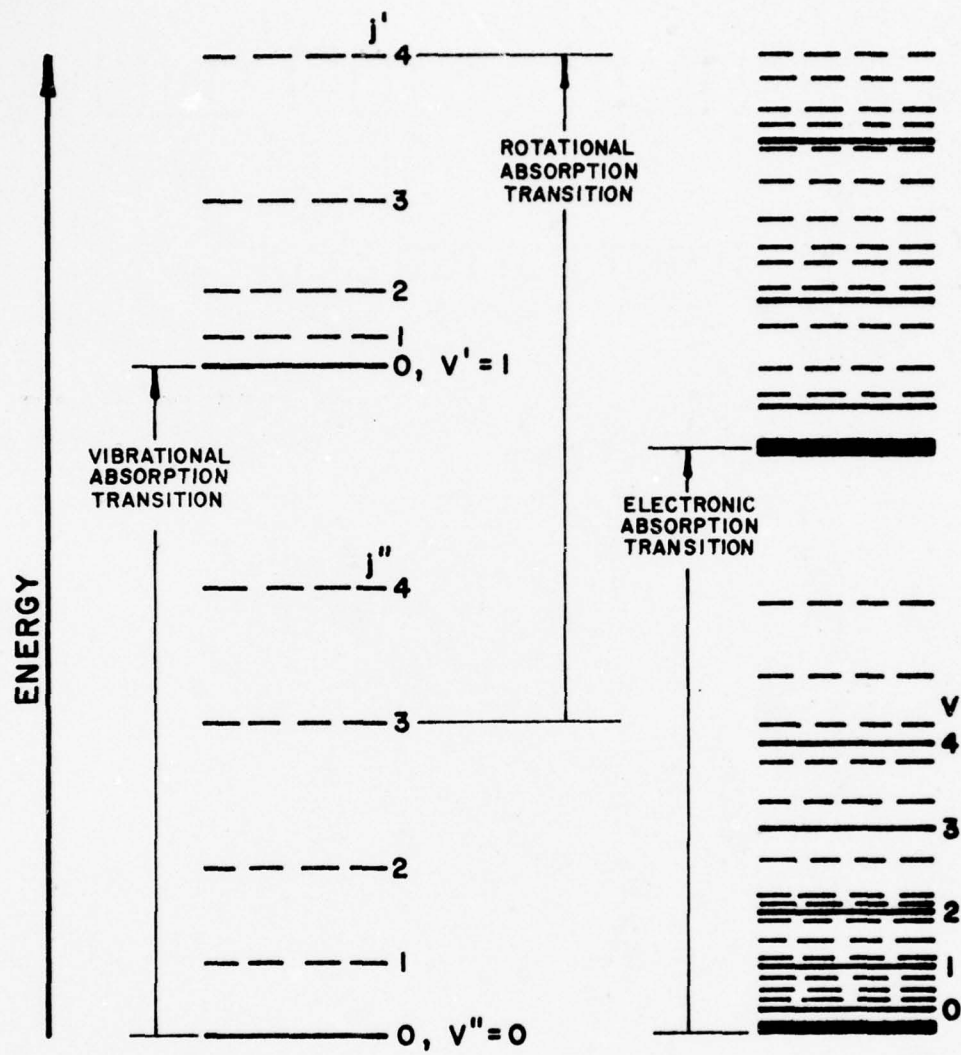


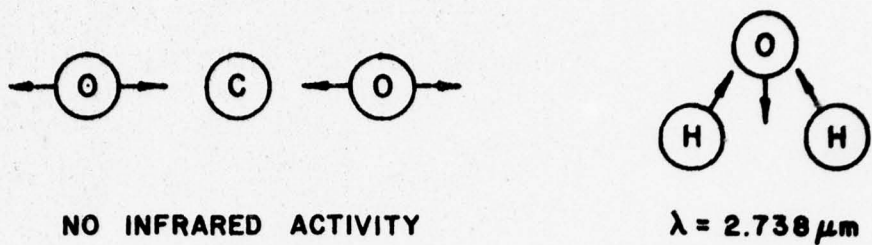
Figure 2.3-1. Diagram of Vibrational and Rotational Levels of Two ³⁷ Electronic States of a Molecule [Adapted from [Orchin]].

The number of different vibrational transitions accompanying a change in electron energy and the number of different rotational transitions associated with a change in the vibrational energy of a molecule may be very large. This is responsible for the extremely complex structure of molecular spectra. Additionally vibrational or rotational levels of a molecule may overlap with each other. Figure 2.3-2 shows the vibrational modes of carbon dioxide and water vapor, two of the atmospheric constituents that have absorption lines in the infrared spectrum.

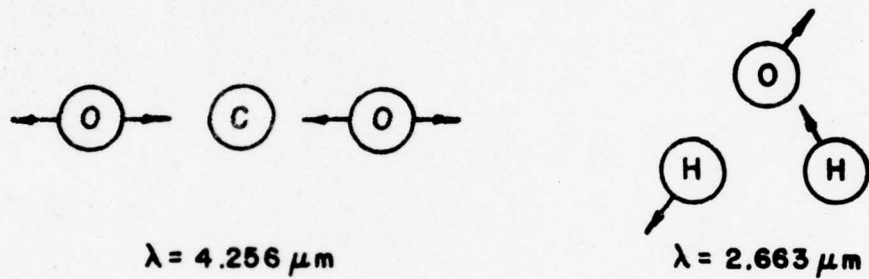
Detailed discussion of the energy level selection rules may be found in Kroto²⁵ or Goody¹⁵. The interaction of electronic, vibrational, and rotational energies may, as a first approximation, be considered as additive. Thus, if the energies were strictly independent, the selection rules for a combined transition could be regarded as a combination of the three separate selection rules. Atoms and molecules can exhibit electronic line spectra, but the overall complexity, overlapping, and simultaneous changes of all three forms of quantized energy of molecules requires band systems.

Lastly, we consider a fundamental property under the classical theory of a molecule. That is the electric dipole moment. This moment is defined as the product of the magnitude of an electric charge and the distance between it and its opposite charge. It is this property by which absorption occurs. The electromagnetic radiation absorption happens when an electric field interacts with the motion of the molecule, changing the dipole moment and bringing about an

SYMMETRIC STRETCHING



ANTI-SYMMETRIC STRETCHING



BENDING

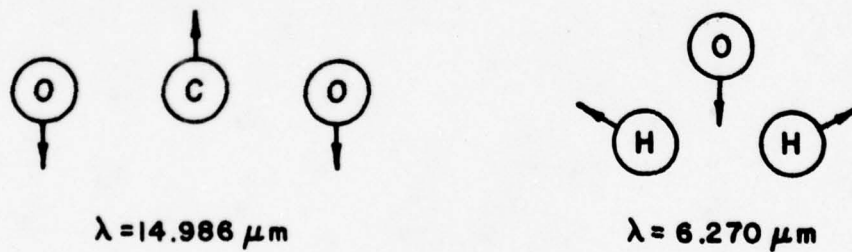


Figure 2.3-2. Vibrational Modes of CO₂ and H₂O [Hudson¹⁸].

energy transition. In symmetric molecules some vibrational modes produce no change in dipole moment. As a consequence, no infrared activity occurs.

2.4 Spectral Line Broadening

Thus far in the discussion of spectral lines it has been stated that the position (frequency) of an absorbing line due to an allowed energy transition may be predicted exactly by Eq. 2.3-2. While in theory this is true, in practice the line that is observed is not a singled frequency slit from the electromagnetic spectrum. The line is widened by a phenomenon termed line broadening. The expansion is due to a variety of reasons [Breene⁴], but only three will be discussed here. Natural line-broadening, Doppler line-broadening, and pressure or Lorentz line-broadening are the main mechanisms considered for atmospheric calculations and are therefore, developed below. The line breath is conventionally taken as the spectral width corresponding to the half maximum intensity points on the curve describing the line. The profiles are assumed symmetric hence, half the line breath is used in characterizing the line shape, and is termed the half width. Figure 2.4-1 depicts the Doppler line shape, the Lorentz line shape and the half width of each.

2.4.1 Natural Broadening

The uncertainty principle states that the product of the uncertainty of our knowledge of the energy and mean life of an atomic state cannot be less than Planck's constant divided by 4π . Since every excited state of a molecule has a finite lifetime, its energy

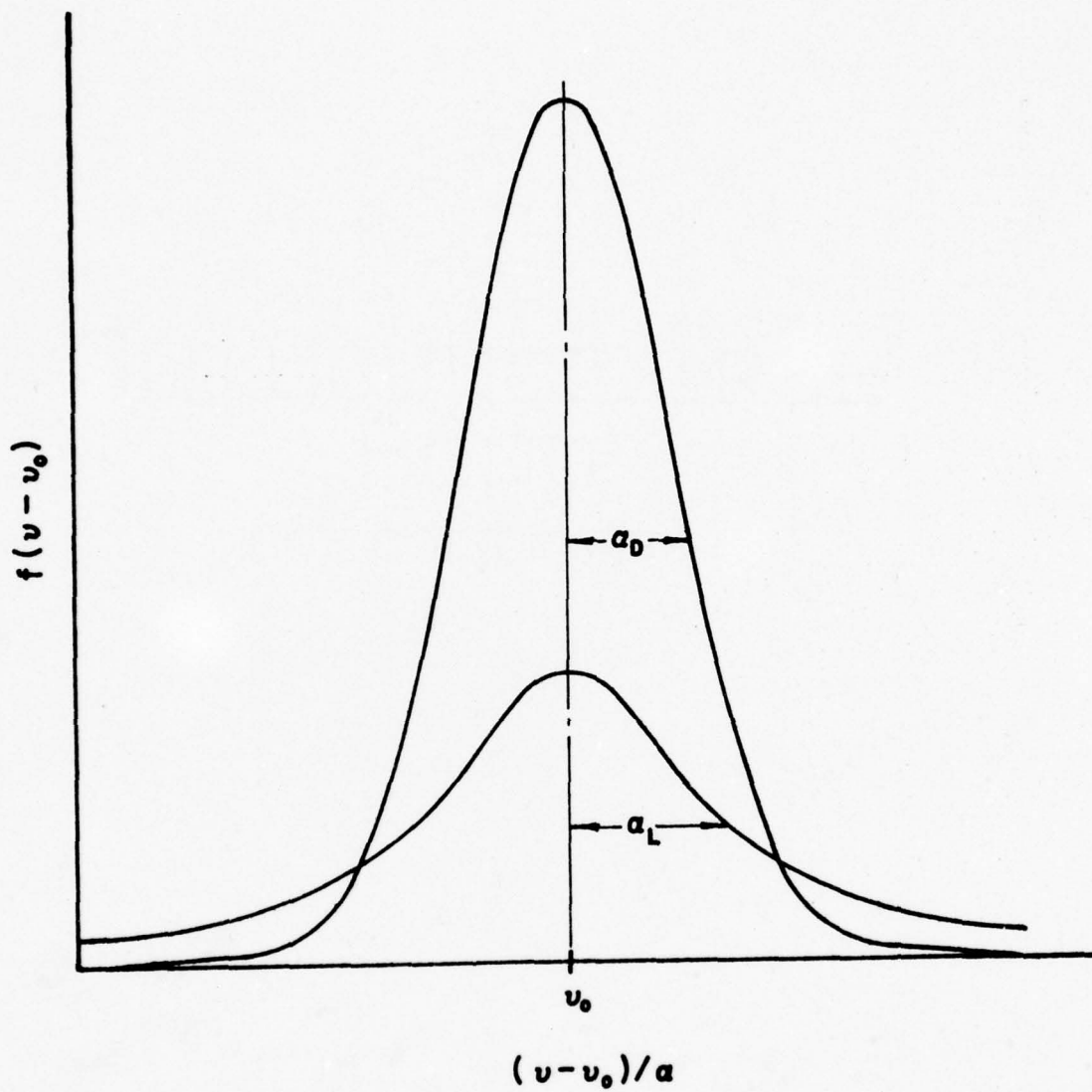


Figure 2.4-1. Doppler and Lorentz Line Shapes and Half Widths [Jaimeson, et al²²].

cannot be measured exactly. Thus, because we do not know precisely a molecule's energy transition, we cannot know absolutely the frequency of emission or absorption [Jamieson, et al²²]. This uncertainty leads to a lower limit of the width of an observed spectral line, termed the natural width (α_N). It is given by

$$\alpha_N = \frac{1}{4\pi\phi_i} \quad , \quad (2.4-1)$$

where ϕ_i is the lifetime of an energy transition. For a typical vibrational transition ϕ_i is of the order of 0.1 seconds [Goody¹⁵]. Thus, from Eq. 2.4-1, α_N is of the order of $3 \cdot 10^{-11} \text{ cm}^{-1}$, in wave numbers. This is trivial when compared to other line widths and is neglected for atmospheric calculations.

2.4.2 Doppler Broadening

If a monochromatic radiation source is moving with velocity whose component in the line of sight to the observer is u , the frequency appears shifted by an amount

$$\Delta\nu = \frac{u}{c} \nu_0 \quad , \quad (2.4-2)$$

compared with the frequency of the source when it is at rest (ν_0). This change is termed the Doppler Effect.

For a stratified atmosphere it may be assumed that the translational states of molecules are in thermodynamic equilibrium and their

velocity u , relative to an observer, is given by the Maxwell velocity distribution [Kuhn²⁶]

$$p(u) = \left(\frac{m}{2\pi kT} \right)^{1/2} \exp \left(- \frac{mu^2}{2kT} \right), \quad (2.4-3)$$

where m is the mass of the molecule,
 k is Boltzman's constant,
and T is temperature in °K.

When $u \ll c$ this probability function for velocity manifests itself in a broadening of the spectral line observed.

Defining the doppler half width at half maximum [Anding²] as

$$\begin{aligned} \alpha_D &= \frac{v_o}{c} \left(\frac{2kT \ln 2}{M} \right)^{1/2} \\ &= 3.58 \cdot 10^{-7} \left(\frac{T}{M} \right)^{1/2} v_o, \end{aligned} \quad (2.4-4)$$

where M is molecular weight, the line shape is predicted by

$$f(v-v_o) = \left(\frac{\ln 2}{\pi} \right)^{1/2} \frac{1}{\alpha_D} \exp \left\{ - \frac{v-v_o}{\alpha_D} \right\}. \quad (2.4-5)$$

Goody¹⁵ gives the two extreme values for α_D as $3.3 \cdot 10^{-2} \text{ cm}^{-1}$ and $3.5 \cdot 10^{-4} \text{ cm}^{-1}$.

2.4.3 Pressure Broadening

The interaction of a radiating particle with another particle has an effect on the spectral line which is very complex in nature. In order to make the problem manageable it is necessary to introduce simplifying assumptions whose justifications are not often obvious and whose validity is limited. The theory of pressure broadening has developed from two opposite viewpoints. Following Lorentz, it is considered that a collision breaks the otherwise unperturbed wave train of a radiating particle. The line width is then determined, not by the natural life time T , but by the shorter time T_c between collisions. A fourier analysis of the wave train leads to a line width proportional to $1/T_c$; the effect is a kinetic one, depending on the relative velocities of the molecules.

The statistical approach was first applied by Holtsmark¹⁷ to the effect of ions on each other. It was later applied by others to the mutual effects of neutral atoms. It neglects the motion of the atoms and regards them as being at rest, but distributed randomly in space. The characteristic frequency of the radiating or absorbing molecule is changed by the presence of another molecule according to some function of the distance separating them. Each molecule can be regarded as emitting one frequency at any given time, but the random effect of many radiating molecules leads to a continuous intensity distribution whose calculation is purely statistical in nature.

The Fourier analysis of the emitted radiation of a particle that has been interrupted by a collision, leads to an expression for the intensity of the disturbed wave function [Breene⁴] of

$$I(\nu) \propto R \left\{ \int_{-\infty}^{\infty} dt \exp(2\pi i(\nu_0 - \nu)t) \overline{\exp 2\pi i \eta(t)} \right\} \quad (2.4-6)$$

where $I(\nu)$ is intensity as a function of ν ,
 R is the operation of taking the real part of the
expression,
 $\eta(t)$ is the phase shift due to interaction as a
function of time, and the bar over the function
indicates a time averaging.

Now if there is negligible phase shift before time t , then an
encounter occurs and the integral terminates, we have

$$\begin{aligned} I(\nu) &\propto R \left\{ \int_0^t dt' \exp(2\pi i(\nu_0 - \nu)t') \right\} \\ &= R \left\{ \frac{1}{2\pi i(\nu_0 - \nu)} \left[\exp(2\pi i \{(\nu_0 - \nu)t\}) - 1 \right] \right\} \\ &= \frac{\sin 2\pi(\nu_0 - \nu)t}{2\pi(\nu_0 - \nu)} \quad (2.4-7) \end{aligned}$$

This result is now averaged over all possible values of t , while
neglecting the time spent in collision. The interruption theory has
now become impact theory.

According to the kinetic theory of gases, the distance (1) traveled between collisions by a molecule with velocity u follows the distribution function

$$p(l) dl = \frac{dl}{\bar{l}_u} \exp(-l/\bar{l}_u) , \quad (2.4-8)$$

where \bar{l}_u is the mean free-path for molecules of velocity u . The distribution function for the time between collisions follows from the substitution $udl = dt$, and is given by

$$p(t) dt = \frac{dt}{T_c} \exp\left(-\frac{t}{T_c}\right) , \quad (2.4-9)$$

where T_c is again the mean time between collisions. Now the product of Eq. 2.4-9 and Eq. 2.4-7, integrated over all time yields [Goody¹⁵]

$$I(v, u) = \frac{1}{(v-v_0)^2 + \left(\frac{1}{2\pi T_c}\right)^2} ,$$

which if normalized so that its area for all v is unity, may be written as

$$f(v, u) = \frac{1}{\pi} \frac{\alpha_L(u)}{(v-v_0)^2 + \alpha_L^2(u)} , \quad (2.4-10)$$

where the Lorentz line width (α_L) is defined as

$$\alpha_L(u) = \frac{1}{2\pi T_c} \quad (2.4-11)$$

The Lorentz line width is very strongly dependent upon pressure and temperature [Zuev⁵⁴] and is often approximated by

$$\alpha_L = \alpha_{L_0} \left(\frac{P}{P_0} \right) \left(\frac{T_0}{T} \right)^n \quad (2.4-12)$$

The subscript zero denotes some reference width calculated at the reference pressure P_0 and temperature T_0 . The exponent n is an empirically derived number, usually set to 0.5.

Having replaced the velocity dependence of α_L with a pressure, temperature relation, the common form of the Lorentz line shape (Pressure Broadening) is given as

$$f(\nu, \alpha_L) = \frac{1}{\pi} \frac{\alpha_L}{(\nu - \nu_0)^2 + \alpha_L^2} \quad (2.4-13)$$

Typical values for α_L range from 0.055 cm^{-1} for methane to 0.11 cm^{-1} for ozone [McClatchey, et. al³¹].

2.5 Summary

A knowledge of the composition and properties of the atmosphere, together with an understanding of molecular energy transitions, and spectral line broadening are the tools to be used for atmospheric absorption computations. It is possible to identify those molecules

that absorb radiation and determine, to some degree of accuracy, the center frequency absorbed. It is also possible to roughly predict the shape of the spectral line, given information on the composition of the atmosphere. This information, when calculated accurately, may be used for the temperature retrieval scheme alluded to in the introduction [McClatchey³³].

CHAPTER III

TRANSMITTANCE AND THE VOIGT FUNCTION IN THE FIFTEEN MICROMETER BAND

3.1 Preface

This Chapter addresses the subject of atmospheric transmittance with the combined effects of Doppler and Pressure line broadening. The definitions of absorption and transmittance are first presented then a function including both types of spectral line spreading is developed. This function is then introduced into the transmittance differential equation and the final form of the transmittance relation is given. Next the frequency band used here is briefly discussed, together with the validity of the assumptions made that limit investigation to this interval. Finally a summary of the important aspects of the chapter is given.

3.2 Absorption and Transmittance

The interaction of radiation with matter can lead to three types of changes in the energy. (1) Reflection, in which a part of the incident energy is deflected back. The reflected radiation as a fraction of that incident is the power of reflection of the substance. (2) Scattering, a part of the radiation energy incident at a definite direction is scattered in all directions. This is caused by an interaction depending on the relationship of the radiation wave length to the scattering particle size or certain optical flaws, such as differences in refractive index in the material. (3) Absorption, by which is designated the conversion of radiation energy into heat. The

portion of the energy transformed, expressed as a fraction of the incident energy, is known as the power of absorption. Chapter two developed the molecular model used for this energy absorption and now the model to predict absorption not on a molecular level, but a quantitative level, is developed.

These three effects depend in a characteristic manner on the wave length of the radiation and also on the specific properties of the substance to be investigated. For the infrared region, only the last effect is important [La Rocca and Turner²⁸]. Therefore it will be discussed exclusively.

The radiant energy of a definite monochromatic frequency ν passing into a body of length Δx , as shown in Fig. 3.2-1, is denoted $I_\nu(X_1)$. The emanating energy is reduced by some amount, proportional to the length Δx , and is denoted $I_\nu(X_2)$.

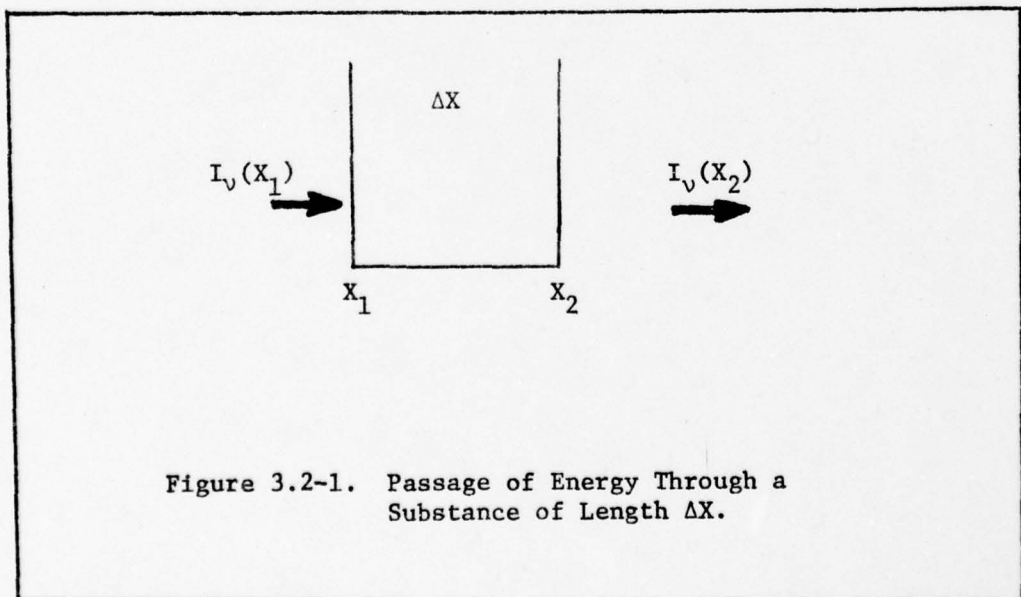


Figure 3.2-1. Passage of Energy Through a Substance of Length ΔX .

For atmospheric purposes it is recognized that the reduction in intensity of the radiation is due to the absorption of a portion of the energy by the molecules present in the path. Figure 3.2-1 is expressed mathematically as

$$I_v(X_2) = \alpha I_v(X_1) \Delta X$$

or in differential form

$$dI_v(X) = -I_v(X) \alpha dX. \quad (3.2-1)$$

The constant of proportionality is termed α and is also called the extinction coefficient. The negative sign is due to the reduction in intensity. Equation 3.2-1 is integrated to obtain

$$\int_{I_v(o)}^{I_v(x)} \frac{d I_v(x)}{I_v(x)} = \int_0^x -\alpha dx,$$

$$\ln \frac{I_v(x)}{I_v(o)} = -\alpha x,$$

and finally

$$I_v(x) = I_v(o) \exp(-\alpha x). \quad (3.2-2)$$

Equation 3.2-2 is known as the absorption law and is usually named after Lambert-Bouguer. The index αx is called the optical

density [Brugel⁶]. The optical density is an index of a power and must be dimensionless. The layer thickness x is usually measured in centimeters, thus the extinction coefficient is expressed in cm^{-1} .

A graphical representation of the optical density (αx), or the radiation energy transmitted ($I_v(x)$), both for a constant layer thickness (x); or the extinction coefficient (α) as a function of frequency, give the spectrum of the substance investigated. However, other quantities are usually used in the representation of spectra, namely the transmittance (τ) or the absorption (A), both given as a percentage of the incident radiation. The first is defined as the ratio of the energy passed to that which was incident. So from Eq. 3.2-2,

$$= \frac{I_v(x)}{I_v(o)} = \exp(-\alpha x). \quad (3.2-3)$$

The absorption (A) is defined as

$$A = 1 - \tau = 1 - \exp(-\alpha x). \quad (3.2-4)$$

Accordingly, the extinction (E) is defined

$$E = -\ln \tau = \ln \frac{1}{\tau} = \ln \frac{I_v(o)}{I_v(x)}. \quad (3.2-5)$$

The law of absorption (Eq. 3.2-2) gives a first quantitative unit for spectral measurements. Obviously, the absorption of a body is larger

the greater the thickness x , or the larger the extinction coefficient α , for the wavelength in question. In the last resort, however, the number of molecules absorbing in the volume is what is responsible for the absorption. Accordingly the extinction coefficient suffices completely for the description of the absorption power of a substance provided the number of molecules in the volume under consideration remains constant. Unfortunately this does not apply to the atmosphere where the number of molecules per unit volume is dependent upon the pressure. Therefore a relation must be derived between the concentration of a substance and the absorption it causes. Since in the atmosphere the number of molecules responsible for the absorption depends directly on the pressure, it is logical to write the extinction as a linear function of the concentration (or density) of the absorbing gas.

$$E = K \rho(x) dx \quad (3.2-6)$$

This equation is referred to as Beer's Law, in honor of its discoverer, A. Beer. Now from Eqs. 3.2-6 and 3.2-5 we obtain

$$\tau = \exp(-K\rho(x)dx). \quad (3.2-7)$$

This combined relationship of Eq. 3.2-6 and Eq. 3.2-5 is known as the Lambert-Beer Law.

For mixtures of absorbing materials the incremental absorption is additive in the absence of chemical interaction [Whiffen⁵¹]. Thus Eqs. 3.2-2 and 3.2-7 may be rewritten as

$$I_{\nu}(x) = I_{\nu}(0) \exp(-\sum_j \alpha_j x), \quad (3.2-8)$$

and

$$\tau = \exp(-\sum_j K_j \rho_j(x) dx), \quad (3.2-9)$$

where the summation over j accounts for the different gases in the atmosphere. Equation 3.2-9 is the basis of the whole infrared spectral analysis. It is true in most cases for monochromatic radiation. However care must be taken when it is applied to a band, as must be done with any measurement instrument. Brugel⁶ contains a discussion of the limits of Eq. 3.2-9.

3.2.1 The Transmittance Differential Equation

While Eq. 3.2-9 is correct, it is not in a convenient form for calculation of atmospheric transmittances from the top of the atmosphere to the bottom (ground level). Beginning with a form of Eq. 3.2-1 and utilizing Beer's Law the starting relation is given as

$$dI = -I K \rho(x) dx. \quad (3.2-10)$$

The expressed dependence of intensity (I) and the absorption coefficient (K) on wavelength, temperature, and pressure is dropped, but still understood. Rearranging 3.2-10 we obtain

$$\frac{dI}{I} = -K \rho(x) dx.$$

The hydrostatic equation (2.2-1) relates density (ρ) to pressure (P) in the manner desired. It is restated below without the negative

sign. For atmospheric considerations we begin at altitude Z and pressure P and move down to altitude $Z-\Delta Z$ and pressure $P+\Delta P$. Also the mixing ratio $M(P)$ is introduced to reflect a relation between total pressure and the pressure of only one gas under consideration. Chapter five contains a detailed explanation of Eq. 3.2-11.

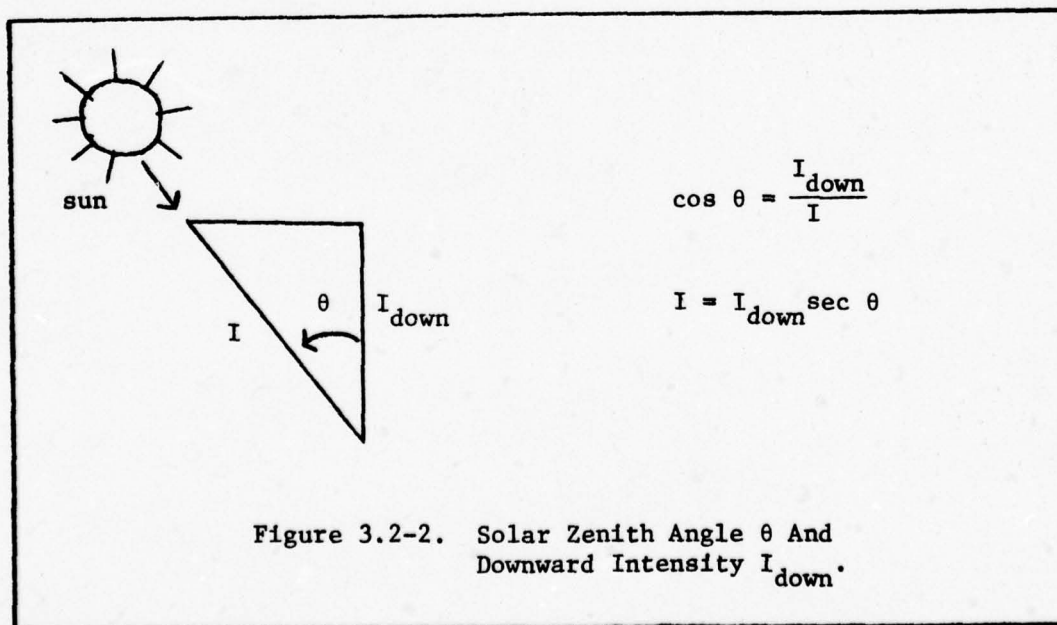
$$\frac{dP}{g} = \frac{1}{M(P)\rho(x)} dx \quad (3.2-11)$$

This yields

$$\frac{dI}{I} = -\frac{KM}{g} dP, \quad (3.2-12)$$

where the dependence of the mixing ratio on pressure is understood.

Instruments measure that portion of the intensity of radiation directed downward only and what needs to be considered is the total intensity. If θ is the solar zenith angle, from Fig. 3.2-2 Eq. 3.2-12 becomes



$$\frac{dI}{I} = -K \frac{M \sec \theta}{g} dP.$$

Integrating this equation from the top of the atmosphere ($P=0, I=I_0$) to a point where the pressure is P and the intensity I , yields,

$$\int_{I=I_0}^{I=I} \frac{dI}{I} = - \frac{\sec \theta}{g} \int_0^P MKdP,$$

$$\ln \frac{I}{I_0} = - \frac{\sec \theta}{g} \int_0^P MKdP,$$

or from the definition of transmittance,

$$\tau = \exp \left\{ - \frac{\sec \theta}{g} \int_0^P KMdP \right\}. \quad (3.2-13)$$

Now at a reference point (T_0, P_0) calculate a reference transmittance τ_0 and let

$$c = \frac{\sec \theta}{g}. \quad (3.2-14)$$

Thus,

$$\tau_0 = \exp \left\{ -c \int_0^{P_0} KMdP \right\},$$

and at any other position given by $P = P_0 + \Delta P$, calculate

$$\tau = \exp \left\{ -c \int_0^{P=P_0+\Delta P} KMdp \right\}.$$

Dividing this expression by the reference transmittance gives

$$\frac{\tau}{\tau_0} = \exp \left\{ -c \left[\int_0^{P_0+\Delta P} KMdp - \int_0^{P_0} KMdp \right] \right\}$$

$$\frac{\tau}{\tau_0} = \exp \left\{ -c \int_{P_0}^{P_0+\Delta P} KMdp \right\}.$$

Now let $P_0 = P_r$, a reference pressure

$\tau_0 = \tau_r$, the associated reference transmittance

$P = P_0 + \Delta P$, and

$$\tau = \tau_r \exp \left\{ -c \int_{P_r}^P KMdp \right\}. \quad (3.2-15)$$

We may place this relation in differential equation form.

$$\frac{\tau}{\tau_r} = \exp \left\{ -c \int_{P_r}^P KMdP \right\}$$

$$\ln \frac{\tau}{\tau_r} = -c \int_{P_r}^P KMdP$$

$$\frac{d}{dP} \left\{ \ln \frac{\tau}{\tau_r} \right\} = \frac{d}{dP} \left\{ -c \int_{P_r}^P KMdP \right\}$$

$$\frac{\tau_r}{\tau} \cdot \frac{1}{\tau_r} \cdot \frac{d\tau}{dP} = \frac{d}{dP} \left\{ -c \int_{P_r}^P KMdP \right\}$$

Using Leibnitz's rule for differentiating an integral [Spiegel⁴⁴],

$$\frac{1}{\tau} \frac{d\tau}{dP} = -c \left[\int_{P_r}^P \frac{d}{dP} (KM) dP + KM \frac{dP}{dv} - KM \frac{dP_r}{dv} \right].$$

Since K is a function of v , the last two terms follow. Neither P nor P_r are functions of v , so $\frac{dP}{dv} = \frac{dP_r}{dv} = 0$.

$$\frac{1}{\tau} \frac{d\tau}{dP} = -c \int_{P_r}^P \frac{d}{dP} (KM) dp$$

Using the fundamental theorem of calculus [Britten, et al⁵],

$$\text{i.e.: if } f(x) = \frac{d}{dx} g(x)$$

$$\text{then } \int f(x) dx = \int \frac{d}{dx} g(x) dx = g(x),$$

subject to boundary conditions;

$$\frac{1}{\tau} \frac{d\tau}{dP} = -cKM.$$

Writing this expression to explicitly show the functional dependence upon frequency, temperature, and pressure and utilizing the knowledge that the extinction coefficient (K) of each gas may be superimposed (as in Eq. 3.2-9), the transmittance differential equation is obtained.

$$\frac{d\tau(\nu, T, P)}{dP} = \left\{ -\frac{\sec \theta}{g} \sum_j K_j(\nu, T, P) M_j(P) \right\} \tau(\nu, T, P). \quad (3.2-16)$$

The iterative solution of this expression yields the desired transmittance values from the top of the atmosphere to ground level.

3.2.2 The Absorption Coefficient $K(\nu, T, P)$

For a given gas there exists a variety of forms for the absorption coefficient $K(\nu, T, P)$ [L'Vov³⁰]. In general the coefficient can be written

$$K_j(\nu, T, P) = \sum_i S_{ij} f(\nu - \nu_{o_{ij}}). \quad (3.2-17)$$

S_i represents the strength of the i th spectral line, ν_{o_i} is the center frequency of the line and the function $f(\nu - \nu_{o_i})$ defines the line shape of the i th line. In theory the contribution of each spectral line is added together (the summation over i) to obtain an absorption coefficient for a molecular species (gas type). Several authors give expressions for the line intensity (S_i) [Goody¹⁵, Hertzberg¹⁶]. Miller, et al.³⁵ gives

$$S_{ij} = S_{o_{ij}} Q_j(T) \left(\frac{T_o}{T}\right)^{C_j} \exp \left\{ \frac{E_{ij}}{kT_o} \left(1 - \frac{T_o}{T}\right) \right\}, \quad (3.2-18)$$

where S_o is a reference strength calculated at (T_o, P_o) ,
 E is the energy of the lower state involved in the molecular transition,
 k is the Boltzman's constant,
 T is temperature in degrees Kelvin, and
 Q is the vibrational partition function.

This strength function is one that currently being used for atmospheric transmittance calculations and is adopted here.

What remains of Eq. 3.2-17 to be specified is the line shape function. Chapter two enumerated the three most important line broadening mechanisms. In practice the investigator must decide if the problem at hand can be resolved by a single broadening function or if a more complicated one is needed to accurately describe the absorption coefficient. There are several approaches to the problem and the interested individual is referred to Miller, *et al.*³⁵, Anding², or La Rocca and Turner²⁸. For rapid line-by-line computation of transmittance at the sacrifice of some accuracy the Lorentz line shape function is generally used [Potter⁴⁰, Gibson¹⁴]. The shape function employed in this work is developed in the next section.

3.3 The Voigt Function

The first twenty years of the twentieth century were marked by considerable achievements in the field of atomic absorption theory. During this period the fundamental relationships between absorption and the atomic constants were established and, as was discussed in Chapter two, the theory for pressure broadening of lines was formulated [Lorentz²⁹]. The theory of Natural and Doppler broadening had been already developed. While several individuals realized that line broadening phenomena could not be completely predicted unless all causes were accounted for, it was W. Voigt⁴⁸ who first proposed that the effects of Doppler and Collision broadening could be dealt with in a single line shape function. Today this relation bears his name.

The relation may be derived by assuming that the line shape function follows a Doppler profile near the center and Lorentz in the wings.

The Lorentz line shape was developed in Chapter two and is restated here.

$$f(\nu - \nu_0) = \frac{1}{\pi} \frac{\alpha_L}{(\nu - \nu_0)^2 + \alpha_L^2} \quad (3.3-1)$$

The Doppler effect that causes a frequency shift of the monochromatic wavelength (ν_0), emitted by a molecule at rest, is written

$$\nu'_0 = \nu_0 \left(1 - \frac{u}{c}\right) \quad (3.3-2)$$

Again u is the line-of-sight velocity component of the molecule.

From Eq. 3.3-2 two relations to be used later are obtained.

$$u^2 = \frac{c^2(\nu'_0 - \nu_0)^2}{\nu_0^2} \quad (3.3-3)$$

$$du = \frac{c}{\nu_0} d\nu'_0 \quad (3.3-4)$$

Now if the translational states of the molecules under consideration are in thermodynamic equilibrium, the fractional number of molecules with velocities between u and $u + du$ is given by the Maxwell velocity distribution $p(u)$.

$$p(u)du = \left(\frac{m}{2\pi kT}\right)^{1/2} \exp\left(-\frac{mu^2}{2kT}\right) du \quad (3.3-5)$$

Substituting Eq. 3.3-3 and 3.3-4 into 3.3-5 yields

$$p(u)du = \left(\frac{m}{2\pi kT}\right)^{1/2} \exp\left[-\frac{mc^2(\nu'_0 - \nu_0)^2}{2kT\nu_0^2}\right] \frac{c}{\nu_0} d\nu'_0 \quad (3.3-6)$$

The contribution to the shaping function from all Doppler shifted components will be the probability function $p(u)du$ times the Lorentz line shape, integrated over all frequencies. It may be expressed as

$$f(\nu - \nu_0) = \int_{-\infty}^{\infty} p(u) f'(\nu - \nu_0) du. \quad (3.3-7)$$

The function $f'(\nu - \nu_0)$ is given by Eq. 3.3-1 with the center frequency of absorption (ν_0) replaced by the Doppler shifted frequency (ν_0'). Thus,

$$f'(\nu - \nu_0) = \frac{1}{\pi} \frac{\alpha_L}{(\nu - \nu_0')^2 + \alpha_L^2}, \quad (3.3-8)$$

and

$$\nu - \nu_0' = (\nu - \nu_0) - (\nu_0' - \nu_0). \quad (3.3-9)$$

Now utilizing Eqs. 3.3-9, 3.3-8, 3.3-6 and 3.3-7 the combined Doppler-Lorentz function is obtained [Voigt⁴⁷].

$$f(\nu - \nu_0) = \int_{-\infty}^{\infty} \frac{1}{\pi} \frac{\alpha_L \exp \left[-\frac{mc^2 (\nu_0' - \nu_0)^2}{2kT\nu_0^2} \right]}{[(\nu - \nu_0) - (\nu_0' - \nu_0)]^2 + \alpha_L^2} \left(\frac{m}{2\pi kT} \right)^{1/2} \frac{c}{\nu_0} d\nu_0' \quad (3.3-10)$$

Defining the variable

$$t = \left(\frac{mc^2}{2kT} \right)^{1/2} \left(\frac{\nu_0' - \nu_0}{\nu_0} \right), \quad (3.3-11)$$

we have immediately,

$$t^2 = \frac{mc^2}{2kT} \left(\frac{v'_o - v_o}{v_o} \right)^2 \quad (3.3-12)$$

and

$$dt = \left(\frac{mc^2}{2kT} \right)^{1/2} \frac{dv'_o}{v_o} \quad (3.3-13)$$

So now Eq. 3.3-10 becomes

$$\begin{aligned} f(v-v_o) &= \frac{1}{\pi} \int_{-\infty}^{\infty} \frac{\alpha_L \exp[-t^2] v_o \left(\frac{2kT}{mc^2} \right)^{1/2}}{[(v-v_o) - (v'_o - v_o)]^2 + \alpha_L^2} \left(\frac{mc^2}{2\pi kT} \right)^{1/2} \frac{1}{v_o} dt. \quad (3.3-14) \\ &= \frac{1}{\pi} \left(\frac{mc^2}{2\pi kT v_o^2} \right)^{1/2} \alpha_L \int_{-\infty}^{\infty} \frac{\exp(-t^2) dt}{\frac{1}{v_o} \left(\frac{mc^2}{2kT} \right)^{1/2} \left\{ [(v-v_o) - (v'_o - v_o)]^2 + \alpha_L^2 \right\}} \\ &= \frac{1}{\pi^{3/2}} \left(\frac{mc^2}{2kT v_o^2} \right)^{1/2} \alpha_L \int_{-\infty}^{\infty} \frac{\left(\frac{mc^2}{2kT v_o^2} \right)^{1/2} \exp(-t^2) dt}{\left[\left(\frac{v-v_o}{v_o} \right) \left(\frac{mc^2}{2kT} \right)^{1/2} - \left(\frac{v'_o - v_o}{v_o} \right) \left(\frac{mc^2}{2kT} \right)^{1/2} \right]^2 + \left(\frac{mc^2}{2kT v_o^2} \right) \alpha_L^2} \end{aligned} \quad (3.3-15)$$

Now using Eq. 3.3-11 again and defining

$$\alpha_D = \left(\frac{2kT}{mc^2} \right)^{1/2} v_o, \quad (3.3-16)$$

$$\frac{\alpha_L}{\alpha_D} = y, \quad \text{and} \quad \frac{v-v_o}{\alpha_D} = x, \quad (3.3-17)$$

$$(3.3-18)$$

where α_D is the Doppler half width, the relation becomes

$$f(v-v_o) = \left(\frac{mc^2}{2kTv_o} \right)^{1/2} \frac{1}{\pi^{3/2}} \int_{-\infty}^{\infty} \frac{y \exp(-t^2) dt}{[x-t]^2 + y^2}. \quad (3.3-19)$$

The absorption coefficient for the mixed Doppler-Lorentz (Voigt) function is then given by Eq. 3.2-17 and the following new definition of strength

$$K_{o_{ij}} = \frac{S_{ij}}{\alpha_D} \left(\frac{1}{\pi} \right)^{1/2}, \quad (3.3-20)$$

where S_{ij} is defined in Eq. 3.2-18. Thus

$$K_j(v, T, P) = \sum_i \frac{K_{o_{ij}}}{\pi} \int_{-\infty}^{\infty} \frac{y \exp(-t^2) dt}{y^2 + (x-t)^2}. \quad (3.3-21)$$

Other derivations of this Voigt profile are given in Penner³⁸, Goody¹⁵, or more recently Young⁵³.

Combining Eq. 3.3-21 and the transmittance differential equation (3.2-16) one obtains the relation for atmospheric transmittance considering the Voigt profile. Several authors assert that this function should be used if completely accurate results are to be obtained [LaRocca and Turner²⁸, Anding², and Rodgers⁴¹]. The summary of this chapter collects all the equations thus far derived that are needed. The evaluation of the Voigt profile is discussed in the next chapter.

Figure 3.3-1 shows the relation between the Doppler line shape, Lorentz line shape and the Voigt profile.

3.4 The Fifteen Micron Band

Figure 3.4-1 shows the electromagnetic spectrum and the nomenclature used for different regions. This work is limited to the so called fifteen micron band. The limits of the band are not well defined and in fact depend much on the instrument used to investigate the region. As the name implies however it is generally around the 15 μ m portion of the spectrum.

The NIMBUS 6 High Resolution Infrared Radiation Sounder (HIRS) is a third generation infrared radiation sounding satellite possessing many new features for greatly improved capability of sounding the earth's atmosphere. The investigations of this work used the specifications of the NIMBUS 6 to calculate the transmittances needed to provide correct temperature soundings. NIMBUS 6 uses seven channels in the fifteen micron band. The channels are monitored by a multi-channel filter radiometer. The band provides better sensitivity to

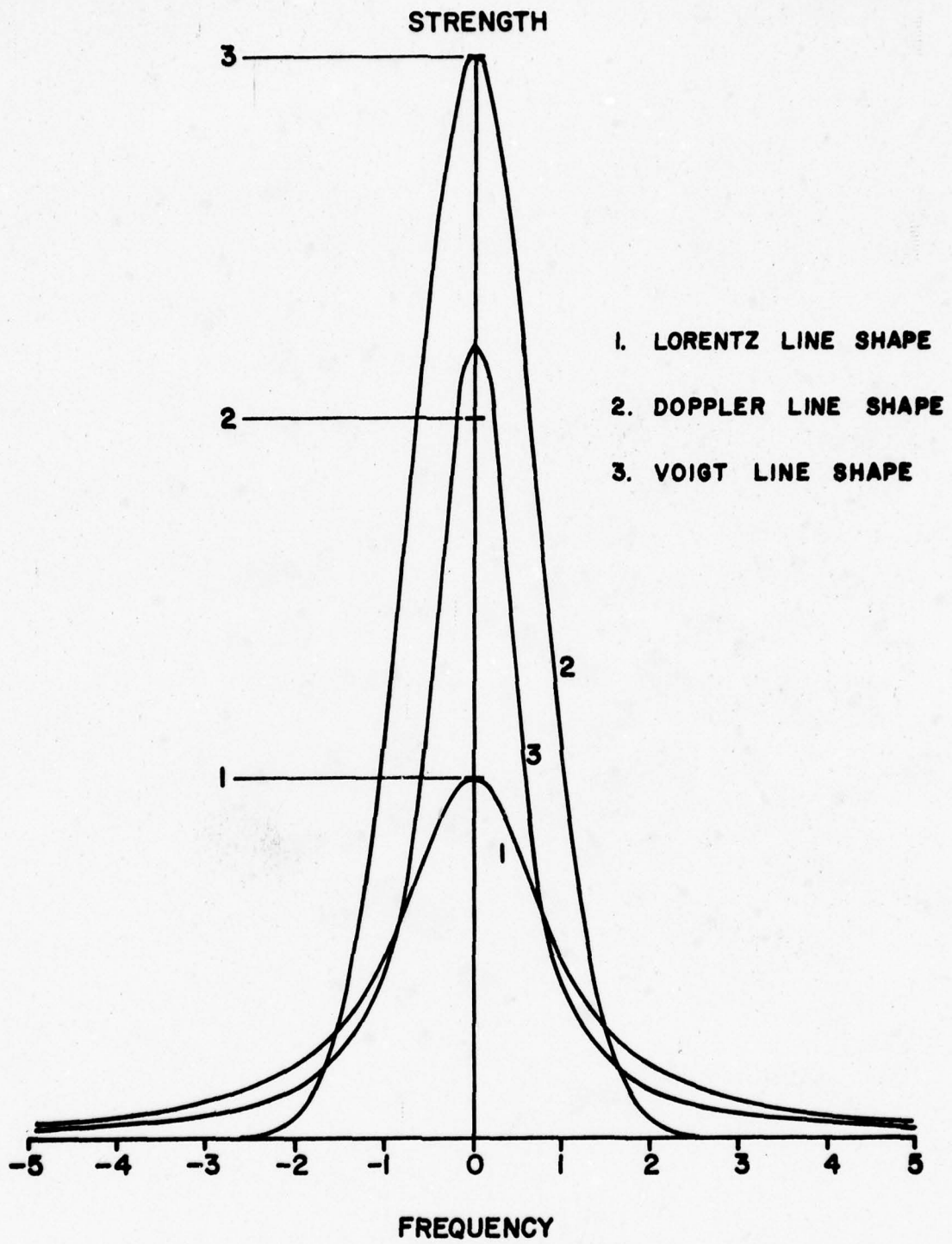


Figure 3.3-1. Doppler, Lorentz and Voigt line shapes.

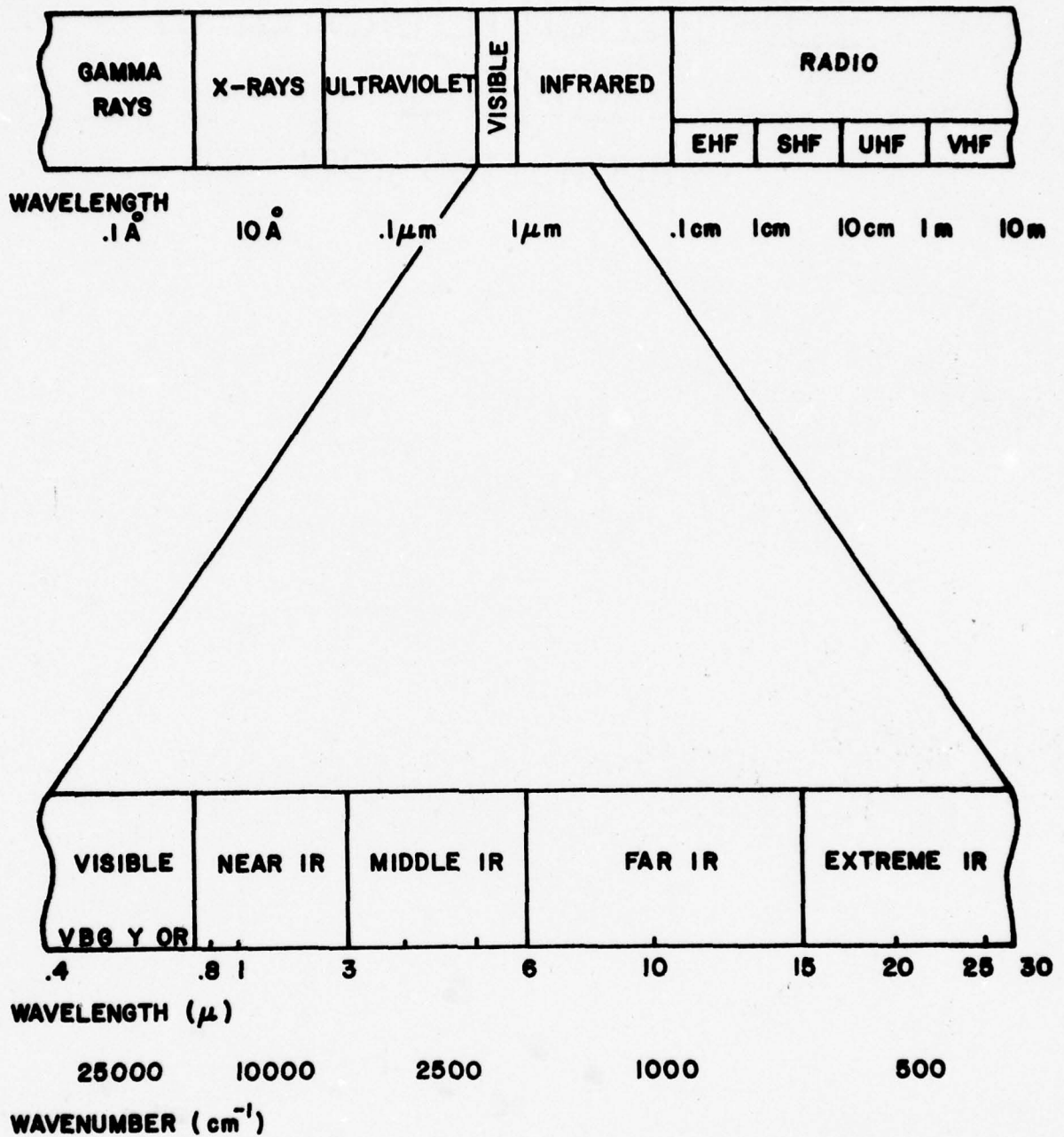


Figure 3.4-1. The Electromagnetic Spectrum.

the temperature of the relatively cold regions of the atmosphere [Sissala⁴³] than can be achieved with the 4.3 μ m band channels. These cooler temperatures correspond to higher altitudes and lower pressures. At these levels the Lorentz line width is reduced and the Doppler line width is broadened. Therefore for most accurate transmittance calculations both line broadening schemes must be represented. For this reason the Voigt profile is used in calculations.

The important engineering aspects of NIMBUS 6 design are depicted in Table 3.4-1 and Fig. 3.4-2.

Channel Number	Central Wavenumber (cm ⁻¹)	Interval Between 50% Response Points (cm ⁻¹)	Primary Absorber	Level of Peak Energy Contribution
1	668	2.8	CO ₂	30mb
2	679	13.7	CO ₂	60mb
3	690	12.6	CO ₂	100mb
4	702	15.9	CO ₂	250mb
5	716	17.5	CO ₂	500mb
6	733	17.6	CO ₂ /H ₂ O	750mb
7	749	18.4	CO ₂ /H ₂ O	900mb

Table 3.4-1. NIMBUS 6 Characteristics.
(Adapted from Sissala⁴³)

Figure 3.4-2 depicts the filter responses for the seven channels of interest. For atmospheric calculations it is necessary to consider

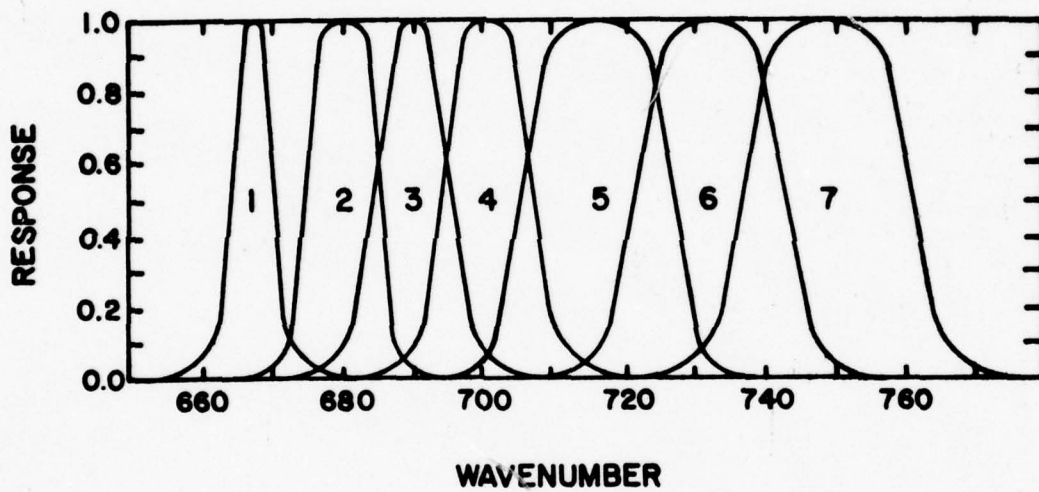


Figure 3.4-2. HIRS filter responses [Sissala⁴³].

all lines whose center frequency (ν_0) is within a channel, for the transmittance of that channel. Thus, for example, the summation over i in Eq. 3.3-21 runs over those lines whose center frequency is between 665.2 cm^{-1} and 670.8 cm^{-1} for channel one. In addition it may be necessary to consider the wings of lines whose center frequency lies outside the channel interval. Figure 3.4-3 depicts such a line (wavenumber ν_{01}). Although the center frequency is outside the channel limits, the right wing of the line contributes to absorption within the channel.

3.5 Summary

The transmittance differential equation to be used in this investigation is given by

$$\frac{d \tau(\nu, T, P)}{dP} = \left\{ - \frac{\sec \theta}{g} \sum_j K_j(\nu, T, P) M_j(P) \right\} \tau(\nu, T, P). \quad (3.2-16)$$

K_j is called the absorption coefficient and has different representations, depending upon the nature of the investigation. For instances where the combined effects of Doppler-Lorentz (Voigt) broadening are to be considered, the absorption coefficient is expressed by the Voigt profile,

$$K_j = \sum_i \frac{k_{0ij}}{\pi} \int_{-\infty}^{\infty} \frac{y \exp(-t^2) dt}{y^2 + (x-t)^2} \quad (3.3-21)$$

where

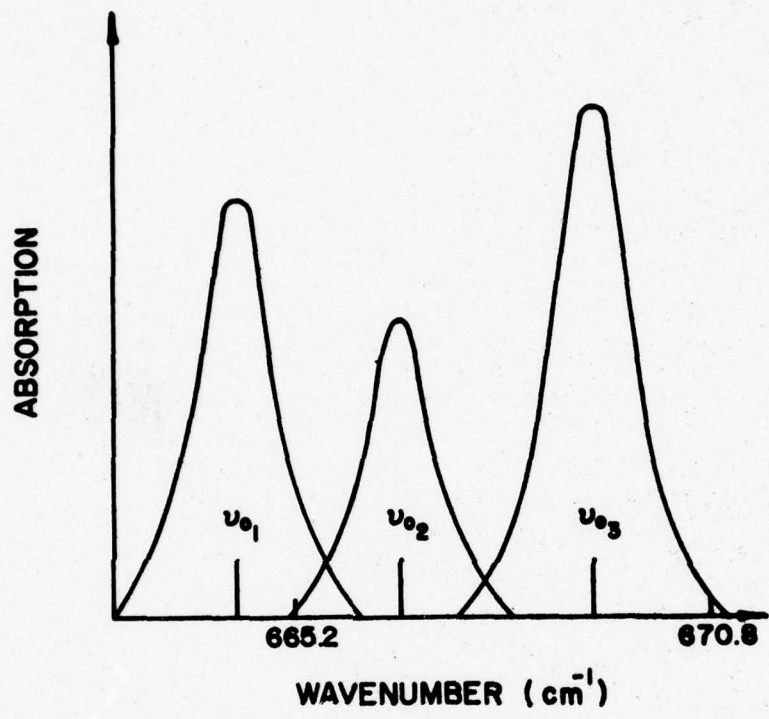


Figure 3.4-3. A spectral line (ν_{01}) that absorbs in channel one although its center is out of the channel.

$$K_{o_{ij}} = \frac{S_{ij}}{\alpha_D} \left(\frac{\ln 2}{\pi} \right)^{1/2} \quad (3.3-20)$$

is the line strength,

$$y = \frac{\alpha_L}{\alpha_D} (\ln 2)^{1/2}, \quad (3.3-17)$$

$$x = \frac{v-v_o}{\alpha_D} (\ln 2)^{1/2}, \quad (3.3-18)$$

$$\alpha_L = \left(\frac{P}{P_o} \right) \left(\frac{T_o}{T} \right)^{1/2} \alpha_o, \quad (2.4-12)$$

$$\alpha_D = 3.58 \cdot 10^{-7} \left(\frac{T}{M} \right)^{1/2} v_o, \quad (2.4-4)$$

$$S_{ij} = S_{o_{ij}} Q_j(T) \left(\frac{T_o}{T} \right)^{C_j} \exp \left\{ \frac{E_{ij}}{kT_o} \left(1 - \frac{T_o}{T} \right) \right\}. \quad (3.2-18)$$

NOTE: The doppler width $\alpha_D (\ln 2)^{1/2}$ is used instead of α_D in all equations [Anding²].

M is the molecular weight, α_L the Lorentz half width, α_D the Doppler half width, Q the vibrational partition function (see Chapter six), E the energy of the lower state of a transition, and k Boltzman's constant. The subscript zero indicates a reference value calculated at (T_o, P_o) , except when used with v. Then it indicates the center frequency of absorption. The subscript j is for gas type and the

subscript i is for the absorbing lines. J runs for all molecular species of concern, while the i counter runs for all the lines that fall within a channel of the instrument used for measurements. The limits of the channel may have to be extended by some amount to account for the wings of lines whose center frequency is outside the channel. The channels used here and their filter responses are depicted in Table 3.4-1 and Fig. 3.4-2 respectively.

CHAPTER IV
COMPUTER ALGORITHMS FOR THE VOIGT PROFILE

4.1 Preface

The Voigt profile developed in chapter three is widely accepted but, until recently, not widely used because it is difficult to quickly evaluate. This chapter presents three methods of evaluation that are easily computerized. The first was developed by John Keilkopf, the second by S. R. Drayson and the last is a new method developed here. In searching for methods to compute the profile, speed and accuracy were the primary concerns. In a line-by-line transmittance model as much as 75% of the computational time may be used to evaluate the Voigt function. Any reduction in calculation time for the function would then obviously have a dramatic effect on the transmittance program execution time.

The accuracy required of any algorithm is about one part in 10^4 . The uncertainty of absorption line parameters limit transmittance accuracy so that this degree of exactness is all that is needed. Function subprograms for each method are listed in appendices.

The results of tests for speed and accuracy of each method are presented last. The design of the examination is specified and the outcome is tabulated. The method selected for use in these transmittance calculations is specified and some comments on its applicability are given.

4.2 J. F. Kielkopf's Voigt Algorithm

The Voigt profile derived in chapter three is written in slightly

different form by Kielkopf²⁴. Following the development of his algorithm the two forms will be related. Starting as Kielkopf, the Voigt profile may be written

$$V(\beta_l, \beta_g; \nu) = \int_{-\infty}^{\infty} \frac{\beta_l/\pi \exp[-(\nu'/\beta_g)^2] d\nu'}{[\beta_l^2 + (\nu - \nu')^2]} \quad (4.2-1)$$

A standardized form of the function that does not change its width or height as a function of parameters is given by

$$U(x) = \frac{V(\beta_l, \beta_g; \beta x)}{I(\beta_l, \beta_g)}, \quad (4.2-2)$$

where $\nu = \beta x$ and the peak value of V is I . For large values of x the function may be approximated by

$$\eta = \frac{l}{l+g^2}, \quad (4.2-3)$$

where

$$l = \beta_l/\beta, \quad (4.2-4)$$

$$g = \beta_g/\beta. \quad (4.2-5)$$

The letters g and l represent the gaussian and lorentzian parts of the line shape respectively. Near the line core, gaussian properties appear in U and an approximation to the standardized function is

$$U(\eta;x) = (1-\eta)G(x) + \eta L(x), \quad (4.2-6)$$

where

$$G(x) = \exp[-(\ln 2)x^2], \quad (4.2-7)$$

and

$$L(x) = \frac{1}{1+x^2}. \quad (4.2-8)$$

A function of the form of Eq. 4.2-6 has substantial errors in the limit as x grows large, however. Therefore corrections and adjustments are made to the relations used for l , g , and U .

The graphs given by Van de Hulst and Reesnick⁴⁶ show that the gaussian and lorentzian portions of a line are related approximately by

$$g^2 = (1/\ln 2)(1-l). \quad (4.2-9)$$

A small quadratic correction results in a highly accurate relation.

$$g^2 = (1/\ln 2)[1 - (1 + \epsilon \ln 2)l + (\epsilon \ln 2)l^2] \quad (4.2-10)$$

$$\epsilon = 0.0990$$

The lorentzian fraction is similarly

$$l = \frac{2}{[1 + \epsilon \ln 2 + [(1 - \epsilon \ln 2)^2 + (4 \ln 2/a^2)]^{1/2}]} \quad (4.2-11)$$

Here a is called the Voigt parameter and is defined as

$$a = \beta_l / \beta_g = \frac{l}{g}. \quad (4.2-12)$$

From Eq. 4.2-4 we have

$$\beta = \beta_g / \ell \quad (4.2-13)$$

Next what is needed is the peak intensity I . It is given in terms of the complementary error function as

$$I(\beta_g, \beta_g) = \frac{a}{\pi^{1/2} \beta_g} \exp(a^2) \operatorname{erfc}(a). \quad (4.2-14)$$

There are a large number of methods to compute the complementary error function. The one chosen here is

$$\operatorname{erfc}(a) = f(a) \exp(-a^2) \quad (4.2-15)$$

where

$$f(a) = \frac{1}{\pi^{1/2}} (b_1 t + b_2 t^2 + b_3 t^3) \quad (4.2-16)$$

and

$$t = \frac{1}{1 + b_0 a} \quad (4.2-17)$$

$$b_0 = 0.47047$$

$$b_1 = 0.61658$$

$$b_2 = -0.16994$$

$$b_3 = 1.32554$$

Combining Eqs. 4.2-14, 15 and 16,

$$I(\beta_g, \beta_g) = \frac{a}{\pi \beta_g} \left(b_1 t + b_2 t^2 + b_3 t^3 \right) \quad (4.2-18)$$

Beginning with Eq. 4.2-6 and adding a correction term, the final form of $U(\eta;x)$ was determined by Kielkopf²⁴ as

$$U(\eta;x) = (1-\eta)G(x) + \eta L(x) + \eta(1-\eta)E(x)[G(x) - L(x)]. \quad (4.2-19)$$

The function $E(x)$ was determined empirically as

$$E(x) = \frac{0.8029 - 0.4207x^2}{1 + 0.2030x^2 + 0.07335x^4}. \quad (4.2-20)$$

Now the relation between the variables of Eq. 4.2-1 and the standard form of the Voigt profile is shown.

$$f(v-v_0) = y/\pi \int_{-\infty}^{\infty} \frac{e^{-t^2}}{y^2 + (x-t)^2} dt, \quad (4.2-21)$$

where

$$x = \frac{v-v_0}{\alpha_D} (\ln 2)^{1/2}, \quad (4.2-22)$$

$$y = \frac{\alpha_L}{\alpha_D} (\ln 2)^{1/2}. \quad (4.2-23)$$

Substituting these definitions in Eq. 4.2-21 yields

$$f(v-v_0) = \frac{1}{\pi} \frac{\alpha_L}{\alpha_D} (\ln 2)^{1/2} \int_{-\infty}^{\infty} \frac{e^{-t^2}}{\left(\frac{\alpha_L}{\alpha_D}\right)^2 \ln 2 + \left[\frac{v-v_0}{\alpha_D} (\ln 2)^{1/2} - t\right]^2} dt$$

$$= \frac{1}{\pi} \frac{\alpha_L}{\alpha_D} (\ln 2)^{1/2} \int_{-\infty}^{\infty} \frac{e^{-t^2} dt}{\frac{\ln 2}{2} \left[\alpha_L^2 + (v-v_0) - \frac{\alpha_D}{(\ln 2)^{1/2}} t \right]^2} .$$

Now let

$$t = v'/\beta_g , \quad (4.2-24)$$

$$v-v_0 = v , \quad (4.2-25)$$

$$\frac{\alpha_D}{(\ln 2)^{1/2}} = \beta_g , \quad (4.2-26)$$

$$\alpha_L = \beta_l , \quad (4.2-27)$$

so that

$$f(v-v_0) = \frac{1}{\pi} \frac{\beta_l}{\beta_g} \int_{-\infty}^{\infty} \frac{\exp \left[-\left(\frac{v'}{\beta_g} \right)^2 \right] \frac{1}{\beta_g} dv'}{\left[\beta_l^2 + (v-v')^2 \right] \left(\frac{1}{\beta_g} \right)^2} .$$

$$f(v-v_0) = \frac{\beta_l}{\pi} \int_{-\infty}^{\infty} \frac{\exp \left[-\left(\frac{v'}{\beta_g} \right)^2 \right] dv'}{\beta_l^2 + (v-v')^2} \quad (4.2-28)$$

This is exactly the form given by Kielkopf²⁴, so the relations of Eqs. 4.2-24, 25, 26, and 27 are those desired.

Now in terms of the line parameters previously defined, the pro-

cedure for the algorithm is summarized.

$$(1) \quad a = \frac{\alpha_L}{\alpha_D} (\ln 2)^{1/2} \quad (4.2-29)$$

$$(2) \quad \ell = \frac{2}{\{1 + \epsilon \ln 2 + [(1 - \epsilon \ln 2)^2 + (4 \ln 2 / a^2)]^{1/2}\}} \quad (4.2-30)$$

$$\epsilon = 0.0990$$

$$(3) \quad g^2 = (1/\ln 2) [1 - (1 - \epsilon \ln 2)\ell + (\epsilon \ln 2)\ell^2] \quad (4.2-31)$$

$$(4) \quad \eta = \frac{\ell}{\ell + g^2}$$

$$(5) \quad \beta = \frac{\alpha_L}{\ell} \quad (4.2-32)$$

$$(6) \quad x = \frac{v - v_0}{\beta} \quad (4.2-33)$$

$$(7) \quad I(\beta_\ell, \beta_g) = \frac{a}{\pi \alpha_L} (b_1 t + b_2 t^2 + b_3 t^3) \quad (4.2-34)$$

$$t = \frac{1}{1 + b_0 a}$$

$$b_0 = 0.47047$$

$$b_1 = 0.61686$$

$$b_2 = -0.16994$$

$$b_3 = 1.32554$$

$$(8) \quad G(x) = \exp[-(\ln 2)x^2] \quad (4.2-35)$$

$$(9) \quad L(x) = \frac{1}{1+x^2} \quad (4.2-36)$$

$$(10) \quad E(x) = \frac{0.8029 - 0.4207x^2}{1 + 0.203x^2 + 0.07335x^4} \quad (4.2-37)$$

$$(11) \quad U(n;x) = (1-n)G(x) + nL(x) + n(1-n)E(x)[G(x) - L(x)] \quad (4.2-38)$$

$$(12) \quad V(\beta_L, \beta_G, \nu) = U(n;x) I(\beta_L, \beta_G) \quad (4.2-39)$$

These twelve steps yield the desired value of the Voigt profile. The accuracy of this method is given [Kielkopf²⁴] as 10^{-4} times the peak intensity. The FORTRAN IV function subprogram implementing this method is listed in Appendix A.

4.3 S. R. Drayson's Voigt Algorithm

In developing a computer algorithm to evaluate the Voigt function, Drayson required accuracy of about one part in 10^4 . Beyond this the chief aim was rapid computation of the function, which is repeated here for clarity.

$$f(\nu-\nu_0) = \frac{y}{\pi} \int_{-\infty}^{\infty} \frac{\exp(-t^2) dt}{y^2 + (x-t)^2} \quad (4.3-1)$$

$$x = \frac{\nu-\nu_0}{\alpha_D} (\ln 2)^{1/2} \quad y = \frac{\alpha_L}{\alpha_D} (\ln 2)^{1/2}$$

It is easily seen from the definition of x that it can assume values that are both positive and negative. However since it is assumed that $f(v-v_0)$ is an even function in x , i.e. $f(x) = f(-x)$, only positive values of x are needed for line broadening problems. Similarly it is seen that y will assume only positive values as long as the Lorentz half-width (α_L) is included. For other applications negative values of y occur [Fried and Conte¹³]. Limiting x and y so that they are greater than or equal to zero defines the first quadrant of the xy plane.

Now consider the complex probability function defined as

$$w(Z) = \frac{i}{\pi} \int_{-\infty}^{\infty} \frac{e^{-t^2}}{Z-t} dt = e^{-Z^2} \left(1 + \frac{2i}{\pi} \int_0^Z e^{-t^2} dt \right), \quad (4.3-2)$$

where $Z = x + iy$, $x \geq 0$, $y > 0$. Separating this function into real and imaginary parts yields

$$\begin{aligned} w(Z) &= \frac{1}{\pi} \int_{-\infty}^{\infty} \frac{ie^{-t^2} dt}{(x+iy) - t} \\ &= \frac{1}{\pi} \int_{-\infty}^{\infty} \frac{ie^{-t^2} dt}{(x-t) + iy} \cdot \frac{(x-t) - iy}{(x-t) - iy} \\ &= \frac{1}{\pi} \int_{-\infty}^{\infty} \frac{y e^{-t^2} + i(x-t)e^{-t^2}}{(x-t)^2 + y^2} dt \end{aligned}$$

$$w(Z) = \frac{1}{\pi} \int_{-\infty}^{\infty} \frac{y e^{-t^2}}{(x-t)^2 + y^2} dt + \frac{i}{\pi} \int_{-\infty}^{\infty} \frac{(x-t)e^{-t^2}}{(x-t)^2 + y^2} dt \quad (4.3-3)$$

It is thus shown that the Voigt profile is the real part of the complex probability function $w(Z)$. Several authors have tabulated values of this function for both the real and imaginary parts, but the most complete account of its mathematical properties appears to be that of Faddeyeva and Terentév¹² or more recently, for atmospheric applications, Armstrong³.

In order to evaluate the real part of $w(Z)$ as rapidly as possible, the xy plane is partitioned as shown in Figure 4.3-1 [Drayson¹¹] and different approximating functions are used in each region.

In Region I $w(Z)$ may be rewritten as

$$\left. \begin{aligned} w(Z) &= e^{-Z^2} + \frac{2i}{\pi^{1/2}} F(Z) \\ F(Z) &= e^{-Z^2} \int_0^Z e^{-t^2} dt \end{aligned} \right\} \quad (4.3-4)$$

For real Z , the function $F(Z)$ is known as Dawson's function. The coefficients (d_n) of a Taylor series expansion of $F(Z)$ about any real point $(x, 0)$, have the relationships

$$d_0 = F(x), \quad d_1 = 1 - 2xd_0, \quad d_{n+1} = -\frac{2}{n+1} (xd_n + d_{n-1}) \quad (4.3-5)$$

for $n = 1, 2, 3, \dots$ [Dawson¹⁰].

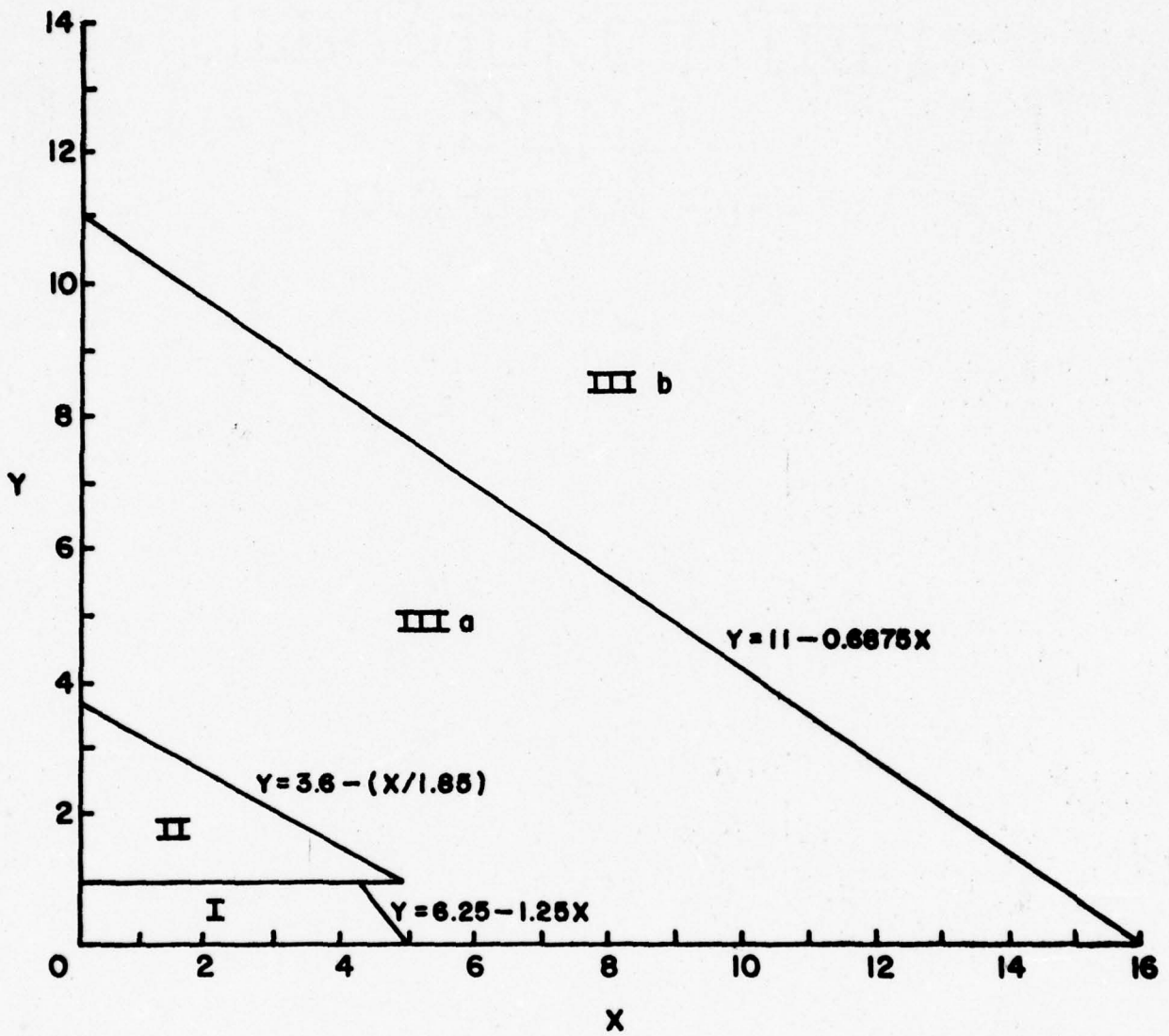


Figure 4.3-1. Computational regions used by Drayson ¹¹.

Thus, for Region I, Dawson's function is first evaluated on the x-axis and a Taylor series is used to find the imaginary part of $F(Z)$ and thus the real part of $w(Z)$.

Dawson's function may be evaluated by series expansion, asymptotic expansion, or a Chebyshev expansion [Hummer¹⁹]. In the method developed for his program Drayson evaluates Dawson's function initially by Chebyshev expansion on the x-axis for $x = 0.1, 0.3, 0.5, \dots, 4.9$. The coefficients d_1, d_2, d_3, d_4 are computed at each point using Eq. 4.3-5 and stored for later use. This process is required only once. Dawson's function is then evaluated for arbitrary x by a Taylor series expansion about the nearest tabulated point ($x = 0.1, 0.3, \dots, 4.9$). The number of terms needed in the series expansion of $F(Z)$ is a function of x and y . To avoid a test for convergence of the series, an empirical function was developed to determine the number of terms required.

For Region II first note that it has been shown by Chebyshev⁹ and later K. A. Posse³⁹ that an integral of the type

$$\int_a^b \frac{p(t)}{Z-t} dt$$

can be represented by the continued fraction

$$\frac{\lambda_0}{Z - \alpha_1 - \frac{\lambda_1}{Z - \alpha_2 - \frac{\lambda_2}{Z - \alpha_3 - \dots}}}$$

where λ_n and α_n are coefficients in a recurrence formula. Fried and Conte¹³ applied this technique to the function $w(Z)$ to obtain its fractional expansion.

$$w(Z) = \frac{1}{\pi^{1/2}} \frac{1}{Z + \frac{1}{Z + \frac{1/2}{Z + \frac{1}{Z + \frac{3/2}{Z + \dots}}}}}$$

$$w(Z) = \frac{1}{\pi^{1/2}} \cdot \frac{1}{Z + \frac{1/2}{Z + \frac{1}{Z + \frac{3/2}{Z + \dots}}}} \dots \frac{n/2}{Z + \dots} \dots \quad (4.3-6)$$

Along the line $y = 1$, which separates Region I and II, the Taylor series and the continued fraction require about the same computational time. The number of terms needed in the fractional expansion varies from $n = 4$ to $n = 19$ [Drayson¹¹]. Again an empirical function was developed to determine the number of terms required and thus avoid a check for convergence.

For Region III the complex argument (Z) has a sufficiently large modulus, i.e. $|Z| = (x^2 + y^2)^{1/2}$, so that Gauss-Hermite quadrature is effective [Faddeyeva and Terentév¹²]. The Voigt profile is approximated by a four-point quadrature in Region IIIa and a two-point quadrature in Region IIIb. The expressions used are

$$\frac{y}{\pi} \int_{-\infty}^{\infty} \frac{e^{-t^2}}{y^2 + (x-t)^2} dt = \frac{y}{\pi} \sum_{i=0}^3 W_i \frac{1}{y^2 + (x-t_i)^2} \quad (4.3-7)$$

in Region IIIa, and

$$\frac{y}{\pi} \int_{-\infty}^{\infty} \frac{e^{-t^2}}{y^2 + (x-t)^2} dt = \frac{y}{\pi} \sum_{i=0}^1 W_i \frac{1}{y^2 + (x-t_i)^2} \quad (4.3-8)$$

in Region IIIb. Here W_i are the weight factors and the t_i 's are the roots of the Hermite polynomial of degree $n+1$. Carnahan, et al.⁸ has an explanation of Gaussian Quadrature methods as well as tables of W_i and t_i for the Gauss-Hermite Quadrature method.

Utilizing the four regions of Fig. 4.3-1 and the three methods described to approximate the real part of Eq. 4.3-2, Drayson has written a FORTRAN IV function subprogram that he claims is accurate to about one part in 10^4 and much more rapid than any other currently available to evaluate the Voigt profile. A listing of the program is contained in Appendix B.

4.4 Proposed Voigt Algorithm

This method begins, as does Drayson's with the complex probability function

$$w(Z) = e^{-Z^2} \left(1 + \frac{2i}{\pi^{1/2}} \int_0^Z e^{t^2} dt \right). \quad (4.4-1)$$

Again, $Z = x + iy$ and $x, y \geq 0$. It was shown in section 4.3 that the real part of this function is the Voigt profile. From the definition of the complementary error function of complex argument,

$$\operatorname{erfc}(-iZ) = \left(1 + \frac{2i}{\pi^{1/2}} \int_0^Z e^{t^2} dt \right). \quad (4.4-2)$$

Therefore

$$w(Z) = e^{-Z^2} \operatorname{erfc}(-iZ), \quad (4.4-3)$$

or in terms of the error function of complex argument

$$w(Z) = e^{-Z^2} \left(1 - \operatorname{erf}(-iZ) \right). \quad (4.4-4)$$

It is possible to approximate $w(Z)$ by utilizing Euler's formula for e^Z and a series expansion of the error function for complex argument. Euler's formula applied here is

$$e^{-Z^2} = \exp(-x^2 + y^2) \left(\cos(2xy) - i \sin(2xy) \right). \quad (4.4-5)$$

The series expansion for the error function is [Salzer⁴²]

$$\operatorname{erf}(-iZ) = \frac{2}{\pi^{1/2}} \sum_{n=0}^{\infty} \frac{(-1)^n}{n! (2n+1)} (-iZ)^{2n+1}. \quad (4.4-6)$$

Combining Eq. 4.4-5 and 4.4-6 into Eq. 4.4-4 yields the algorithm desired.

It was noted, however, that for large modulus the series expansion of the error function required upwards of 50 terms for convergence. Therefore, the xy plane was divided in a manner similar to that of Drayson. The difference is that there are only three regions and two approximating functions. Figure 4.4-1 depicts the three regions.

The series is used in Region I. In order to avoid testing for convergence a computer routine was developed to determine the number of terms of the series required for various values of x and y in the

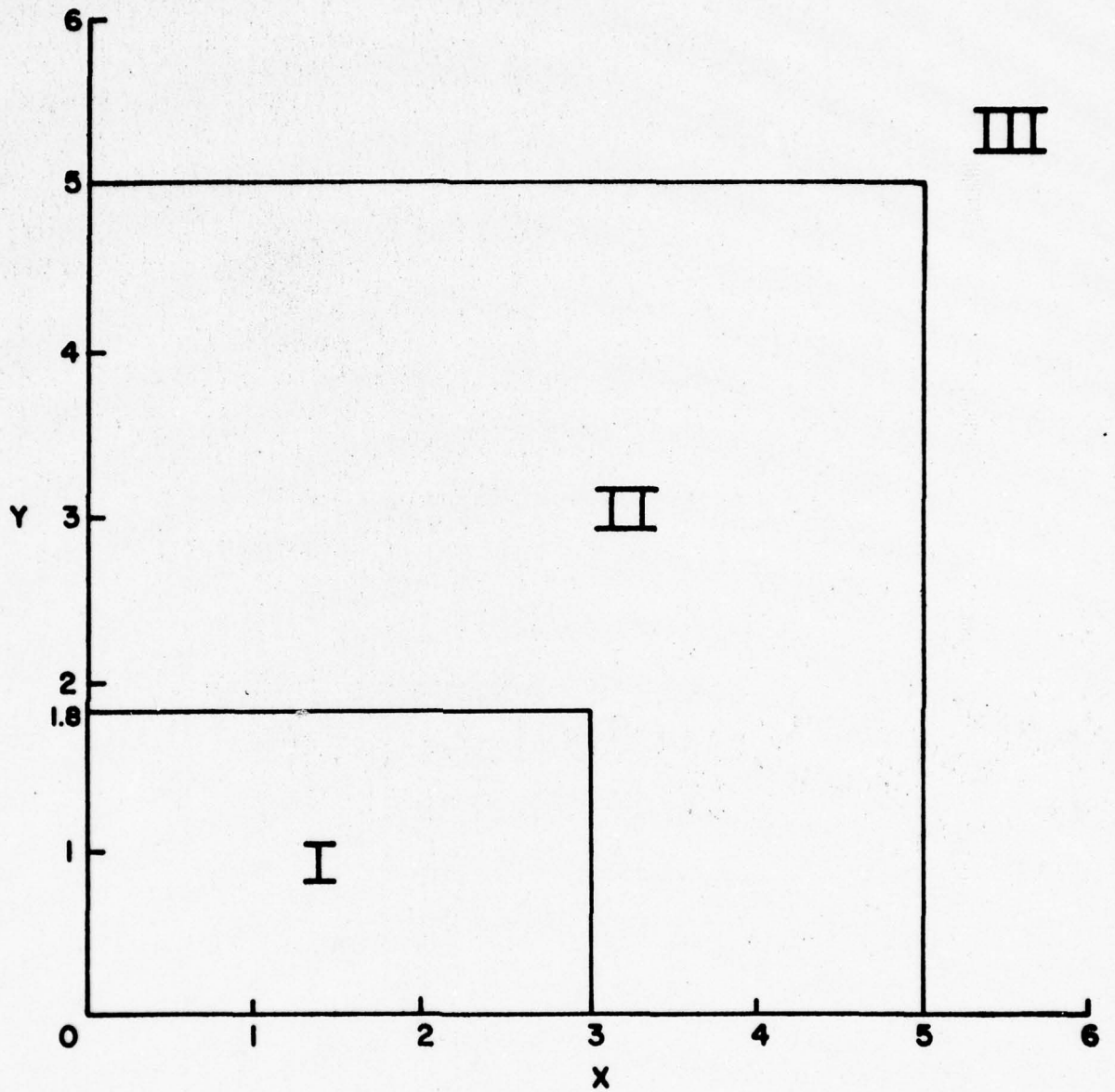


Figure 4.4-1. Regions proposed by this work.

region. The results of that routine are shown in Fig. 4.4-2. It was noticed that if the points of $x = 0.1$ and $x = 2.0$ are used (a rough linear fit), the lines for different values of y have the same slope. The line just moves up for increasing values of y . Therefore the relation used to fix the number of terms was chosen to be

$$N = 6.842 x + 8. \quad (4.4-7)$$

The position of this line with respect to the test results is also shown in Fig. 4.2-2. In implementation the value of N is truncated to yield an integer. The minimum for N was set to 8 to assure convergence. The single exception is for $x = 0$. Then the number of terms is set to 15.

The limits of the regions depicted in Fig. 4.4-1 were chosen after analyzing different approximations for $w(Z)$. It was decided that a quadrature of the integral would be the simplest and most accurate for regions two and three. Using a modified Gauss-Laguerre quadrature, Abramowitz¹ obtains two approximations that are used for $w(Z)$. The limits expressed by Abramowitz were modified since a reduced accuracy from that which he specified was acceptable. For Region II a three point formula yields

$$w(Z) = iZ \left(\frac{A_1}{Z^2 - A_2} + \frac{A_3}{Z^2 - A_4} + \frac{A_5}{Z^2 - A_6} \right). \quad (4.4-8)$$

$$A_1 = 0.4613135$$

$$A_2 = 0.1901635$$

$$A_3 = 0.9999216$$

$$A_4 = 1.7844927$$

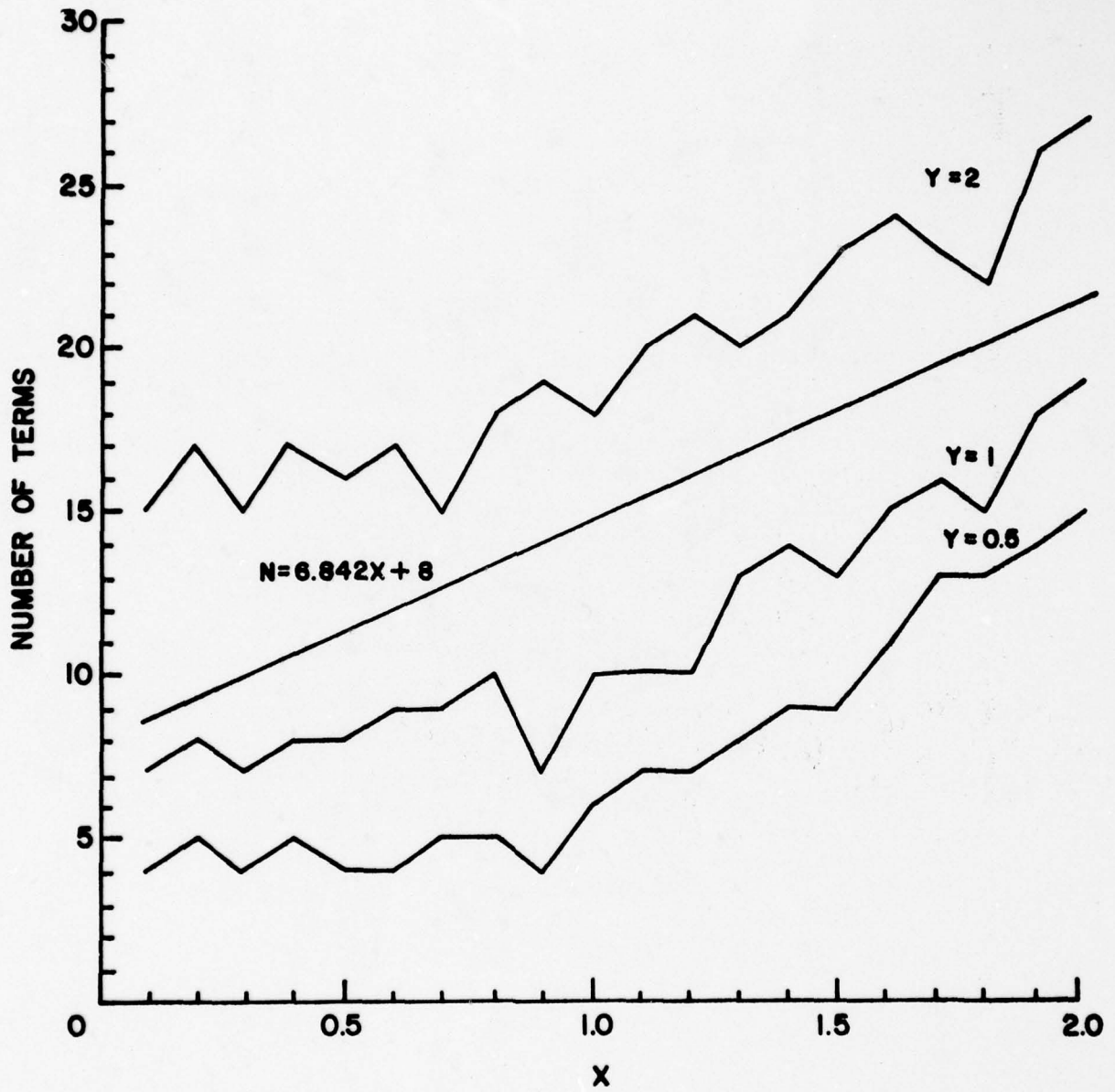


Figure 4.4-2. Number of series terms required for convergence.

$$A_5 = 0.002883894$$

$$A_6 = 5.5253437$$

Only the real part of equation 4.4-8 is required, so the relation is separated into real and imaginary parts.

$$w(Z) = iZ \left\{ \frac{A_1}{(x^2 - y^2 - A_2) + i2xy} + \frac{A_3}{(x^2 - y^2 - A_4) + i2xy} + \frac{A_5}{(x^2 - y^2 - A_6) + i2xy} \right\}$$

$$= iZ \left\{ \frac{A_1(x^2 - y^2 - A_2) - i2A_1xy}{(x^2 - y^2 - A_2)^2 + (2xy)^2} + \frac{A_3(x^2 - y^2 - A_4) - i2A_3xy}{(x^2 - y^2 - A_4)^2 + (2xy)^2} + \right.$$

$$\left. \frac{A_5(x^2 - y^2 - A_6) - i2A_5xy}{(x^2 - y^2 - A_6)^2 + (2xy)^2} \right\}$$

$$= iZ \left\{ \frac{A_1(x^2 - y^2 - A_2)}{(x^2 - y^2 - A_2)^2 + (2xy)^2} + \frac{A_3(x^2 - y^2 - A_4)}{(x^2 - y^2 - A_4)^2 + (2xy)^2} + \frac{A_5(x^2 - y^2 - A_6)}{(x^2 - y^2 - A_6)^2 + (2xy)^2} \right\}$$

R

$$-i \left(\frac{2A_1xy}{(x^2 - y^2 - A_2)^2 + (2xy)^2} + \frac{2A_3xy}{(x^2 - y^2 - A_4)^2 + (2xy)^2} + \frac{2A_5xy}{(x^2 - y^2 - A_6)^2 + (2xy)^2} \right)$$

I

$$= iZ(R - iI)$$

$$= (-y + ix)(R - iI)$$

The real part of this relation is

$$R\{w(Z)\} = -yR + xI.$$

In terms of the constants and x and y

$$R\{w(Z)\} = A_1 \frac{2x^2y - (x^2 - y^2 - A_2)y}{(x^2 - y^2 - A_2)^2 + (2xy)^2} + A_3 \frac{2x^2y - (x^2 - y^2 - A_4)y}{(x^2 - y^2 - A_4)^2 + (2xy)^2} + A_5 \frac{2x^2y - (x^2 - y^2 - A_6)y}{(x^2 - y^2 - A_6)^2 + (2xy)^2}. \quad (4.4-9)$$

Equation 4.4-9 is the expression used in Region II. It is accurate to about two parts in 10^4 for any (x,y) in the region.

For Region III a two point Gauss-Laguerre quadrature formula gives

$$w(Z) = iZ \left(\frac{B_1}{Z^2 - B_2} + \frac{B_3}{Z^2 - B_4} \right) \quad (4.4-10)$$

$$B_1 = 0.5124242$$

$$B_2 = 0.2752551$$

$$B_3 = 0.05176536$$

$$B_4 = 2.724745$$

Following the same procedure as before, the real portion of the function can be ascertained as

$$R\{w(Z)\} = B_1 \frac{2x^2y - (x^2 - y^2 - B_2)y}{(x^2 - y^2 - B_2)^2 + (2xy)^2} + B_3 \frac{2x^2y - (x^2 - y^2 - B_4)y}{(x^2 - y^2 - B_4)^2 + (2xy)^2}. \quad (4.4-11)$$

This expression is accurate to about one part in 10^4 for (x,y) in Region III. The FORTRAN IV program implementing Eqs. 4.4-4, 4.4-9, and 4.4-11 is listed in Appendix C.

4.5 Comparison of Voigt Algorithms

In order to select one of the previous methods for evaluation of the Voigt function it was necessary to design computer programs to verify the accuracy of each method and establish some relative times for execution. Additionally the ease of implementation and program size of each method had to be considered.

It was assumed that any time savings in the computation of the parameters x and y would be as beneficial to one method as another. Therefore the execution time of a method is defined to be the time that expires from the issuance of a call statement to the return of a value by the subroutine. Compilation time of the program was not included nor was any input or output. Timing of the routines became a problem and several methods of time determination were tried. In the end it was decided to use the execution time returned by the operating system of the computer. That should account for all the time that a program has control of the central processing unit (CPU) and is probably as accurate as any timing routine.

Accuracy determinations were somewhat simpler. Faddeyeva and Terentév¹² have tabulated values for $\bar{w}(Z)$ when $0 < x < 5$ and $0 < y < 5$ to six decimal figures. For regions outside of that range Drayson's¹¹ method was used to set the true value of $w(Z)$. It was assumed that since his work had been published it would be as accurate as he claimed.

All programs were processed by an IBM 360/65 computer.

4.5.1 Accuracy Tests

Three separate tests were conducted to determine the accuracy of each method. As an initial screening Kielkopf's method and the method proposed here were pitted against Drayson's method. A synopsis of the results are shown in Table 4.5-1.

This first test was conducted using double precision operations to increase accuracy in all measurements. The table does not show all the digits used, which is why entries such as the one for $x = 0.5$, $y = 4.0$ appear to have no error when actually there is a slight difference. As the table indicates, Kielkopf's method has accuracy errors that are relatively large. Examination of his values with true, tabulated values [Faddeyeva and Terentév¹²] revealed unacceptable margins of error. Thus the same conclusion drawn by Drayson in his search for an accurate Voigt Algorithm was reached. Kielkopf's method is not accurate enough for atmospheric work [Drayson¹¹].

The second test was designed to verify the accuracy of both the proposed method and Drayson's method. The regions used by the proposed method were selected, one at a time, and one hundred values of the function were computed by each method. The computed values were compared to those tabulated by Faddeyeva and Terentév¹² for $0 < x < 5$, $0 < y < 5$. In Region III, where $x > 5$, $y > 5$ the values returned by the two methods were compared with each other, since no tabulated values were available.

Figure 4.5-1 depicts the regions used by the proposed method.

x	y	True Value (Drayson's)	Kielkopf's Value	Proposed Value	Percent Relative Error	
					Kielkopf	Proposed
0.1	1.0	.426050	.426182	.426042	$3.09 \cdot 10^{-4}$	$1.84 \cdot 10^{-3}$
0.3	1.0	.413984	.415461	.413989	$3.56 \cdot 10^{-3}$	$1.21 \cdot 10^{-3}$
0.5	1.0	.391218	.394833	.391236	$9.24 \cdot 10^{-3}$	$4.71 \cdot 10^{-3}$
0.1	2.0	.254974	.254805	.254970	$6.62 \cdot 10^{-4}$	$1.56 \cdot 10^{-5}$
0.3	2.0	.251677	.244411	.251692	$2.88 \cdot 10^{-2}$	$5.96 \cdot 10^{-5}$
0.5	2.0	.245279	.224884	.245226	$8.31 \cdot 10^{-2}$	$2.16 \cdot 10^{-4}$
0.1	3.0	.178842	.180084	.178841	$6.94 \cdot 10^{-3}$	$4.11 \cdot 10^{-4}$
0.3	3.0	.177581	.171631	.177581	$3.35 \cdot 10^{-2}$	$2.78 \cdot 10^{-4}$
0.5	3.0	.175105	.155897	.175105	$1.09 \cdot 10^{-1}$	$2.56 \cdot 10^{-5}$
0.1	4.0	.136923	.139572	.136924	$1.93 \cdot 10^{-2}$	$1.28 \cdot 10^{-3}$
0.3	4.0	.136329	.132635	.136330	$2.70 \cdot 10^{-2}$	$1.05 \cdot 10^{-3}$
0.5	4.0	.135155	.119779	.135155	$1.13 \cdot 10^{-1}$	$6.60 \cdot 10^{-4}$
0.1	5.0	.110663	.114381	.110664	$3.35 \cdot 10^{-2}$	$2.78 \cdot 10^{-4}$
0.3	5.0	.110341	.108533	.110342	$1.63 \cdot 10^{-2}$	$2.20 \cdot 10^{-4}$
0.5	5.0	.109702	.092719	.109703	$1.55 \cdot 10^{-1}$	$1.75 \cdot 10^{-4}$

Table 4.5-1. Initial accuracy tests. Drayson's values used as true. (Not all digits shown in value columns.)

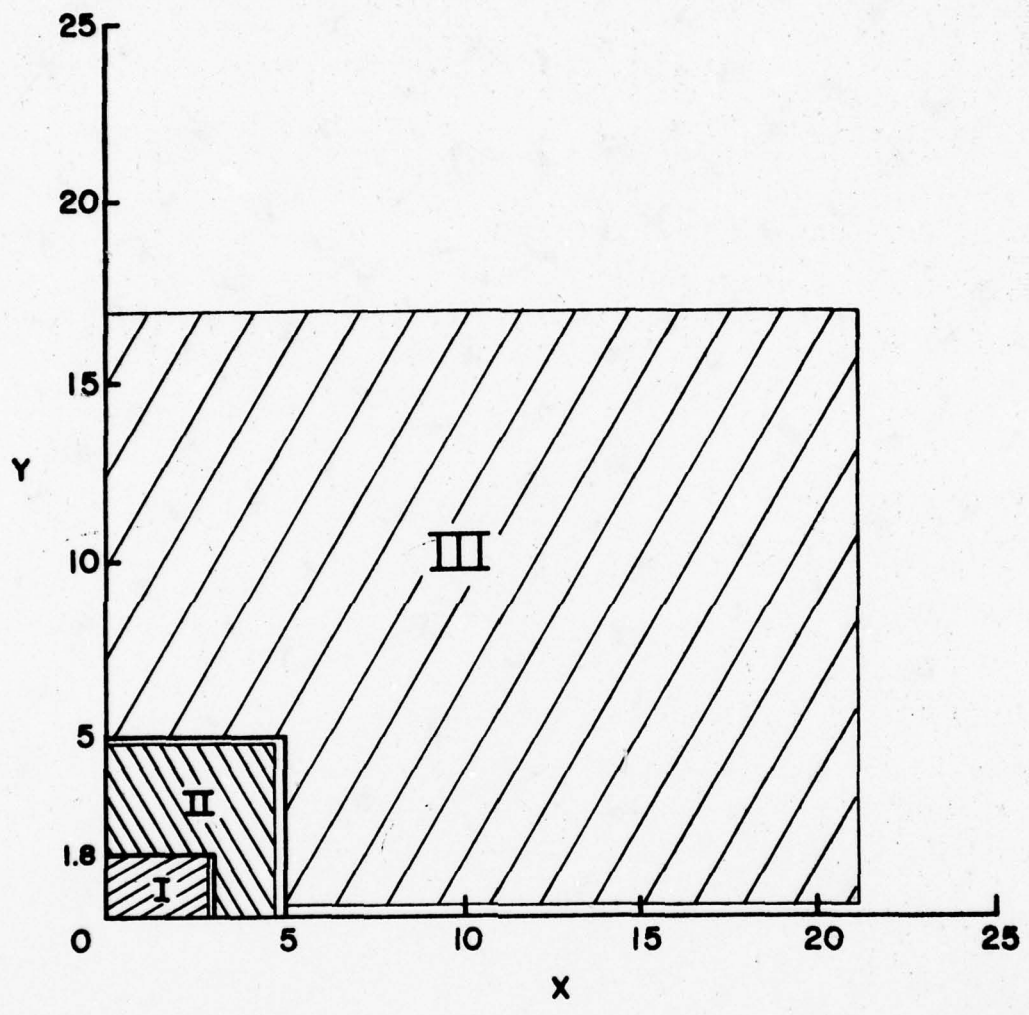


Figure 4.5-1. Coverage of proposed regions by accuracy test two.

The shaded areas are the range of the points used for comparison.
The points were selected to include as much of the area of each region
as possible. In Region I

$y = 0$ to 1.8 in increments of 0.2,

$x = 0$ to 2.7 in increments of 0.3.

In Region II

$y = 2$

$y = 2.5$ to 4.6 in increments of 0.3,

$x = 0$ to 4.5 in increments of 0.5,

and $y = 0$ to 3.5 in increments of 0.5,

$x = 3$ to 4.6 in increments of 0.4.

In Region III

$y = 5$ to 17 in increments of 3.0,

$x = 2$ to 11 in increments of 1.0,

and $y = 0.5$ to 5 in increments of 0.5,

$x = 5$ to 21 in increments of 4.0.

The results of this test are summarized in Table 4.5-2. The peak deviation in Region I for the proposed method is larger than the peak for Drayson, but the actual error for that single point was only three parts in 10^4 . The root mean square error was well within acceptable limits.

For Region II the peak deviations were nearly the same, while the root mean square error for the proposed method was better than Dray-

Region	Drayson's Method		Proposed Method	
	Peak Deviation	RMS Deviation	Peak Deviation	RMS Deviation
I	$1.72504 \cdot 10^{-5}$	$4.29676 \cdot 10^{-7}$	$3.89991 \cdot 10^{-4}$	$4.07495 \cdot 10^{-6}$
II	$1.41329 \cdot 10^{-3}$	$1.41402 \cdot 10^{-4}$	$1.41342 \cdot 10^{-3}$	$1.42011 \cdot 10^{-5}$
III	$*3.41969 \cdot 10^{-6}$	$*6.03836 \cdot 10^{-8}$	$*3.41969 \cdot 10^{-6}$	$*6.03836 \cdot 10^{-8}$

*Deviation of one method from another.

Table 4.5-2. Results of accuracy test two.

son's. In Region III the deviation of one method from the other is small, reflecting the two different quadrature techniques used.

The final accuracy test used the regions suggested by Drayson, one at a time. Figure 4.5-2 depicts the coverage of each area. Rather than using tabulated values, the results obtained with Drayson's method were compared to those obtained using the proposed method. Table 4.5-3 summarizes the results of the test.

It is clearly seen from Table 4.5-2 and Table 4.5-3 that the proposed method yields values of the Voigt profile that are accurate enough for atmospheric work. Root-mean-square errors indicate accuracies that normally exceed tabulated values of the profile.

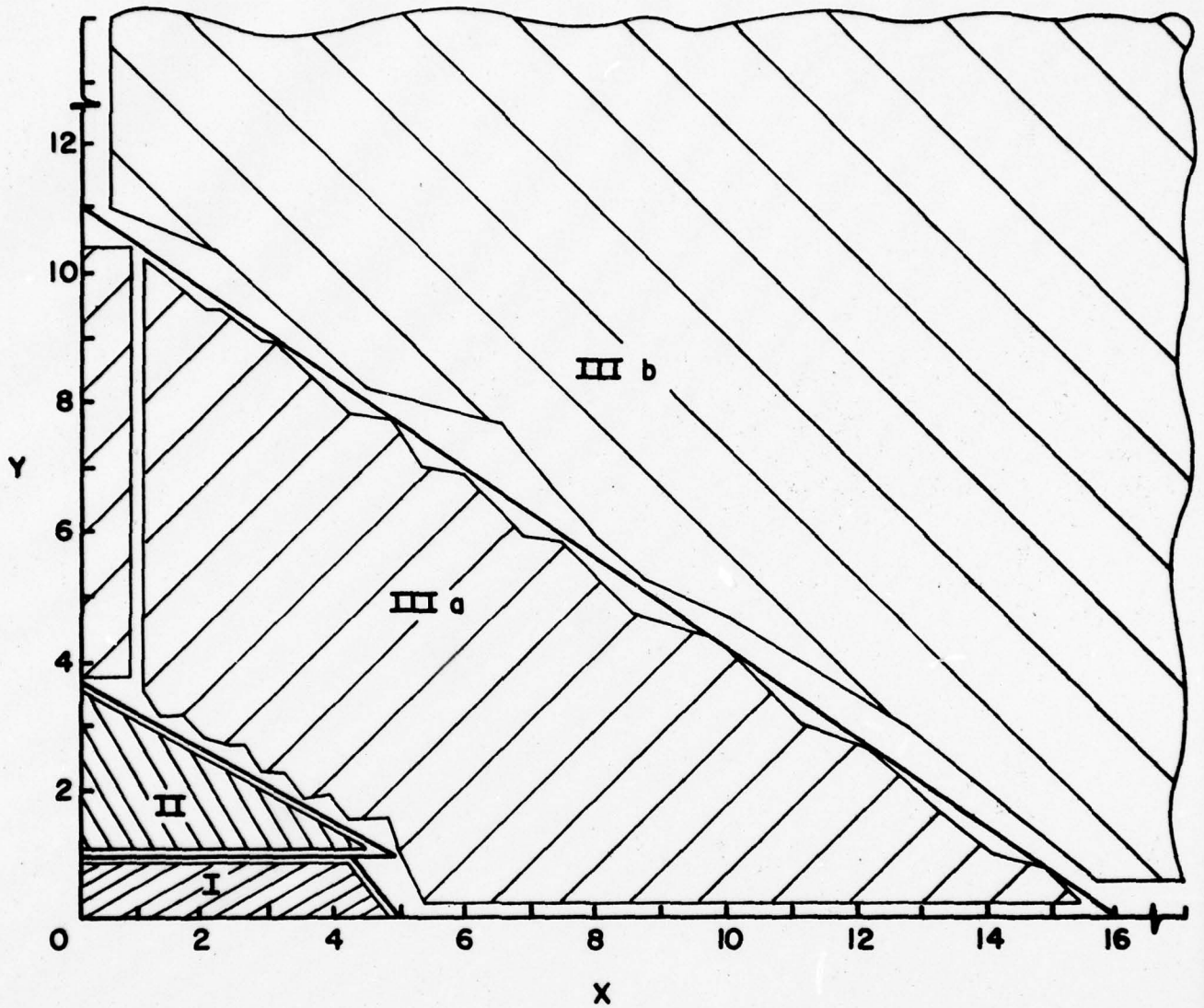


Figure 4.5-2. Coverage of Drayson's regions for accuracy test three.

Region	Peak Deviation	RMS Deviation	Number Points Used
I	$5.27915 \cdot 10^{-5}$	$2.46145 \cdot 10^{-7}$	452
II	$3.44067 \cdot 10^{-3}$	$1.34552 \cdot 10^{-5}$	283
IIIa	$6.92595 \cdot 10^{-6}$	$2.06357 \cdot 10^{-8}$	744
IIIb	$3.41969 \cdot 10^{-6}$	$1.99151 \cdot 10^{-8}$	420

Table 4.5-3. Deviations of Proposed method from Drayson's method using Drayson's regions.

4.5.2 Execution Time Tests

Four tests were conducted utilizing Drayson's method and the proposed method in an effort to determine which algorithm would save the most computer execution time. For each of the tests a small main routine was written that fixed the values of x and y and then called the routine being tested. The master program of some tests performed input/output or accuracy measurements. The other main routines performed no extraneous operations. The tests involved merely replacing that portion of the program implementing Drayson's method with the proposed method and resubmitting the job for execution.

The first test used the regions of the proposed method, selecting points from one region at a time. This is a slightly biased test since the proposed algorithm remained in one region while Drayson's algorithm jumped from region to region, depending on the value of the parameters. However Drayson contended that his method was the most rapid available, and placed no stipulations on how parameters were selected. The main routine for this test performed input and output as well as accuracy measurements for both methods. Therefore, the times were somewhat over true execution time, but reflected the relative speed of each method. Table 4.5-4 lists the results of this test. The method proposed in this work reduced the time to approximate the Voigt profile by an average of 26.6%.

A second test was conducted using the regions proposed by Drayson, selecting points from one region at a time. This has the same bias as the first test except that it is in Drayson's favor this time.

Region	Drayson's Method		Proposed Method	
	CPU Seconds	%	CPU Seconds	%
I	4.05	100	2.92	72.09
II	4.14	100	3.00	72.46
III	3.87	100	2.92	75.45

Table 4.5-4. Results of time tests conducted using regions and points indicated in Fig. 4.5-1.

One hundred points were selected from each region. The results of the test are shown in Table 4.5-5. The main routine for this test performed output operations as well as calling the method being tested. The method proposed by this work reduced the time to approximate the Voigt profile by an average of 27.5%.

An offshoot of the accuracy test conducted using the regions and points shown in Fig. 4.5-2 was that the times for execution were available. This comprised the third speed test. The main routine in this case performed output and deviation analysis in addition to calling the Voigt algorithm. Again the times were somewhat in excess of true execution time, but still reflected the relative speed of each method. Table 4.5-6 summarizes this test. The proposed method reduced the time to evaluate the Voigt profile by an average of 29.5%.

A final test was conducted that did not use regions. Ten-thousand points were selected as follows

$$y = 0 \text{ to } 19.8 \text{ in increments of } 0.2,$$
$$x = 0 \text{ to } 24.75 \text{ in increments of } 0.25.$$

The master routine performed no input or output and no other calculations. This was strictly comparing the time for Drayson's method and the proposed method to evaluate ten-thousand points. The results are enumerated in Table 4.5-7.

4.5.3 The Selected Voigt Algorithm

In view of the results of the time tests conducted the selection was not difficult. Both methods yield the accuracy necessary for good

AD-A052 685

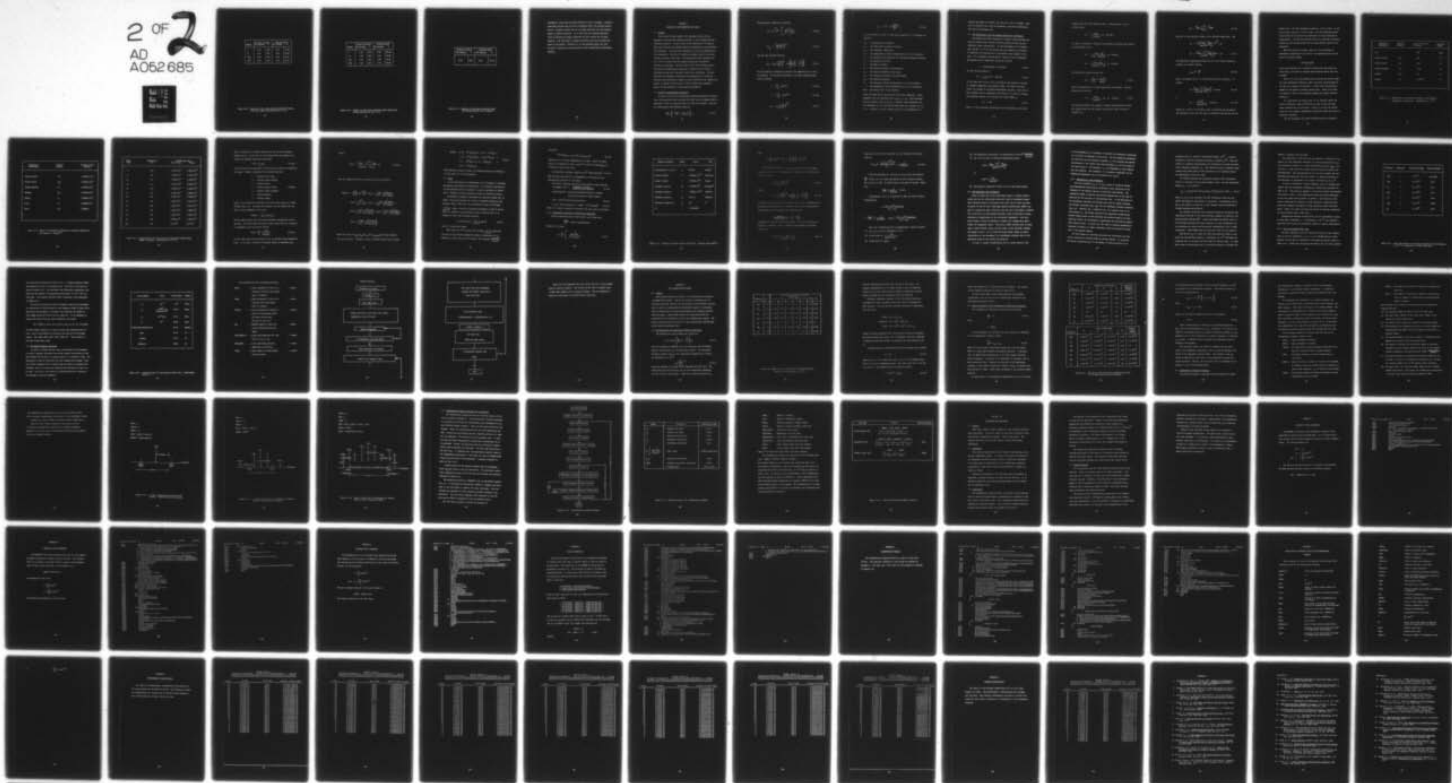
TEXAS UNIV AT EL PASO DEPT OF ELECTRICAL ENGINEERING
A COMPUTATIONAL METHOD FOR SPECTRAL MOLECULAR ABSORPTION USING --ETC(U)
MAY 77 P C VAN DERWOOD

F/G 4/1

UNCLASSIFIED

NL

2 OF 2
AD
A052 685



END
DATE
FILMED
5-78

DDC

Region	Drayson's Method		Proposed Method	
	CPU Seconds	%	CPU Seconds	%
I	3.30	100	2.37	71.81
II	3.22	100	2.52	78.26
IIIa	3.90	100	2.52	64.61
IIIb	3.59	100	2.70	75.21

Table 4.5-5. Results of time tests conducted using 100 points from each region indicated in Fig. 4.2-1.

Region	Drayson's Method		Proposed Method	
	CPU Seconds	%	CPU Seconds	%
I	3.45	100	2.29	66.38
II	3.12	100	2.49	79.80
IIIa	3.72	100	2.69	72.31
IIIb	3.69	100	2.42	65.58

Table 4.5-6. Results of time tests conducted using regions and points indicated in Fig. 4.5-2.

Drayson's Method		Proposed Method	
CPU Seconds	%	CPU Seconds	%
3.15	100	2.25	71.42

Table 4.5-7. Results of time tests conducted using ten-thousand points and no regions.

atmospheric calculation and both methods are easy to program. Drayson's algorithm contains some 64 source statements while the proposed method has 40. Drayson's method was run in single precision and the proposed method in double precision. It is felt that the proposed algorithm could be executed in single precision and still retain the accuracy required. The conversion to single precision would only increase the speed of the method. Therefore it is the proposed method that will be used to evaluate the Voigt profile in the transmittance differential equation.

CHAPTER V

ABSORPTION LINE PARAMETERS AND UNITS

5.1 Preface

This chapter brings together the remaining topics that are necessary to develop the computer solution to the transmittance differential equation. A brief review of the equations to be used is given and the known and unknown quantities appearing in the relations are identified. The input data necessary to solve the equations are also identified. The value of physical constants used in the calculations is given at this time. The mixing ratio $M(P)$ introduced in Eq. 3.2-11 is derived and the combined extinction coefficient relation is developed. Then the units of all the relations used in this work are dimensionally analyzed to assure they are correct. Additionally some unit conversion factors are introduced. The data available as atmospheric absorption line parameters are presented together with some general remarks on their derivation and compilation. Finally a computer routine that is used to handle the tremendous amount of data available is developed and explained.

5.2 Review of Transmittance Equations

In order to solve the transmittance equation developed in chapter three the quantities that are known and those that are unknown must be specified. First all equations that are used are restated. They are the transmittance differential equation,

$$\frac{d\tau}{dP} = \left\{ -\frac{\sec \theta}{g} \sum_j K_j M_j(P) \right\} \tau. \quad (5.2-1)$$

The absorption coefficient relations,

$$K_j = \sum_i \frac{K_{oij}}{\pi} \int_{-\infty}^{\infty} \frac{y e^{-t^2} dt}{y^2 + (x-t)^2}, \quad (5.2-2)$$

$$K_{oij} = \frac{S_{ij}}{\alpha_D} \left(\frac{\ln 2}{\pi} \right)^{1/2}, \quad (5.2-3)$$

and the line strength function

$$S_{ij} = S_{oij} Q_j \left(\frac{T_o}{T} \right)^{c_j} \exp \left\{ \frac{E_{ij}}{kT_o} \left(1 - \frac{T_o}{T} \right) \right\}. \quad (5.2-4)$$

For the purpose of dimensional analysis the summations over i and j are dropped. The variables appearing in the above equations must also be defined,

$$y = \frac{\alpha_L}{\alpha_D} (\ln 2)^{1/2}, \quad (5.2-5)$$

$$x = \frac{v-v_o}{\alpha_D} (\ln 2)^{1/2}, \quad (5.2-6)$$

$$\alpha_L = \alpha_o \frac{P}{P_o} \left(\frac{T_o}{T} \right)^{1/2}, \quad (5.2-7)$$

$$\alpha_D = 3.58 \cdot 10^{-7} \left(\frac{T}{M}\right)^{1/2} \nu_0 \cdot \quad (5.2-8)$$

It is seen that in order to solve these equations it is necessary to specify:

- S_0 ... a reference line strength,
- Q ... the vibrational partition function,
- T_0 ... the reference temperature,
- T ... the temperature at which transmittance is to be calculated,
- c ... the exponent that expresses the rotational partition function,
- E ... the energy of the line,
- k ... Boltzman's constant,
- M ... The molecular weight of the absorber,
- ν_0 ... the center wavenumber of the line,
- α_0 ... the reference Lorentzian line half-width,
- P_0 ... the reference pressure,
- P ... the pressure at which transmittance is to be calculated,
- ν ... the wavenumber at which transmittance is to be calculated,
- $M(P)$. the mixing ratio of the absorber.

These variables may be grouped into four broad categories. Those dependent upon the absorbing line (S_0 , E , ν_0 , α_0), those dependent upon the absorber type or gas (Q , c , M , $M(P)$), those dependent upon the atmosphere (T , P), and finally those that are constant (T_0 , P_0 , k , ν). Actually ν is not constant since if the transmittance at

another wavenumber is desired, the value of ν must be changed. Data must be obtained then, from the atmosphere, from the absorbing gas, and from the absorbing line.

5.3 The Mixing Ratio and The Combined Extinction Coefficient

The mixing ratio $M(P)$ introduced in chapter three expresses the relation between total pressure and the pressure of only one gas (absorber) under consideration. In the development of the Lambert Beer law (Eq. 3.2-7) it was stated that the reduction in intensity of radiation was proportional to the amount of gas present in the path. If u represents the gas amount, then du is the incremental gas amount and the Lambert-Beer Law may be written

$$\tau = \exp(-K\rho(x)dx) = \exp(-Kdu). \quad (5.3-1)$$

So that the gas amount is

$$du = \rho_{\text{gas}}(x) dx. \quad (\text{gm/cm}^2) \quad (5.3-2)$$

If the right side of Eq. 5.3-2 is divided by the density of the gas at standard temperature and pressure (STP), the units of the gas amount are changed to centimeter-atmospheres (cm-atm). This unit is more commonly used in atmospheric work since it is easier to compute the equivalent amount of an absorber in a path length as

$$\Delta L = cRP \quad (5.3-3)$$

where c is the fractional concentration of the absorber, R the path

length (cm), and P the pressure (atm). Converting Eq. 5.3-2 to cm-atm yields

$$du = \frac{\rho_{\text{gas}}}{\rho_{\text{gas(STP)}}} dx \quad (\text{cm-atm}).$$

In order to introduce a mixing ratio multiply and divide the relation by the density of air.

$$du = \frac{\rho_{\text{air}} \rho_{\text{gas}}}{\rho_{\text{air}} \rho_{\text{gas(STP)}}} dx \quad (\text{cm-atm})$$

$$du = \frac{\rho_{\text{air}} \rho_{\text{gas}}}{\rho_{\text{gas(STP)}} \rho_{\text{air}}} dx \quad (\text{cm-atm})$$

Now define the density mixing ratio

$$M_d = \frac{\rho_{\text{gas}}}{\rho_{\text{air}}} \frac{d \text{ gm/cm}^3}{\text{gm/cm}^3}, \quad (5.3-4)$$

where the densities are at some temperature and pressure. Now gas amount may be written

$$du = \frac{\rho_{\text{air}}}{\rho_{\text{gas(STP)}}} M_d dx. \quad (\text{cm-atm}) \quad (5.3-5)$$

The relation between the volumetric mixing ratio measured in parts per million (ppm) and the density mixing ratio (M_d) is given by [Weast⁴⁹] as

$$M_d = \frac{M_{\text{ppm}} \cdot 10^{-6} \cdot M_{\text{t gas}}}{M_{\text{t air}}} , \quad (5.3-6)$$

where M_t is the molecular weight of air and gas respectively. Now

$$du = \frac{\rho_{\text{air}} M_{\text{ppm}} \cdot M_{\text{t gas}} \cdot 10^{-6}}{\rho_{\text{gas(STP)}} M_{\text{t air}}} dx$$

$$du = \frac{M_{\text{ppm}} \cdot 10^{-6} M_{\text{t gas}} \rho_{\text{air}}}{\rho_{\text{gas(STP)}} M_{\text{t air}}} dx. \quad (5.3-7)$$

The hydrostatic approximation given by Eq. 2.2-1 relates density to pressure in a manner desired,

$$\rho_{\text{air}} dx = \frac{dP}{g} , \quad (5.3-8)$$

Here P is pressure and g is the acceleration due to gravity. So finally

$$du = \frac{M_{\text{ppm}} \cdot 10^{-6} M_{\text{t gas}} dP}{\rho_{\text{gas(STP)}} M_{\text{t air}} g} \quad (\text{cm-atm}) \quad (5.3-9)$$

or

$$du = \frac{M_d dP}{\rho_{\text{gas(STP)}} g} \quad (\text{cm-atm}). \quad (5.3-10)$$

Either Eq. 5.3-9 or 5.3-10 may be used to calculate the gas amount. The selection of one over the other is dependent upon the gas and the

mixing ratio. For most atmospheric gases Eq. 5.3-9 is used. In the case of water vapor Eq. 5.3-10 is used. The calculated gas amount is multiplied by the extinction coefficient in the calculation of transmittance. As might be expected there is a different extinction coefficient (K) and gas amount (du) for each absorber (gas) in the atmosphere.

When more than one absorber (gas) is to be considered in atmospheric transmittance the index of the exponential must be the sum of all optical depths.

$$\tau = \exp\left(-\sum_j K_j M_j dP\right).$$

Since every absorber has a different mixing ratio and extinction coefficient, each must be computed and multiplied before they can be added.

Table 5.3-1 lists the mixing ratios in parts per million (ppm) for those atmospheric absorbers whose fractional concentrations do not vary as a function of altitude. It also lists the molecular weights of the gases of constant mixing ratio. Table 5.3-2 gives the density at STP of the atmospheric gases that absorb infrared radiation.

For cases where the mixing ratio is not constant (water and ozone) a different value of M(P) must be used at each altitude where Transmittance is calculated. Table 5.3-3 lists the mixing ratios for the variable atmospheric constituents water and ozone at different altitudes.

For the atmosphere only seven absorbers need be considered.

Atmospheric Constituent	Chemical Formula	Parts per Million by Volume	Molecular Weight
Air		10^6	28.97
Carbon Dioxide	CO ₂	330	44
Nitrous Oxide	N ₂ O	0.28	44
Carbon Monoxide	CO	0.075	28
Methane	CH ₄	1.6	16
Oxygen	O ₂	$2.095 \cdot 10^5$	32

Table 5.3-1. Mixing Ratios and Molecular Weights of Non-Varying Atmospheric Constituents. [McClatchey, et al.³¹]

Atmospheric Constituent	Chemical Formula	Density at STP (gm/cm ³)
Carbon Dioxide	CO ₂	1.9768441 · 10 ⁻³
Nitrous Oxide	N ₂ O	1.9781371 · 10 ⁻³
Carbon Monoxide	CO	1.2510101 · 10 ⁻³
Methane	CH ₄	7.1678376 · 10 ⁻⁴
Oxygen	O ₂	1.4286545 · 10 ⁻³
Ozone	O ₃	2.1436282 · 10 ⁻³
Water	H ₂ O	1.0000010

Table 5.3-2 Density of Atmospheric Absorbers at Standard Temperature and Pressure. [Nelson³⁶]

Height (Km)	Temperature (°K)	Mixing Ratio (M_d)	
		Water Vapor	Ozone
0	294	$1.1754 \cdot 10^{-2}$	$5.0378 \cdot 10^{-8}$
5	267	$1.3867 \cdot 10^{-3}$	$9.1527 \cdot 10^{-8}$
10	235	$1.5388 \cdot 10^{-4}$	$2.1639 \cdot 10^{-7}$
15	216	$3.6122 \cdot 10^{-6}$	$9.0304 \cdot 10^{-7}$
20	218	$4.7604 \cdot 10^{-6}$	$3.5967 \cdot 10^{-6}$
25	224	$1.5625 \cdot 10^{-5}$	$6.9962 \cdot 10^{-6}$
30	234	$2.7231 \cdot 10^{-5}$	$1.5128 \cdot 10^{-5}$
35	245	$1.6873 \cdot 10^{-5}$	$1.4112 \cdot 10^{-5}$
40	258	$1.2913 \cdot 10^{-5}$	$1.2312 \cdot 10^{-5}$
45	270	$1.0814 \cdot 10^{-5}$	$7.3989 \cdot 10^{-6}$
50	276	$6.6232 \cdot 10^{-6}$	$4.5204 \cdot 10^{-6}$
70	218	$2.0876 \cdot 10^{-6}$	$1.2824 \cdot 10^{-6}$
100	210	$2.0 \cdot 10^{-6}$	$8.6 \cdot 10^{-8}$

Table 5.3-3. Mixing Ratios for Water Vapor and Ozone from A Midlatitude Summer Atmosphere. [McClatchey, et al.³²]

Five of these have a constant mixing ratio and two have variable mixing ratios. In any case we are concerned with the product $K du$. Define the combined extinction coefficient

$$ABSK = \sum_j K_j du_j \quad (5.3-11)$$

Let the value of the subscript j vary from one to seven to account for all gases. Further, establish the following relations

- 1 ... denotes water vapor,
- 2 ... denotes carbon dioxide,
- 3 ... denotes ozone,
- 4 ... denotes nitrous oxide, (5.3-12)
- 5 ... denotes carbon monoxide,
- 6 ... denotes methane,
- 7 ... denotes oxygen.

$K_1 du_1$ is the extinction coefficient for water vapor, $K_2 du_2$ for carbon dioxide, and so on. Defining the variable L as the counter for the level of the atmosphere we can write

$$ABSK(L) = \sum_{j=1}^7 K_j(L) du_j(L)$$

The gas amount $du_j(L)$ will have seven different expressions; one for each gas. For water vapor and ozone the gas amount will be a function of atmospheric level and can be written

$$du(L) = \frac{dP}{g} \frac{M_d(L)}{\rho_{\text{gas}}(\text{STP})} \quad (5.3-13)$$

For the other gases the gas amount is not so dependent upon atmospheric level. It is only a function of pressure (which is dependent upon

level),

$$du(L) = \frac{M_{\text{ppm}} \cdot 10^{-6} \text{ Mt}_{\text{gas}}}{\rho_{\text{gas(STP)}} \text{ Mt}_{\text{air}} \text{ g}} dP. \quad (5.3-14)$$

Thus the combined extinction coefficient can be written as

$$\begin{aligned} \text{ABSK(L)} = \frac{dP}{g} & \left\{ K_1(L) \frac{M_d(L)}{1.0} + K_2(L) \frac{(330 \cdot 10^{-6})(44)}{(1.97 \cdot 10^{-3})(28.97)} \right. \\ & K_3(L) \frac{M_d(L)}{2.14 \cdot 10^{-3}} + K_4(L) \frac{(.28 \cdot 10^{-6})(44)}{(1.97 \cdot 10^{-3})(28.97)} + \\ & K_5(L) \frac{(.075 \cdot 10^{-6})(28)}{(1.25 \cdot 10^{-3})(28.97)} + K_6(L) \frac{(1.6 \cdot 10^{-6})(16)}{(7.16 \cdot 10^{-4})(28.97)} + \\ & \left. K_7(L) \frac{(2.095 \cdot 10^{-1})(32)}{(1.42 \cdot 10^{-3})(28.97)} \right\}, \end{aligned}$$

where the value of M_{ppm} , Mt_{gas} , Mt_{air} and $P_{\text{gas(STP)}}$ have been inserted into the equations. Assuming a value of 980.665 cm/sec^2 for g yields

$$\begin{aligned}
\text{ABSK(L)} = & \{1.02 \cdot 10^{-3} K_1(L) M_d(L) + 2.59 \cdot 10^{-4} K_2(L) + \\
& 4.76 \cdot 10^{-1} K_3(L) M_d(L) + 2.19 \cdot 10^{-7} K_4(L) + \\
& 5.9 \cdot 10^{-8} K_5(L) + 1.25 \cdot 10^{-6} K_6(L) + \\
& 1.65 \cdot 10^{-1} K_7(L)\} dp
\end{aligned}
\tag{5.3-15}$$

This relation is used to obtain the combined extinction coefficient at each level (L) of the atmosphere.

5.4 Units

In the calculation of transmittance it is necessary to determine gas amounts and extinction coefficients. For different applications or when different data is available, it may be necessary to convert units. Therefore a brief treatise is given on conversion factors.

According to Avogadro's hypothesis the molecular weight (M), in grams, of any gas occupies 22.4 liters at standard temperature and pressure (STP). Hence one cubic centimeter of gas at STP weighs

$\frac{M}{2.24 \cdot 10^4}$ grams. Since one centimeter-atmosphere at STP is equivalent to a length of one centimeter of gas at STP per cm^2 , it is possible to write the following relation

$$1 \text{ cm-atm of gas} = \frac{M}{2.24 \cdot 10^4} \text{ gm-cm}^2, \tag{5.4-1}$$

where M is molecular weight.

Also since one cm^3 of gas at STP contains $\frac{1}{2.24 \cdot 10^4}$ moles and one mole of gas contains Avogadro's number of molecules, it is possible to write that one cm^3 of gas at STP contains $\frac{6.02 \cdot 10^{23}}{2.24 \cdot 10^4}$

molecules,

$$1(\text{cm-atm})_{\text{STP}} = 2.69 \cdot 10^{19} \text{ molecules/cm}^2 \quad (5.4-2)$$

Equation 5.4-1 is valid independent of the gas. Since for water vapor it is possible to write 1 gm-cm^2 in terms of $(\text{cm-atm})_{\text{STP}}$ it is shown for water vapor that

$$1 \text{ precipitable centimeter (H}_2\text{O)} = 3.34 \cdot 10^{22} \text{ (molecules/cm}^2\text{)} \quad (5.4-3)$$

Thus the unit molecule/cm² is independent of the nature of the absorbing gas and basic to all gases.

Some other relations that have proven useful in this work are:

$$\text{wavenumber (cm}^{-1}\text{)} = \frac{\text{frequency (1/sec)}}{\text{speed of light (cm/sec)}} \quad (5.4-4)$$

$$\begin{aligned} \text{energy(joules)} &= \text{energy (wavenumbers)} \cdot \text{Planck's constant} \\ &(\text{joules-sec}) \cdot \text{speed of light (cm/sec)} \end{aligned}$$

$$E(j) = [E(\text{cm}^{-1})][h(j\text{-sec})][c(\text{cm/sec})] \quad (5.4-5)$$

$$1 \text{ atm} = 1013.25 \text{ milibars} = 1.01325 \cdot 10^5 \text{ newtons/m}^2 \quad (5.4-6)$$

Table 5.4-1 lists the physical constants that were used in this work.

5.4.1 Dimensional Analysis of Transmittance Equations

From the equations used in this work it can be seen that

$$\frac{\text{KMdP}}{g} \text{ must be dimensionless.}$$

Equation 5.2-2 gives

$$K = \frac{K_0}{\pi} \int_{-\infty}^{\infty} \frac{ye^{-t^2} dt}{y^2 + (x-t)^2}, \quad (5.4-7)$$

Physical Constant	Symbol	Value	Unit
Acceleration of gravity	g	980.665	cm/sec ²
Planck constant	h	$6.626196 \cdot 10^{-34}$	Joule-sec
Speed of light	c	$2.997925 \cdot 10^{10}$	cm/sec
Avogadro constant	N _A	$6.022169 \cdot 10^{23}$	molecule ⁻¹
Boltzman constant	k	$1.380622 \cdot 10^{-23}$	Joule/°K
Reference Pressure	P ₀	1013.25	millibars
Reference Temperature	T ₀	296	°K
Pi	π	3.141592654	

Table 5.4-1. Physical constants used in this work. (Adapted from Weast⁴⁹).

with

$$y = \frac{\alpha_L}{\alpha_D} (\ln 2)^{1/2} \quad \text{and} \quad x = \left(\frac{\nu - \nu_0}{\alpha_D} \right) (\ln 2)^{1/2} .$$

Provided that $\alpha_L, \alpha_D, \nu, \nu_0$ all have units of cm^{-1} the integral portion of Eq. 5.4-7 is dimensionless. Therefore K will have units of K_0 , given by

$$K_0 = \frac{S}{\alpha_D} \left(\frac{\ln 2}{\pi} \right)^{1/2}, \quad (5.4-8)$$

where

$$S = S_0 Q \left(\frac{T_0}{T} \right)^{C_j} \exp \left\{ \frac{E}{kT_0} \left(1 - \frac{T_0}{T} \right) \right\}. \quad (5.4-9)$$

As long as T_0 and T have the same units their ratio is dimensionless. The partition function Q has a numerical value and is dimensionless and the index of the exponential is dimensionally

$$\frac{(\text{Joules})}{(\text{Joules}/^{\circ}\text{K})(^{\circ}\text{K})} \left(1 - \frac{^{\circ}\text{K}}{^{\circ}\text{K}} \right),$$

provided the energy E is given in joules. If it is not it must be converted. (See Eq. 5.4-5). Therefore the strength S will have units of S_0 .

$$S \stackrel{d}{=} S_0 \stackrel{d}{=} \frac{\text{cm}^{-1}}{\text{molecule} - \text{cm}^{-2}} \quad (5.4-10)$$

From Eq. 5.4-8 it can be seen that K_0 , and therefore K will have units of

$$K \stackrel{d}{=} K_0 \stackrel{d}{=} \frac{\text{cm}^{-1}}{\frac{\text{molecule} \cdot \text{cm}^{-2}}{\text{cm}^{-1}}} = \frac{\text{cm}^2}{\text{molecules}} \quad (5.4-11)$$

From the discussion of section 5.3 recall that the quantity $\frac{\text{MdP}}{g}$ of Eq. 5.4-7 is really gas amount du and is given by either Eq. 5.3-9 or 5.3-10. In either case it has units of cm-atm . Therefore

$$\frac{\text{KMdP}}{g} \stackrel{d}{=} \frac{\text{cm}^2}{\text{molecule}} \cdot \text{cm-atm}$$

Utilizing Eq. 5.4-2 it is possible to make the above relation dimensionless.

$$1 = \frac{2.69 \cdot 10^{19} \text{ molecules}}{\text{cm}^3 \cdot \text{atm}}$$

$$1 \cdot \frac{\text{KMdP}}{g} \stackrel{d}{=} \frac{\text{cm}^2}{\text{molecules}} \cdot \text{cm-atm} \cdot \frac{2.69 \cdot 10^{19} \text{ molecules}}{\text{cm}^3 \cdot \text{atm}}$$

Thus, all calculations will be dimensionally correct provided

- (1) $\alpha_L, \alpha_D, \nu, \nu_0$ are in wavenumbers (cm^{-1}),
- (2) S_0 has units of $\frac{\text{cm}^{-1}}{\text{molecule} \cdot \text{cm}^{-2}}$,
- (3) E has units of joules,

- (4) The extinction coefficient K is multiplied by $2.69 \cdot 10^{19} \frac{\text{molecules}}{\text{cm}^3 \text{-atm}}$,
- (5) Eq. 5.2-1 is used to calculate transmittance where

$$M_j(P) = \frac{M_{\text{ppm}} \cdot 10^{-6} \cdot M_{t_{\text{gas}}}}{\rho_{\text{gas(STP)}} M_{t_{\text{air}}}}$$

or

$$M_j(P) = \frac{M_d}{\rho_{\text{gas(STP)}}$$

- (6) The physical constants of Table 5.4-1 are used where needed.

5.5 The Absorption Line Parameters

About 10 years ago various individuals began to compile spectroscopic data on the vibrational-rotational lines of atmospheric gases. This continued mostly as individual work until about 5 years ago when an effort at the Air Force Cambridge Research Laboratories (AFCL) was made to continue the data collection with the aim of providing a complete set of data for all vibrational-rotational lines of naturally occurring molecules of significance in the terrestrial atmosphere. With such data at hand it would be possible to compute the transmittance appropriate for atmospheric paths. The work at AFCL includes data on water vapor, carbon dioxide, ozone, nitrous oxide, carbon monoxide, methane, and oxygen to date. All of these molecules except oxygen are minor constituents of the atmosphere, but nonetheless represent most of the absorption lines in the visible and infrared.

In order to compute transmittance due to a given spectral line

in the atmosphere it is necessary to describe the absorption coefficient as a function of frequency of each line. The four essential parameters for each line are the resonance frequency ν_0 , the intensity per absorbing molecule S , the Lorentz line width parameter α_0 , and the energy of the lower state E . The frequency, ν_0 , is independent of both temperature and pressure. The intensity, S , is pressure independent and its temperature dependence can be calculated from ν and E .

5.5.1 Derivation of Line Parameters

The four parameters ν_0 , E , S , and α_0 must of course be derived from experimental observations, subjected to data reduction in the framework of the general theories of molecular spectroscopy. The complexity needed to approach the problem depends both on the type of molecule and the accuracy of observational data. In the derivation of the parameters, equations and methods were used for linear triatomic and diatomic molecules (CO_2 , N_2O , CO) and nonlinear triatomic molecules (H_2O , O_3). Methane, CH_4 , a spherical top, is a special case, as is the diatomic O_2 . The energy states and the transition probabilities between energy states of the molecules are defined primarily by their numerical values, as established by experiments and the quantum numbers which identify them. In nearly all the cases of interest mathematical relations of greater or lesser complexity relate the numerical properties to the quantum numbers.

For both linear and nonlinear molecules the vibrational and rotational states may be characterized by quantum numbers. To calculate the purely vibrational part of the energy of linear molecules it is

necessary first to compute an unperturbed energy, G_v^{up} . A similar procedure is used for nonlinear molecules to compute G_v^{up} . Then the effects of resonance perturbations are incorporated to obtain the molecular vibrational energies, G_v . This method was used to generate those energy levels which have not been observed; for all observed states the experimental values were used.

For linear molecules the rotational energy of each vibrational state is a function of the quantum numbers J and l , and the vibrational energy, G_v . It is given by

$$E_{v,j} = G_v + B_v [J(J+1) - l^2] - D_v [J(J+1) - l^2]^2 + H_v [J(J+1) - l^2]^3 + \dots \quad (5.5-1)$$

where B_v , D_v , H_v are constants for each vibrational state that are either determined by observation or calculated. The equations for B_v and D_v are similar to those for G_v and likewise require modification through resonance perturbation.

For nonlinear molecules the rotational levels are calculated from complicated functions of the three different moments of inertia of the molecule model [Hertzberg¹⁶]. Having determined the energy states of the different molecules and their isotopes, the line frequencies (ν_0) are determined by taking the differences corresponding to all allowed transitions. These depend upon the selection rules for the molecule.

Half-widths (α_0) of lines are taken from observed values or computed for each molecular species. McClatchey, et al.³¹ discusses the procedure used to calculate the half width of each gas type. In cases where there is insufficient data to warrant inclusion of variable half

widths, a constant value was used.

The intensities of the lines are calculated as a function of frequency (ν), the vibrational intensity of a nonrotating molecule (S_V), the rotational intensity of a rigid nonvibrating molecule (S_{ROT}), and a factor, F , that takes into account that both forms of motion occur simultaneously. The representations of F are quite complex and very dependent upon molecular type and isotope. A complete discussion of the derivation of parameters can be found in McClatchey, et al.³¹.

In order to establish a minimum intensity value, an extreme atmospheric path was considered, assuming gas concentration specified in Table 5.3-1. This path was tangent to the earth's surface and extended from space to space. Lines yielding less than 10 percent absorption at the line center would normally be omitted. This absolute cutoff was not maintained in regions of strong absorption (relatively weak lines were dropped) and regions of weak absorption (most lines were kept). Table 5.5-1 gives the mean half-widths and minimum intensities for each molecule used in this work.

Utilizing the methods outlined above and the experimental results of many other scientists, R. A. McClatchey, et al.³¹, has compiled a data tape that contains the parameters needed to compute transmittance.

5.5.2 The Line Parameter Data Tape

The data compilation thus far described resulted in the accumulation of the four quantities ν_0 , S , E , α_0 for 108,000 spectral lines between 1 μm and the far infrared for the molecular species listed in Table 5.5-1. Additional identifying information has also been supplied

Molecule	Identifier	Intensity Minimum	Mean Half-Width
H ₂ O	1	3 10 ⁻²⁷	not given
CO ₂	2	2.2 10 ⁻²⁶	0.07
O ₃	3	3.5 10 ⁻²⁴	0.11
N ₂ O	4	3.0 10 ⁻²³	0.08
CO	5	8.3 10 ⁻²³	0.06
CH ₄	6	3.3 10 ⁻²⁴	0.055
O ₂	7	3.7 10 ⁻³⁰	0.06

Table 5.5-1. Mean half-widths and intensity minimums used by McClatchey, et al.³¹ in compilation of AFCRL data tape.

for each line as indicated in Table 5.5-2. A standard computer format was adopted for card or card-image input. The units of the data are given in Table 5.5-2. The rotational and vibrational identifiers, the date, and the isotope are explained by McClatchey, et al.³¹, but not used here. The molecule (columns 78-80) correspond to the identifier of Table 5.5-1.

The data are frequency ordered on magnetic tape and are contained in records each of which contain 40 card images as shown in Table 5.5-2. Each record is preceded by a variable that indicates the number of card images within the record (in all cases 40). It is necessary to decode each record from the tape according to the format

I10, 40(F10.3, E10.3, F5.3, F10.3, 5A6, A5, I3, I4, I3) 23A30.

The last format (23A30) is to read the space that separates each record. End of file markers are placed on the tape at the following points: 500, 1000, 2000, 5000, 7500, 10000 cm^{-1} . This results in the tape having seven files.

5.6 The DATSET Computer Subroutine

In order to utilize the data tape of McClatchey it was necessary to write a computer subroutine that would transfer that portion of the data needed from the tape to computer memory or if desired to disk. The subroutine is used in conjunction with the transmittance program. Some job control language (JCL) is needed with the routine to identify the different files of the tape and establish the disk space if that is to be used. The flow of the routine is outlined below and a listing of the program is given in Appendix D.

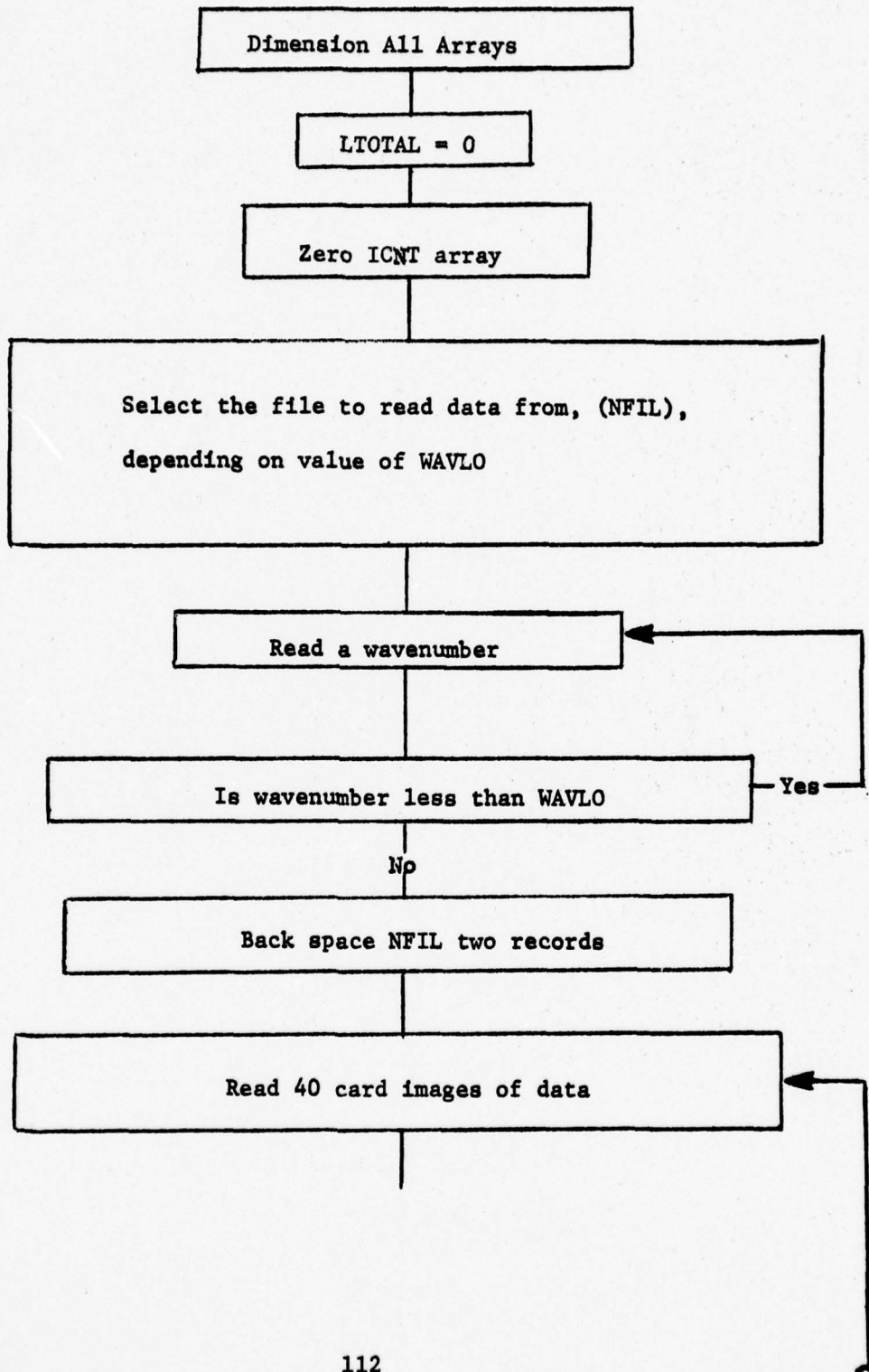
Data element	Units	Card Column	Format
ν_0	cm^{-1}	1-10	F10.3
S_0	$\frac{\text{cm}^{-1}}{\text{molecule-cm}^2}$	11-20	E10.3
α_0	$\text{cm}^{-1}/\text{atm}$	21-25	F5.3
E	cm^{-1}	26-35	F10.3
Rotational-Vibration ID		36-70	5A6,A5
Date		71-73	I3
Isotope		74-77	I4
Molecule		78-80	I3

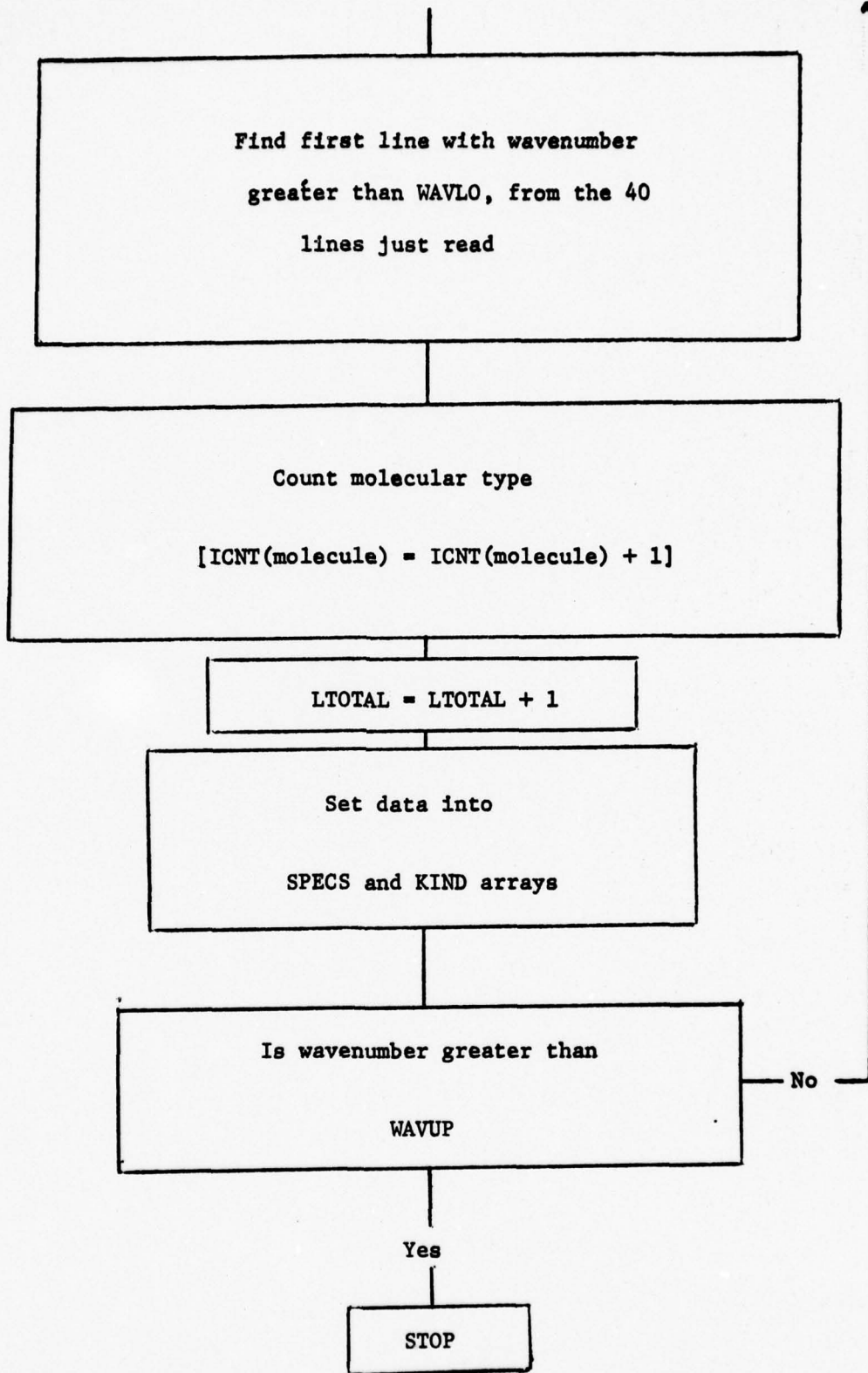
Table 5.5-2. Computer format of each spectral line's data. [McClatchey, et al.³¹]

The subroutine has the following parameters:

WAVLOlower wavenumber of data to be extracted from data tape (lower limit of channel)input
WAVUPupper wavenumber of data to be extracted from tape (upper limit of channel)input
ICNT(T)Array containing the number of spectral lines between wavlo and wavup, by gas type. (1= H ₂ O, 2= CO ₂ , etc.)output
MAXMaximum number of lines that can be transfered from tape (3000)input
SPECS(3000,4)Array containing data for each line (ν_0 , S_0 , E , α_0)output
KIND(3000)Array containing molecular identifier of each lineoutput
LTOTALTotal number of lines between wavlo and wavupoutput

DATSET Flowchart





There are error messages that will inform the user if the program does not execute properly. The routine can be used to transfer data to disk (see comment card in program listing). The JCL necessary to define the files must be included before using disk.

CHAPTER VI

THE TRANSMITTANCE PROGRAM

6.1 Preface

This chapter presents the object of the previous five chapters, a transmittance program. Before the routine is presented the vibrational partition function (Q) is developed, the iterative solution used to solve the transmittance differential equation is explained, and the methods used to compute monochromatic and averaged transmittance are given. These final details are incorporated with the equations thus far developed to yield the transmittance program. The chapter concludes with the results of some transmittance calculations in the fifteen micrometer band.

6.2 The Rotational and Vibrational Partition Functions

The equation for line strength may be given as

$$S = S_o Q_R \exp \left\{ \frac{E}{kT_o} \left(1 - \frac{T_o}{T} \right) \right\} Q_V \quad (6.2-1)$$

The line strength is dependent upon the rotational and vibrational modes of the molecule in a characteristic manner. The rotational partition function (Q_R) is very temperature dependent and is given by [McClatchey, et al.³¹]

$$Q_R = \left(\frac{T_o}{T} \right)^{C_j}, \quad (6.2-2)$$

where the exponent C_j assumes values dependent upon gas type. The vibrational partition function (Q_V) is also temperature dependent, but not in such a clear manner. Table 6.2-1 gives the value of C_j

Molecule	C _j	Vibrational Partition Function						
		Temperature						
		175	200	225	250	275	296	325
H ₂ O	1.5	1.0	1.0	1.0	1.0	1.0	1.0	0.999
CO ₂	1.0	1.082	1.072	1.058	1.041	1.019	1.0	0.970
O ₃	1.5	1.042	1.038	1.033	1.024	1.013	1.0	0.981
N ₂ O	1.0	1.108	1.094	1.075	1.051	1.025	1.0	0.963
CO	1.0	1.0	1.0	1.0	1.0	1.0	1.0	1.0
CH ₄	1.5	1.007	1.007	1.006	1.005	1.003	1.0	0.996
O ₂	1.0	1.0	1.0	1.0	1.0	1.0	1.0	0.999

Table 6.2-1. Rotational and Vibrational Partition Functions.
 (Adapted from McClatchey, et al.³¹)

and the vibrational functions that are used in this work. For computer implementation it is simple enough to use the different values for C_j from a look-up array, however a speedy and accurate method is needed for the vibrational partition function.

Therefore regression analysis of the vibrational points was performed for linear, quadratic, and cubic fits to determine the best relation. For each gas the following functions of temperature (T) were tried.

$$\text{Linear...} Q_v = A_1 T + A_2$$

$$\text{Quadratic...} Q_v = B_1 T^2 + B_2 T + B_3$$

$$\text{Cubic...} Q_v = C_1 T^3 + C_2 T^2 + C_3 T + C_4$$

Linear fits were abandoned after the partition function was graphed and several lines were tried. For the quadratic and cubic relations a computer routine was written to determine the coefficients B_1 and C_1 .

In matrix form the vibrational partition functions can be written

$$Q_v = AT, \quad (6.2-3)$$

where Q_v is a (7 x 1) partition array, A is a (7 x 3) unknown array, and T is a (3 x 1) temperature array. For cubic fit A is (7 x 4) and T is (4 x 1). The unknown array A is given by [Burr⁷]

$$A = [T^t T]^{-1} [T^t Q_v], \quad (6.2-4)$$

where the superscript (t) indicates matrix transpose. The results of the regression analysis are given in Table 6.2-2.

In view of the small errors associated with the quadratic coefficients, they are used in the transmittance program for the vibrational partition function.

6.3 Euler's Solution of the Transmittance Differential Equation

The transmittance differential equation may be written

$$\frac{d\tau}{dP} = \sigma\tau, \quad (6.3-1)$$

where

$$\sigma = \sum_j K_j M_j.$$

If the atmosphere is stratified and every layer has a different σ , the transmittance relation becomes

$$\frac{d\tau_\ell}{dP} = \sigma_{\ell+1} \tau_{\ell+1}, \quad (6.3-2)$$

where dP is the pressure difference between the ℓ and $\ell+1$ layers. This is a first-order ordinary differential equation. A solution, $\tau(P)$, is desired that satisfies Eq. 6.3-2 and a single specified initial condition. In general it is impossible to determine $\tau(P)$ in exact analytical form. Instead, the interval in the independent variable, P , over which a solution is desired, $[0, P_0]$, is divided into sub-intervals or steps. These steps correspond to the pressure differences dP .

An application of the Runge-Kutta algorithms to Eq. 6.3-2 results

Molecule	Quadratic Coefficients			Error of Quadratic Formula
	B_1	B_2	B_3	
H ₂ O	$-9.88 \cdot 10^{-8}$	$4.49 \cdot 10^{-5}$	0.99	$9.6 \cdot 10^{-3}\%$
O ₃	$-2.16 \cdot 10^{-6}$	$6.77 \cdot 10^{-4}$	0.98	$2.1 \cdot 10^{-2}\%$
CO ₂	$-2.54 \cdot 10^{-6}$	$5.16 \cdot 10^{-4}$	1.07	$1.3 \cdot 10^{-2}\%$
N ₂ O	$-2.81 \cdot 10^{-6}$	$4.28 \cdot 10^{-4}$	1.12	$2.5 \cdot 10^{-2}\%$
CO	0.0	0.0	1.0	0.0 %
CH ₄	$-6.00 \cdot 10^{-7}$	$2.28 \cdot 10^{-4}$	0.98	$1.3 \cdot 10^{-2}\%$
O ₂	$-9.89 \cdot 10^{-8}$	$4.49 \cdot 10^{-5}$	0.99	$9.6 \cdot 10^{-3}\%$

Molecule	Cubic Coefficients				Error of Cubic Formula
	C_1	C_2	C_3	C_4	
H ₂ O	$-1.68 \cdot 10^{-9}$	$1.16 \cdot 10^{-6}$	$-2.63 \cdot 10^{-4}$	1.02	$8.9 \cdot 10^{-3}\%$
O ₃	$1.08 \cdot 10^{-9}$	$-2.98 \cdot 10^{-6}$	$8.76 \cdot 10^{-4}$	0.97	$2.2 \cdot 10^{-2}\%$
CO ₂	$-1.67 \cdot 10^{-9}$	$1.16 \cdot 10^{-6}$	$-2.63 \cdot 10^{-4}$	1.02	3.9 %
N ₂ O	$8.85 \cdot 10^{-9}$	$-9.46 \cdot 10^{-6}$	$2.05 \cdot 10^{-3}$	0.99	$2.9 \cdot 10^{-2}\%$
CO	$-6.38 \cdot 10^{-14}$	$4.77 \cdot 10^{-11}$	$-1.16 \cdot 10^{-7}$	1.00	$2.8 \cdot 10^{-8}\%$
CH ₄	$-6.91 \cdot 10^{-10}$	$-8.19 \cdot 10^{-8}$	$1.01 \cdot 10^{-4}$	0.99	$1.3 \cdot 10^{-2}\%$
O ₂	$-1.68 \cdot 10^{-9}$	$1.16 \cdot 10^{-6}$	$-2.63 \cdot 10^{-4}$	1.01	$8.9 \cdot 10^{-3}\%$

Table 6.2-2. Regression coefficients for quadratic and cubic fit of Vibrational Partition Function.

in the improved Euler's method or Heun's method [Carnahan, et al.⁸] of solution of the differential equation. The desired solution of Eq. 6.3-2 is thus given as

$$\tau_{\ell+1} = \tau_{\ell} + \frac{dP}{2} \left\{ \sigma\tau_{\ell} + \sigma\bar{\tau}_{\ell+1} \right\} \quad (6.3-3)$$

where

$$\bar{\tau}_{\ell+1} = \tau_{\ell} + dP\sigma\tau_{\ell} ; \quad (6.3-4)$$

subject to the initial condition (top of the atmosphere)

$$\tau(0) = 1 . \quad (6.3-5)$$

Euler's algorithm may be viewed as a predicting equation for $\bar{\tau}_{\ell+1}^{-1}$ (the first approximation to $\tau_{\ell+1}$), whereas Eq. 6.3-3 may be considered a correcting equation to produce an improved estimate of $\tau_{\ell+1}$. Equation 6.3-3 is used iteratively to produce a sequence of corrected $\tau_{\ell+1}$ values. A maximum of ten iterations per atmospheric layer is allowed in the program.

This procedure results in values of transmittance for every layer of the atmosphere, beginning at $P=0$, $\tau=1$ and continuing to the bottom of the atmosphere (ground level). The variable σ must of course be computed for each layer of the atmosphere utilizing the proper equations. However, the calculation of σ is sovereign of the solution τ , and is done independently.

6.4 Transmittance Iteration Technique

This section explains a technique that was developed to enable

the transmittance program to calculate either a monochromatic transmission or an averaged channel transmission. In addition, the option to extend the channel limits was incorporated into the program.

In calculating the transmission at a single frequency the effects of all lines within a specified range of that frequency are added together. This range is denoted by the variable SEARCH. When calculating the transmittance of a channel, the distance BOUND is used to extend the limits of the channel and thus account for lines that contribute to absorption within the channel, but whose center frequency ν_0 is out of the channel (see Fig. 3.4-3). To calculate the transmittance for a band the monochromatic transmittances are calculated at several frequencies and then averaged over the band.

The following variables are defined below and used in the transmittance program, iteration loop.

- WAVLO... Lower wavenumber of channel.
- WAVUP... Upper wavenumber of channel.
- SEARCH... The range about a single frequency within which the effects of spectral lines are added together.
- CNTR... The single frequency at which transmittance is calculated.
- BOUND... Amount by which the limits of a channel are enlarged to consider lines that absorb within the channel, but whose center frequency, ν_0 , is outside of the channel.
- SPACE... The distance between the single frequencies at which transmittances are calculated.

INTVLS... The number of intervals the channel is divided into, minus one.

INCR... The number of intervals the channel is divided into. Also, the number of transmittance calculations made within a channel.

The increment loop proceeds as follows during the transmittance program execution:

- (1) The variables BOUND and INTVLS are read as input data.
- (2) The lower limit, WAVLO, and the upper limit, WAVUP, of the channel are read as input data.
- (3) The limits of the channel are adjusted by the amount BOUND.
- (4) The absorption line parameters (ν_0, S, E, α) of lines between the adjusted WAVLO and WAVUP limits are transferred from tape to computer memory.
- (5) The variable SEARCH is set equal to BOUND. If BOUND was zero, SEARCH is set equal to half the channel width.
- (6) The channel is divided into the desired number of intervals (INTVLS+1) and the variable SPACE is set equal to the distance between transmission calculation points, $SPACE = \frac{WAVUP - WAVLO}{INTVLS}$.
- (7) The first frequency of transmission calculation, CNTR, is set to WAVLO. If only one transmittance calculation is to be made in a channel, CNTR is set to the channel center frequency.
- (8) The upper limit, UP, and lower limit, DOWN, are set to $CNTR \pm SEARCH$ respectively. This causes the transmittance calculations to include lines within the distance SEARCH of CNTR.

- (9) Transmission computations are made for the frequency CNTR.
 - (10) If another transmittance calculation is to be performed in this channel, the value of CNTR is changed to $CNTR + SPACE$ (go to step 9) if not, another channel is done (go to step 2).
 - (11) After all channels are completed the program terminates.
- Figures 6.4-1, 6.4-2, and 6.4-3 graphically display this procedure for three increment options.

INCR = 1
INTVLS = 0
BOUND = 0
CNTR = (WAVUP + WAVLO)/2
SEARCH = (WAVUP-WAVLO)/2

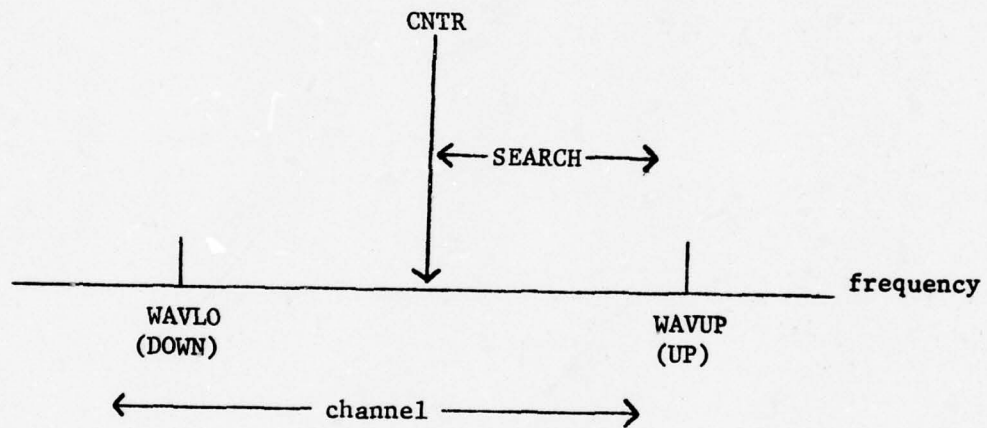


Figure 6.4-1. A single transmission calculation per channel. Channel limits not adjusted.

INCR = 1
INTVLS = 0
BOUND = 5
CNTR = (WAVUP + WAVLO)/2
SEARCH = BOUND

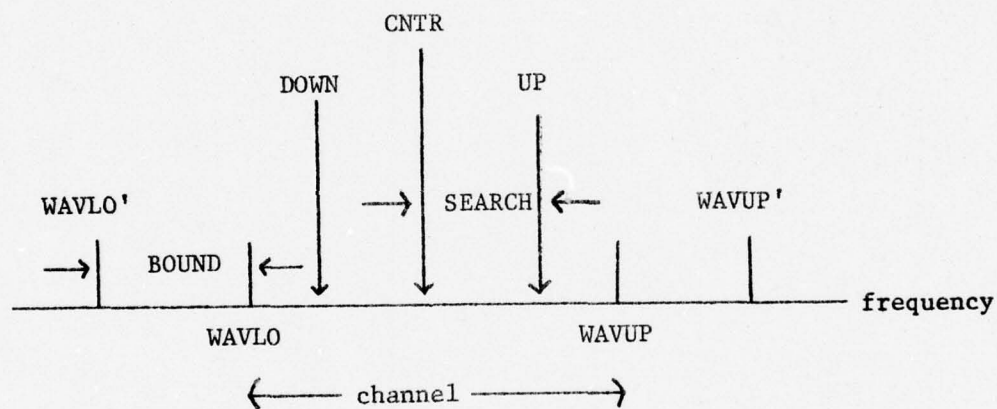


Figure 6.4-2. A single transmission calculation per channel. Channel limits adjusted by BOUND.

INTVLS = 2
 INCR = 3
 BOUND = 5
 CNTR = WAVLO, WAVLO + SPACE, WAVUP
 SEARCH = BOUND
 SPACE = (WAVUP - WAVLO) / INTVLS

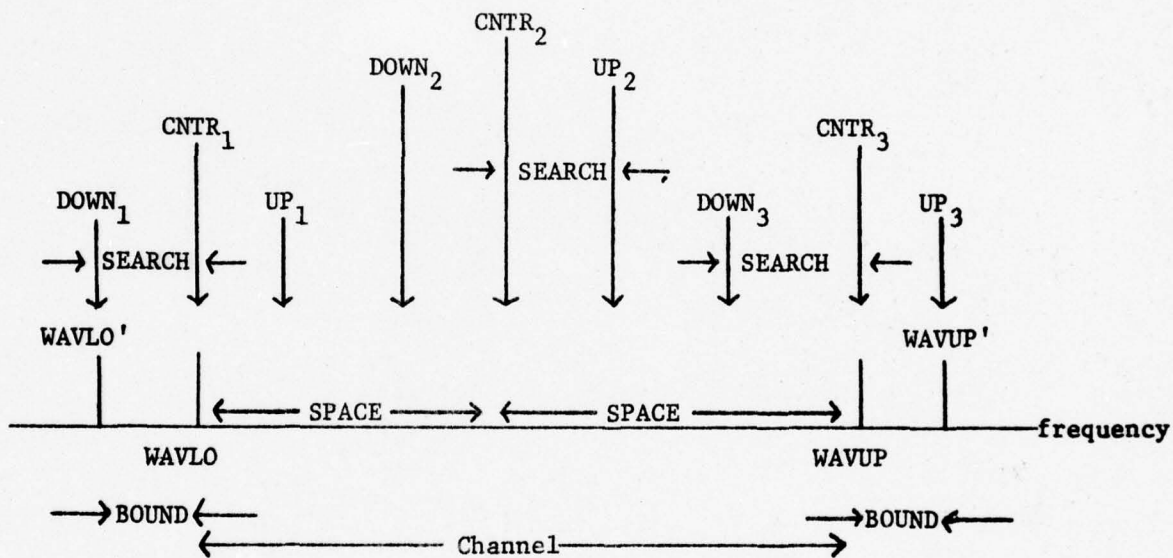


Figure 6.4-3. Three transmittance calculations per channel.
 Channel limits adjusted by BOUND.

6.5 Transmittance Program Flowchart and Utilization

The transmittance program written as the final product of this work is listed in Appendix E. The equations and relations necessary to calculate the line-by-line transmittance were implemented in the most efficient manner possible. There are five main portions of the program. First, all initializations and one-time computations are made. Second the calculations and data transfer peculiar to a channel are completed. The third step is the increment loop. It sets how many and where (frequencies) transmittance calculations are to be performed. Fourth, the equations that are a function of atmospheric level (altitude) are processed. The fifth and final step is the line loop. It considers only the appropriate spectral lines in the transmission calculations. The output is a set of transmittance values for each layer of the atmosphere. A general flowchart is given in Fig. 6.5-1.

A major portion of the program transfers data or determines which spectral lines to use in calculations. The absorption coefficient computation occurs in the line loop and utilizes the equations indicated in Table 6.5-1.

The program was written in FORTRAN IV for an IBM 360/65 computer [20, 21]. It utilizes two subroutines; DATSET to transfer data from tape to core and ZVOIGT to compute the voigt line shape. Both subroutines are explained in other sections and have listings in the appendices. The job control language (JCL) necessary to read the data tape is listed in Appendix D with the DATSET routine.

The card input required to execute the program is:

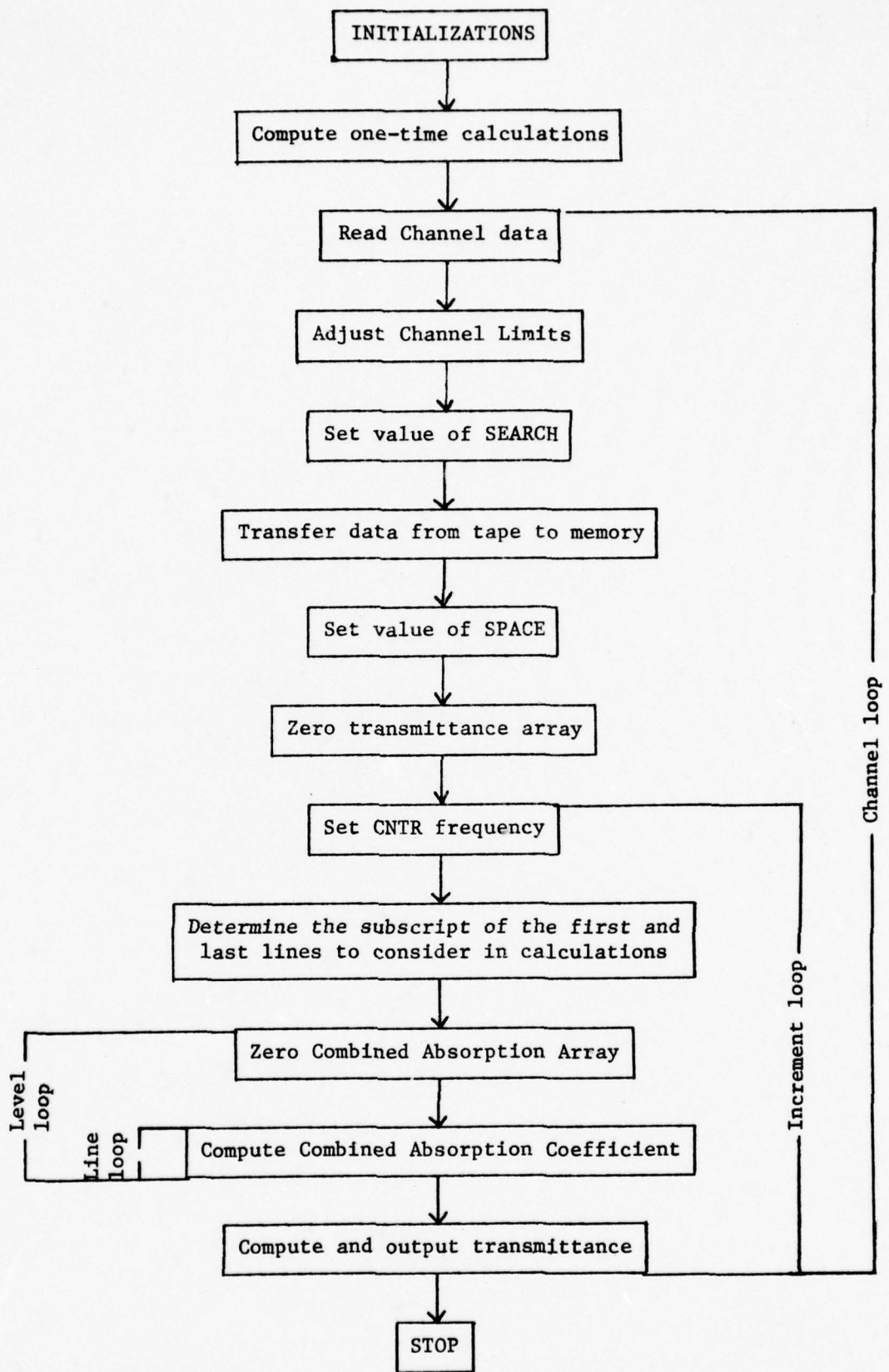


Figure 6.5-1. Transmittance Program Flowchart.

Symbol	Definition	Equation(s) Used
α_D	Doppler line width	2.4-4
α_L	Lorentz line width	2.4-12
y	Doppler-Lorentz ratio	4.3-1
K_0	Absorption coefficient	3.3-20
x	Wavenumber difference	4.3-1
$\frac{1}{\pi} \int_{-\infty}^{\infty} \frac{ye^{-t^2} dt}{y^2+(x-t)^2}$	Voigt shape	ZVOIGT subroutine
$\sum_j K_j$	Extinction coefficient	3.2-21
ABSK	Combined extinction coefficient	5.3-15
τ	Transmittance	6.3-3, 6.3-4

Table 6.5-1. Equations used in the transmittance program.

NCHNL...	Number of channels
LEVS...	Number of atmospheric layers
BOUND...	Extention amount of channel limits
INTVLS...	Number of channel intervals, minus one
PRESS(LEVS)...	Pressure for each layer
TEMP(LEVS)...	Temperature for each layer
H2OMIX(LEVS)...	Water vapor concentration for each layer
O3MIX(LEVS)...	Ozone concentration for each layer
WAVLO...	Lower channel limit (for each channel)
WAVUP...	Upper channel limit (for each channel)

Figure 6.5-2 shows the input format and order required.

The transmittance program was executed for the following input data. NCHNL=7, LEVS=33, BOUND=0, INTVLS=0

The channel limits for each channel were taken from Table 3.4-1.

The pressure, temperature, water vapor concentration and ozone concentration were taken from McClatchey, et al.³² and are similar to Table 5.3-3. The results of this monochromatic layer transmittance for each channel are given in Appendix G. Other computations were made utilizing several frequencies per channel (INTVLS \neq 0) to test the iteration portion of the program. The transmittance of a single channel using INTVLS = 10 is given in Appendix H for comparison with the monochromatic calculation.

Card Name	Format	Number Required																
Level-Channel Data	<table style="margin-left: auto; margin-right: auto;"> <tr> <td style="border: 1px solid black; width: 10px;"></td> <td style="border: 1px solid black; width: 10px;"></td> <td style="border: 1px solid black; width: 10px;"></td> <td style="border: 1px solid black; width: 10px;"></td> <td style="border: 1px solid black; width: 10px;"></td> <td style="border: 1px solid black; width: 10px;"></td> <td style="border: 1px solid black; width: 10px;"></td> <td style="border: 1px solid black; width: 10px;"></td> </tr> <tr> <td style="text-align: center;">NCHNL</td> <td></td> <td style="text-align: center;">LEVS</td> <td></td> <td style="text-align: center;">BOUND</td> <td></td> <td style="text-align: center;">INTVLS</td> <td></td> </tr> </table> 1X I3 1X I3 1X F10.3 1X I4									NCHNL		LEVS		BOUND		INTVLS		1
NCHNL		LEVS		BOUND		INTVLS												
Atmosphere Data	<table style="margin-left: auto; margin-right: auto;"> <tr> <td style="border: 1px solid black; width: 10px;"></td> <td style="border: 1px solid black; width: 10px;"></td> <td style="border: 1px solid black; width: 10px;"></td> <td style="border: 1px solid black; width: 10px;"></td> <td style="border: 1px solid black; width: 10px;"></td> <td style="border: 1px solid black; width: 10px;"></td> <td style="border: 1px solid black; width: 10px;"></td> <td style="border: 1px solid black; width: 10px;"></td> </tr> <tr> <td style="text-align: center;">PRESS(I)</td> <td></td> <td style="text-align: center;">TEM(I)</td> <td></td> <td style="text-align: center;">H2OMIX(I)</td> <td></td> <td style="text-align: center;">O3MIX(I)</td> <td></td> </tr> </table> 6X E9.3 F5.1 1X E9.3 1X E9.3									PRESS(I)		TEM(I)		H2OMIX(I)		O3MIX(I)		LEVS
PRESS(I)		TEM(I)		H2OMIX(I)		O3MIX(I)												
Channel limits Data	<table style="margin-left: auto; margin-right: auto;"> <tr> <td style="border: 1px solid black; width: 10px;"></td> <td style="border: 1px solid black; width: 10px;"></td> <td style="border: 1px solid black; width: 10px;"></td> <td style="border: 1px solid black; width: 10px;"></td> </tr> <tr> <td></td> <td style="text-align: center;">WAVLO</td> <td></td> <td style="text-align: center;">WAVUP</td> </tr> </table> 1X F10.3 1X F10.3						WAVLO		WAVUP	NCHNL								
	WAVLO		WAVUP															

Figure 6.5-2. Input data format and number required.

CHAPTER VII

DISCUSSION AND CONCLUSION

7.1 Preface

This final chapter briefly comments on this research and draws some conclusions. It was the object of this work to develop a fast monochromatic transmittance program. That has been done. The chapter ends with a note on what future, related works might investigate.

7.2 Discussion

This work was approached with the intent of developing a line-by-line transmission model. To construct that model the physics of the atmosphere and some molecular theory of gases was introduced. It is hoped that the development of the transmittance algorithm proceeded in a fluid manner and with enough detail to enable the reader to follow.

During the development of the equations that were needed, an algorithm to quickly evaluate the Voigt function was born. It is sincerely hoped that this Voigt algorithm proves to be a valuable one for atmospheric work.

7.3 Conclusions

The transmittance program written as a result of this work was used to compute the monochromatic transmission for channels in both the 15 and 4.3 micrometer band. Also, averaged transmittances were computed for selected channels. In all cases the program executed properly and returned values that seemed to be correct.

The results of the program were not compared with any other, as they were not available. However, the extinction coefficients computed in the program were compared to those computed in a completely different manner; in a program written by Mr. T. Potter.⁴⁰ The agreement of the coefficients computed in the two different methods was excellent. From these coefficients it is a simple matter to compute transmittance, so it is assumed that if the extinction coefficients were correct the transmittances would be correct.

The single most important conclusion is that the Voigt algorithm developed in this work is a rapid and accurate method to evaluate the Voigt profile. The results of tests that were made with the algorithm surpassed all expectations (see chapter four).

7.4 Ongoing Research

It is my opinion that the Voigt algorithm developed here can be improved. First, the routine need not be double precision. I believe that it is possible to obtain very good results with a single precision routine. Secondly, the series used for the algorithm in Region I could be expanded to thirty terms and a Chebyshev economization used to reduce the number of terms. This would increase speed and maintain the desired accuracy.

The results of this transmittance program need to be compared with some other results. Although the values appear to be correct, they need confirmation. Once the validity of the method is established, additional data needs to be obtained so the transmittance of the

atmosphere can be more closely tabulated. For this the atmosphere should be divided into 100 layers. Additionally, the transmittance computed for a channel needs to be convolved with a slit function corresponding to the HIRS instrument.

Finally a more efficient routine needs to be developed to yield an averaged transmittance. The method used in this work is very time consuming. To calculate a single monochromatic transmittance takes about 15 CPU seconds. If a step of 0.01 wavenumbers is used for a channel with a width of 20 wavenumbers, it means 2000 single evaluations or about 8 hours of computation time. A better system must be developed.

APPENDIX A

KIELKOPF'S VOIGT ALGORITHM

The FORTRAN IV subroutine that implements Kielkopf's Voigt algorithm is listed on the following page. It is a double precision routine that has three parameter inputs and a single parameter output. The input parameters are

$$\begin{aligned} \text{BL} &= \alpha_L \\ \text{BG} &= \alpha_D / (\ln 2)^{1/2} \\ \text{and } v &= \frac{v-v_0}{\alpha_D} (\ln 2)^{1/2} \end{aligned}$$

The value of the Voigt Function is returned as the variable VGT when the main program contains the following statement

```
CALL COEFF(BL, BG, V, VGT).
```

```
0001      SUBROUTINE COEF(BL,BG,V,VGT)
0002      IMPLICIT REAL*8(A-Z)
0003      DATA TWO/2.0000000/
0004      A=BL/BG
0005      AL=2./(1.+0.99*DLOG(TWO)+DSQRT((1.-0.99*DLOG(TWO))**2+
1         (4.*DLOG(TWO))/(A*A)))
0006      G2=(1./DLOG(TWO))/(1.-AL)
0007      B=BL/AL
0008      ETA=AL/(AL+G2)
0009      X=V/B
0010      GX=DEXP(-(DLOG(TWO)*X*X))
0011      ALX=1./(1.+X*X)
0012      EX=(.8029-.4207*X*X)/(1.+2.030*X*X+.07335*X*X*X*X)
0013      UX=(1.-ETA)*GX+ETA*ALX+ETA*(1.-ETA)*EX*(GX-ALX)
0014      T=1./(1.+4.7047*A)
0015      XI=A*(.61686*T-.16994*T*T+1.32554*T*T*T)/(3.141592654*BL)
0016      VGT=XI*UX*(1.772453851/(BL/BG))
0017      RETURN
0018      END
```


APPENDIX B

DRAYSON'S VOIGT ALGORITHM

The FORTRAN IV function subprogram that uses the four regions proposed by Drayson is a single precision routine. The variable VOIGT is set equal to the Voigt function value in the subprogram when the main routine executes a call statement, i.e.,

$$\text{SHAPE} = \text{VOIGT}(X, Y).$$

The parameters X and Y are:

$$Y = \frac{\alpha_L}{\alpha_D} (\ln 2)^{1/2}$$

$$X = \frac{\nu - \nu_0}{\alpha_D} (\ln 2)^{1/2}$$

The program listing begins on the next page.

```

0071      FUNCTION VOIGT(X,Y)
0072      REAL R(22)/0.,.7093602E=7/,RI(15),XN(15)/10.,9.,2*8.,7.,6.,5.,4.,
1       7*3./,YN(15)/3*.6.,.5,2*.4,4*.3,1.,.9.,.8,2*.7/,
2       D0(25),D1(25),D2(25),D3(25),D4(25),HN(25),
3       H/.701/,XX(31)/.5246476,1.65068,.7071068/,
3       HH(3)/.2562121,.2584268E=1,.2820948/,
4       NBY?(19)/9.5,9.,.8.5,8.,.7.5,7.,.6.5,6.,.5.5,5.,.4.5,4.,.3.5,3.,.2.5,
5       2.,.1.5,1.,.5/,
6       C(21)/.7093602E=7,=.2518434E=6,=.8566874E=6,=.2787538E=5,
7       .366074E=5,=.2565551E=4,.7223775E=4,=.1933631E=3,.4899520E=3,
7       -.1173267E=2,.2648762E=2,=.5623190E=2,.1119601E=1,=.2084976E=1,
8       .3621573E=1,=.58514112E=1,.8770816E=1,=.121664,.15584,=.184,.2/
      LOGICAL TRU/.FALSE./
      IF(TRU) GO TO 104
      TRU=.TRUE.
      DO 101 I=1,15
0007      101 RI(I)=-I/2.
0008      DO 103 I=1,25
0009      HN(I)=H*(I-.5)
0010      CO=4.*HN(I)*HN(I)/25.-2.
0011      DO 102 J=2,21
0012      102 B(J+1)=CO*B(J)-3(J-1)+C(J)
0013      DO(I)=HN(I)*(B(22)-B(21))/5.
0014      D1(I)=1.-2.*HN(I)*DO(I)
0015      D2(I)=(HN(I)*D1(I)+DO(I))/RI(2)
0016      D3(I)=(HN(I)*D2(I)+D1(I))/RI(3)
0017      103 D4(I)=(HN(I)*D3(I)+D2(I))/RI(4)
0018      104 IF(X=5.) 105,112,112
0019      105 IF(Y=1.) 110,110,106
0020      106 IF(X.GT.1.85*(3.6-Y)) GO TO 112
0021      IF(Y.LT.1.45) GO TO 107
0022      I=Y+Y
0023      GO TO 108
0024      107 I=11.*Y
0025      108 J=X+X+1.85
0026      MAX=XN(J)*YN(I)+.46
0027      MIN=MINO(16,21-2*MAX)
0028      UU=Y
0029      VV=X
0030      DO 109 J=MIN,19
0031      U=NBY2(J)/(UU*UU+VV*VV)
0032      UU=Y+U*UU
0033      109 VV=X-U*VV
0034      VOIGT=UU/(UU*UU+VV*VV)/1.772454
0035      RETURN
0036      110 Y2=Y*Y
0037      IF(X+Y.GE.5.) GO TO 113
0038      N=X/H
0039      DX=X-HN(N+1)
0040      U=((D4(N+1)*DX+D3(N+1))*DX+D2(N+1))*DX+D1(N+1)*DX+D0(N+1)
0041      V=1.-2.*X*U
0042      VV=EXP(Y2-X*X)*CCS(2.*X*Y)/1.128379-Y*V
0043      UU=-Y
0044      MAX=5.+(12.5-X)*.8*Y
0045      DO 111 I=2,MAX,2
0046      U=(X*V+U)/RI(I)
0047      V=(X*U+V)/RI(I+1)
0048      UU=-UU*Y2

```

```
0049      111 VV=VV+V*UU
0050      VOIGT=1.128379*VV
0051      RETURN
0052      112 Y2=Y*Y
0053      IF (Y.LT.11.-.6875*X) GO TO 113
0054      U=X-XX(3)
0055      V=X+XX(3)
0056      VOIGT=Y*(HH(3)/(Y2+U*U)+HH(3)/(Y2+V*V))
0057      RETURN
0058      113 U=X-XX(1)
0059      V=X+XX(1)
0060      UU=X-XX(2)
0061      VV=X+XX(2)
0062      VOIGT=Y*(HH(1)/(Y2+U*U)+HH(1)/(Y2+V*V)+HH(2)/(Y2+UU*UU)+
1      HH(2)/(Y2+VV*VV))
0063      RETURN
0064      END
```

APPENDIX C

PROPOSED VOIGT ALGORITHM

The implementation of the proposed Voigt algorithm utilizing three regions of the XY plane is a FORTRAN IV function subprogram. The routine sets the variable ZVOIGT equal to the value of the Voigt profile, for the parameters

$$Y = \frac{\alpha_L}{\alpha_D} (\ln 2)^{1/2}$$

$$\text{and } X = \frac{v-v_0}{\alpha_D} (\ln 2)^{1/2} .$$

The call statement required in the main program is

$$\text{SHAPE} = \text{ZVOIGT} (X,Y).$$

The program listing is on the next page.

```

0001      FUNCTION ZVOIGT(X,Y)
0002      IMPLICIT REAL*8(A-H,O-Z)
0003      REAL*8 AN(30)/1.0000000,=.33333333,.10000000,=.238095238E-1,
1      4.62962963E-3,-7.57575757E-4,1.068376069E-4,-1.322751323E-5,
2      1.45891691E-6,-1.450385222E-7,1.312253296E-8,-1.089222104E-9,
3      9.350702795E-11,-5.947794016E-12,3.955429516E-13,
4      -2.46682701E-14,1.448326465E-15,-8.032735012E-17,
5      4.221407289E-18,-2.177855192E-19,
+      1.002516493E-20,-4.551846759E-22,1.977064754E-23,
+-8.230149299E-25,3.289260349E-26,-1.264107899E-27,4.67848352E-29,
+      -1.669761793E-30,5.754191644E-32,-1.916942862E-33/,
+      A1/.46131350/,
6      A2/.19016350/,A3/.C9999216/,A4/1.78449270/,A5/.002883894/,
7      A6/5.52334370/,B1/.51242424/,B2/.27525510/,B3/.05176536/,
8      B4/2.72474500/,PI/SQ/1.128379167/

0004      S=X*X-Y*Y
0005      T=2.*X*Y
0006      IF(Y.GE.5..OR.X.GE.5) GO TO 111
0007      IF(Y.GE.1.8 .OR. X.GE.3.0) GO TO 112
0008      XSER=Y
0009      YSER=-X
0010      XN=Y
0011      YN=-X
0012      X2=-S
0013      Y2=-T
0014      N=6.842*X+8.0
0015      IF(N.GT.29) N=29
0016      IF(X.EQ.0.0) N=15
0017      DO 10 I10=1,N
0018      XNEW=XN*X2-YN*Y2
0019      YNEW=Y2*XN+YN*X2
0020      XSER=XSER+XNEW*AN(I10+1)
0021      YSER=YSER+YNEW*AN(I10+1)
0022      XN=XNEW
0023      YN=YNEW
0024      1) CONTINUE
0025      ZVOIGT=DEXP(-S)*(DCOS(-T)*(1.-PISQ*XSER)+PISQ*DSIN(-T)*YSER)
0026      RETURN
0027      112 R=T*T
0028      T=T*X
0029      F=S-A6
0030      G=S-A4
0031      H=S-A2
0032      ZVOIGT=A1*((T-H*Y)/(H*H+R))+A3*((T-G*Y)/(G*G+R))+
1      A5*((T-F*Y)/(F*F+R))
0033      RETURN
0034      111 R=T*T
0035      T=T*X
0036      F=S-B2
0037      G=S-B4
0038      ZVOIGT=B1*((T-F*Y)/(F*F+R))+B3*((T-G*Y)/(G*G+R))
0039      RETURN
0040      END

```

APPENDIX D

DATSET SUBROUTINE

The data processing routine used by the transmittance program to transfer data from tape to computer memory or disk is listed on the next page. The parameters of the FORTRAN IV subroutine are explained in section 5.6. The following JCL must be included for program execution. It defines the seven files of the tape so that the routine can more quickly select that portion of the tape from which to read data.

```
//GO.FT11FOO1 DD UNIT=2400,DSN=F1L1,  
// LABEL=(02,BLP,IN),DISP=OLD,VOL=SER=TOO388,  
// DCB=(RECFM=F,BLKSIZE=3900)
```

Seven of these cards must be used, the remaining six are exactly the same except as shown.

```
...GO.FT12FOO1...DSN=F1L12...LABEL=(05,BLP,IN)...  
...GO.FT13FOO1...DSN=F1L13...LABEL=(08,BLP,IN)...  
...GO.FT14FOO1...DSN=F1L14...LABEL=(11,BLP,IN)...  
...GO.FT15FOO1...DSN=F1L15...LABEL=(14,BLP,IN)...  
...GO.FT16FOO1...DSN=F1L16...LABEL=(17,BLP,IN)...  
...GO.FT17FOO1...DSN=F1L17...LABEL=(20,BLP,IN)...
```

The routine can transfer 3000 lines of data to core. If disk is to be used the necessary JCL and DEFINE FILE statements must be included, and in the DATSET routine the comment card used and the

```
SPECS(...)=  
and KIND (...)= Cards
```

removed.

```

0001      SUBROUTINE DATSET(WAVLO,WAVUP,ICNT,MAX,SPECS,KIND,LTOTAL)
0002      DIMENSION IDATE(40),ISO(40),MOL(40),GBG(23),ICNT(7)
0003      DIMENSION WAV(40),STRGH(40),WDTH(40),ENGY(40),ROTI(40,5),VIB(40)
0004      DIMENSION SPECS(3000,4),KIND(3000)
0005      LTOTAL=0
0006      DO 40 I40=1,7
0007          40 ICNT(I40)=0
0008              NFIL=11
0009                  IF(WAVLO.GT.500.0) NFIL=12
0010                      IF(WAVLO.GT.1000.0) NFIL=13
0011                          IF(WAVLO.GT.2000.0) NFIL=14
0012                              IF(WAVLO.GT.5000.0) NFIL=15
0013                                  IF(WAVLO.GT.7500.0) NFIL=16
0014                                      IF(WAVLO.GT.10000.0) NFIL=17
0015          07 READ(NFIL,01,END=99) NUM,FREQ
0016          01 FORMAT(I10,F10.3)
0017              IF(FREQ.LT.WAVLO) GO TO 07
0018              BACKSPACE NFIL
0019              BACKSPACE NFIL
0020          23 READ(NFIL,11,END=98) NUM,(WAV(K),STRGH(K),WDTH(K),
1 ENGY(K),(ROTI(K,J),J=1,5),VIB(K),IDATE(K),ISO(K),
1 MOL(K),K=1,40),(GBG(M),M=1,23)
0021          11 FORMAT(I10,40(F10.3,E10.3,F5.3,F10.3,5A6,A5,I3,I4,I3),23A30)
0022              DO 10 I10=1,NUM
0023                  KMOL=MOL(I10)
0024                  MOLF=10*KMOL
0025                  IF(WAV(I10).LT.WAVLO) GO TO 10
0026                  IF(WAV(I10).GT.WAVUP) GO TO 13
0027                  ICNT(KMOL)=ICNT(KMOL)+1
C          WRITE(MOLF,ICNT(KMOL)) WAV(I10),STRGH(I10),WDTH(I10),ENGY(I10)
0028                  LTOTAL=LTOTAL+1
0029                  IF(LTOTAL.GT.MAX) GO TO 97
0030                  SPECS(LTOTAL,1)=WAV(I10)
0031                  SPECS(LTOTAL,2)=STRGH(I10)
0032                  SPECS(LTOTAL,3)=WDTH(I10)
0033                  SPECS(LTOTAL,4)=ENGY(I10)
0034                  KIND(LTOTAL)=MOL(I10)
0035          1) CONTINUE
0036              GO TO 23
0037          13 CONTINUE
0038              REWIND NFIL
0039              GO TO 999
0040          99 WRITE(6,21) NFIL
0041          21 FORMAT(1X,35HLOWER WAVE NUMBER NOT FOUND ON TAPE,/,
1 1X,15HFILE NUMBER IS:,(I10,/,1X,18HPROGRAM TERMINATED,/)
          STOP
0042          98 WRITE(6,31) NFIL,WAV(40),WAVUP
0043          31 FORMAT(//,2X,31HEND OF FILE ENCOUNTERED ON FILE,I3,/,2X,
1 34HBEFORE UPPER WAVE NUMBER WAS FOUND,/,2X,
2 20HLAST WAVE NUMBER IS:,(F10.3,3X,
3 25HUPPER LIMIT SPECIFIED WAS,(5X,F10.3,/,2X,
4 18HPROGRAM CONTINUING,/)
0045              REWIND NFIL
0046                  NFIL=NFIL+1
0047                  IF(NFIL.GE.17) NFIL=17
0048                  GO TO 23
0049          97 WRITE(6,41) (ICNT(M),M=1,7),WAV(40)
0050          41 FORMAT(//,1X,31HEXPECTED RECORD NUMBER EXCEEDED,/,1X,

```

FORTRAN IV G LEVEL 21

DATSET

DATE = 77108

11/01/30

```
1 34HNUMBER OF RECORDS OF EACH TYPE IS: ,/,2X,7(16,2X),/,  
2 20HLAST WAVE NUMBER IS: ,2X,F10.3,/,2X,18HPROGRAM CONTINUING,///  
0051 ICNT(KMOL)=ICNT(KMOL)-1  
0052 REWIND NFIL  
0053 999 RETURN  
0054 END
```


APPENDIX E

TRANSMITTANCE PROGRAM

The transmittance program written as a result of this work follows. The important variables of the routine are defined in Appendix F. The logic and a flow chart for the program is contained in Chapter six.


```

0046      CHECK=SPEC(S(I70,1))
0047      IF(CHECK.GE.DOWN) GO TO 13
0048      70 CONTINUE
0049      IFIRST=1
0050      GO TO 23
0051      13 IFIRST=I70
0052      23 CONTINUE
0053      DO 80 I80=IFIRST,LEND
0054      CHECK=SPEC(S(I80,1))
0055      IF(CHECK.GE.UP) GO TO 33
0056      80 CONTINUE
0057      ILAST=LEND
0058      GO TO 43
0059      33 ILAST=I80
0060      43 CONTINUE
    
```

C
C
C
 LEVEL LOOP

```

0061      DO 30 I30=1,LEVS
0062      DO 50 I50=1,7
0063      ABSK(I30,I50)=0.0
0064      50 CONTINUE
    
```

C
C
C
 LINE LOOP

```

0065      DO 90 I90=IFIRST,ILAST
0066      ITYPE=KIND(I90)
0067      AD=3.587-07*SQRT(TEMP(I30)/WTMOL(ITYPE))
0068      X4=X1(I30)**CJ(ITYPE)*QV(I30,ITYPE)
0069      ALFAD=AD*SPEC(S(I90,1))
0070      ALFAL=X2(I30)*SPEC(S(I90,3))
0071      YFAC=ALG2/ALFAD
0072      U=ALFAL*YFAC
0073      RKQ=(DEXP(X3(I30)*SPEC(S(I90,4)))*SPEC(S(I90,2))*X4)*YFAC
0074      Y=DABS(CNTR-SPEC(S(I90,1)))*YFAC
0075      SHAPE=ZVOIGT(Y,U)
0076      ABSK(I30,ITYPE)=ABSK(I30,ITYPE)+RKQ*SHAPE
0077      90 CONTINUE
0078      30 CONTINUE
    
```

C
C
C
 ABSORPTION COEFFICIENT * MIXING RATIO

```

0079      DO 130 I130=1,LEVS
0080      ABSK(I130,1)=(ABSK(I130,1)*2.743475499D16+H2CMIX(I130)+
1  ABSK(I130,2)*6.954682447D15+ABSK(I130,3)*1.27962331D19+
2  03MIX(I130)+ABSK(I130,4)*5.897035858D12+
3  ABSK(I130,5)*1.589430793D12+ABSK(I130,6)*3.381698754D13+
4  ABSK(I130,7)*4.443139014D18)*(SQRP IV)
0081      130 CONTINUE
    
```

C
C
C
 TRANSMITTANCE

```

0082      LSTOP=LEVS-1
0083      TAU=1.
0084      DO 150 I150=1,LSTOP
0085      INUM=1
0086      HSTEP=(PRESS(I150+1)-PRESS(I150))/1000.
0087      TPRED=TAU-HSTEP*ABSK(I150,1)*TAU
    
```

```
0088      63  TAUNEW=TAU-(HSTEP/2.)*(ABS(K(I150,1))*TAU+ABS(K(I150+1,1)*TPRED)
0089      IF (GABS (TPRED)-TAUNEW).LE-.0001.OR.(INUM.GE.10) GO TO 53
0090      TPRED=TAUNEW
0091      INUM=INUM+1
0092      GO TO 63
0093      53  TAU=TAUNEW
0094      K=(I15)+1
0095      TRANS(K)=TRANS(K)+TAU
0096      150 CONTINUE
0097      CNTR=CNTR+SPACE
0098      50  CONTINUE
0099      TRANS(1)=INCR
0100      WAVLO=WAVLO+30UND
0101      WAVUP=WAVUP-80UND
0102      WRITE(6,31) I20,WAVLO,WAVUP
0103      31  FORMAT(1H1,51X,14PC HANNEL NUMBER,1X,I2,/,25X,
1  23HBEGINNING WAVE NUMBER OF,1X,F10.3,1X,3HAND,1X,
2  20HENDING WAVE NUMBER OF,1X,F10.3,/,25X,70(1H*),/,)
0104      WRITE(6,101)
0105      LEVEL=LEVS
0106      DO 140 I140=1,LEVS
0107      TRANS(I140)=TRANS(I140)/INCR
0108      WRITE(6,91) LEVEL,PRESS(I140),TEMP(I140),TRANS(I140)
0109      LEVEL=LEVS-I140
0110      101 FORMAT(/,19X,5HLEVEL,11X,8HPRESSURE,15X,11HT EMERATURE,9X,
1  22HAVERAGED TRANSMITTANCE,/,16X,85(1H*))
0111      91  FORMAT(20X,I3,11X,D10.4,17X,F5.1,14X,D17.10)
0112      140 CONTINUE
0113      20  CONTINUE
0114      STOP
0115      END
```

APPENDIX F

DEFINITION OF VARIABLES USED IN THE TRANSMITTANCE

PROGRAM

The following is a list of the important variables and their definition, used in the transmittance program.

ABSK(33,7)	Array of absorption coefficients
ALFAL	α_L
ALFAD	α_D
AIG2	$(\ln 2)^{1/2}$
BOUND	Amount by which channel limits are changed.
CJ(7)	Array of rotational partition function exponents.
CNTR	Frequency at which transmittance is calculated.
DOWN	Lower limit of the range of lines included in transmittance calculations.
EGY	Energy of a line (E) = SPECS(I,4).
FREQ	Line wavenumber (ν_0) = SPECS(I,1).
HIGH	Line strength (S) = SPECS(I,2).
HSTEP	dP in bars.
H2OMIX(33)	Array of water vapor concentrations.
IFIRST	Subscript of the lower limit line used in transmittance calculations.
ILAST	Subscript of the upper limit line used in transmittance calculations.

INTVLS	Number of intervals in a channel.
KIND(3000)	Array of molecular types.
LEVS	Number of layers of the atmosphere.
NCHNL	Number of channels.
O3MLX(33)	Array of ozone concentrations.
PO	Reference pressure = 1013.17mb.
PRESS(33)	Array of layer pressures.
QV(33,7)	Array of vibration partition functions.
SEARCH	Range from CNTR within which effects of lines are added together.
SHAPE	Voigt profile value.
SIZE	Line width (α_0) = SPECS(I,3).
SPACE	Distance between points where transmittance is computed.
TAU	Iterative transmittance.
TAUNEW	Corrected iterative transmittance.
TEMP(33)	Array of layer temperatures.
TO	Reference temperature = 296.
TPRED	Predicted transmittance.
TRANS(33)	Transmittances of each layer.
U	$\frac{\alpha_L}{\alpha_D} (\ln 2)^{1/2}$
UP	Upper limit of the range of lines included in transmittance calculations.
WAVLO	Channel lower limit.
WAVUP	Channel upper limit.
WTMOL(7)	Molecular weights of atmospheric gases.

Y

$$\frac{v-v_0}{\alpha_D} (\ln 2)^{1/2}$$

APPENDIX G

MONOCHROMATIC TRANSMITTANCES

The results of monochromatic transmittance calculations for the seven channels of the HIRS are listed. The frequency at which the transmittance was computed was the channel center-frequency. Only lines between the channel limits were used.

CHANNEL NUMBER 1
 BEGINNING WAVENUMBER OF 665.200 AND ENDING WAVENUMBER OF 670.800

LEVEL	PRESSURE	TEMPERATURE	AVERAGED TRANSMITTANCE
33	0.3000E-03	210.0	0.1000000000 01
32	0.6710E-01	218.0	0.999999 320 00
31	0.9510E 00	276.0	0.99998918350 00
30	0.1760E 01	270.0	0.99997533330 00
29	0.3330E 01	258.0	0.99994430430 00
28	0.6520E 01	245.0	0.99987048950 00
27	0.1320E 02	234.0	0.99970339910 00
26	0.2770E 02	224.0	0.99938433670 00
25	0.3220E 02	223.0	0.99930258840 00
24	0.3760E 02	222.0	0.99921257620 00
23	0.4370E 02	220.0	0.99911961300 00
22	0.5100E 02	219.0	0.99901778600 00
21	0.5950E 02	218.0	0.99890878590 00
20	0.6950E 02	217.0	0.99879009500 00
19	0.8120E 02	216.0	0.99866044700 00
18	0.9500E 02	216.0	0.99851623960 00
17	0.1110E 03	216.0	0.99835706470 00
16	0.1300E 03	216.0	0.99817582630 00
15	0.1530E 03	216.0	0.99796458620 00
14	0.1790E 03	216.0	0.99773405050 00
13	0.2090E 03	222.0	0.99747757100 00
12	0.2430E 03	229.0	0.99719837260 00
11	0.2810E 03	235.0	0.99689389680 00
10	0.3240E 03	242.0	0.99657307980 00
9	0.3720E 03	248.0	0.99622502110 00
8	0.4260E 03	255.0	0.99584771810 00
7	0.4870E 03	261.0	0.99543699850 00
6	0.5540E 03	267.0	0.99500102640 00
5	0.6280E 03	273.0	0.99453442030 00
4	0.7100E 03	279.0	0.99403218440 00
3	0.8020E 03	285.0	0.99348372730 00
2	0.9020E 03	290.0	0.99290212630 00
1	0.1013E 04	294.0	0.99227078150 00

CHANNEL NUMBER 2
 BEGINNING WAVENUMBER OF 665.300 AND ENDING WAVENUMBER OF 692.700

LEVEL	PRESSURE	TEMPERATURE	AVERAGED TRANSMITTANCE
33	0.3000E-03	210.0	0.10000000700 01
32	0.6710E-01	218.0	0.10000000700 01
31	0.9510E 00	276.0	0.99999997250 00
30	0.1760E 01	270.0	0.99999999330 00
29	0.3330E 01	258.0	0.99999999370 00
28	0.6520E 01	245.0	0.99999997520 00
27	0.1320E 02	234.0	0.99999989440 00
26	0.2770E 02	224.0	0.99999951950 00
25	0.3220E 02	223.0	0.99999934730 00
24	0.3760E 02	222.0	0.99999917580 00
23	0.4370E 02	220.0	0.99999878640 00
22	0.5100E 02	219.0	0.99999833920 00
21	0.5950E 02	217.0	0.99999772990 00
20	0.6950E 02	217.0	0.99999689090 00
19	0.8120E 02	216.0	0.99999574100 00
18	0.9500E 02	216.0	0.99999415450 00
17	0.1110E 03	216.0	0.99999200650 00
16	0.1300E 03	216.0	0.99998972660 00
15	0.1530E 03	216.0	0.99998479750 00
14	0.1790E 03	216.0	0.99997920050 00
13	0.2090E 03	222.0	0.99997176490 00
12	0.2430E 03	229.0	0.99996221840 00
11	0.2810E 03	235.0	0.99995019060 00
10	0.3240E 03	242.0	0.99993492040 00
9	0.3720E 03	248.0	0.99991587560 00
8	0.4260E 03	255.0	0.99989204760 00
7	0.4870E 03	261.0	0.99986221750 00
6	0.5540E 03	267.0	0.99982604000 00
5	0.6280E 03	273.0	0.99978220100 00
4	0.7100E 03	279.0	0.99972921000 00
3	0.8020E 03	285.0	0.99966468720 00
2	0.9020E 03	290.0	0.99958893910 00
1	0.1013E 04	294.0	0.99949849900 00

CHANNEL NUMBER 3
 BEGINNING WAVENUMBER OF 677.400 AND ENDING WAVENUMBER OF 702.600

LEVFL	PRESSURE	TEMPERATURE	AVERAGED TRANSMITTANCE
33	0.3700E-03	210.0	0.1000000000 01
32	0.6710E-01	218.0	0.1000000000 01
31	0.9510E 00	276.0	0.9999999999 00
30	0.1760E 01	270.0	0.9999999999 00
29	0.3350E 01	258.0	0.9999999999 00
28	0.6520E 01	245.0	0.9999999967 00
27	0.1320E 02	234.0	0.9999999867 00
26	0.2770E 02	224.0	0.9999999431 00
25	0.3220E 02	223.0	0.9999999235 00
24	0.3760E 02	222.0	0.9999998962 00
23	0.4370E 02	220.0	0.9999998605 00
22	0.5100E 02	219.0	0.9999998109 00
21	0.5950E 02	218.0	0.9999997437 00
20	0.6950E 02	217.0	0.9999996517 00
19	0.8120E 02	216.0	0.9999995265 00
18	0.9500E 02	216.0	0.9999993541 00
17	0.1110E 03	216.0	0.9999991205 00
16	0.1300E 03	216.0	0.9999987961 00
15	0.1530E 03	216.0	0.9999983352 00
14	0.1790E 03	216.0	0.9999977244 00
13	0.2090E 03	222.0	0.9999968936 00
12	0.2430E 03	229.0	0.9999957783 00
11	0.2810E 03	235.0	0.9999943110 00
10	0.3240E 03	242.0	0.9999923668 00
9	0.3720E 03	248.0	0.9999898332 00
8	0.4260E 03	255.0	0.9999865384 00
7	0.4870E 03	261.0	0.9999822295 00
6	0.5540E 03	267.0	0.9999767394 00
5	0.6280E 03	273.0	0.9999699206 00
4	0.7100E 03	279.0	0.9999612582 00
3	0.8020E 03	285.0	0.9999502341 00
2	0.9020E 03	290.0	0.9999367155 00
1	0.1013E 04	294.0	0.9999198948 00

CHANNEL NUMBER 4
 BEGINNING WAVENUMBER OF 686.100 AND ENDING WAVENUMBER OF 717.900

LEVEL	PRESSURE	TEMPERATURE	AVERAGED TRANSMITTANCE
33	0.3000E-03	210.0	0.1000000000 01
32	0.6710E-01	218.0	0.1000000000 01
31	0.9510E 00	276.0	0.9999999980 00
30	0.1760E 01	270.0	0.9999999940 00
29	0.3330E 01	258.0	0.9999999770 00
29	0.6520E 01	245.0	0.9999999100 00
27	0.1320E 02	234.0	0.9999999650 00
26	0.2770E 02	224.0	0.9999999010 00
25	0.3220E 02	223.0	0.9999998620 00
24	0.3760E 02	222.0	0.9999998580 00
23	0.4370E 02	220.0	0.9999998320 00
22	0.5100E 02	219.0	0.9999998000 00
21	0.5950E 02	218.0	0.9999997620 00
20	0.6950E 02	217.0	0.9999997160 00
19	0.8120E 02	216.0	0.9999996650 00
18	0.9500E 02	216.0	0.9999995910 00
17	0.1110E 03	216.0	0.9999995050 00
16	0.1300E 03	216.0	0.9999993950 00
15	0.1530E 03	216.0	0.9999992530 00
14	0.1790E 03	216.0	0.9999990800 00
13	0.2090E 03	222.0	0.9999988500 00
12	0.2430E 03	229.0	0.9999985230 00
11	0.2810E 03	235.0	0.9999981740 00
10	0.3240E 03	242.0	0.9999974580 00
9	0.3720E 03	248.0	0.9999966310 00
8	0.4260E 03	255.0	0.9999955240 00
7	0.4870E 03	261.0	0.9999940480 00
6	0.5540E 03	267.0	0.9999921650 00
5	0.6230E 03	273.0	0.9999897460 00
4	0.7100E 03	279.0	0.9999866640 00
3	0.8020E 03	285.0	0.9999826930 00
2	0.9020E 03	290.0	0.9999778820 00
1	0.1013E 04	294.0	0.9999716880 00

CHANNEL NUMBER 5
 BEGINNING WAVENUMBER OF 698.500 AND ENDING WAVENUMBER OF 733.500

LEVEL	PRESSURE	TEMPERATURE	AVERAGED TRANSMITTANCE
33	0.3000E-03	210.0	0.1000000000 01
32	0.6710E-01	218.0	0.1000000000 01
31	0.9510E 00	276.0	0.1000000000 01
30	0.1760E 01	270.0	0.1000000000 01
29	0.3330E 01	258.0	0.9999999999 00
28	0.6520E 01	245.0	0.9999999999 00
27	0.1320E 02	234.0	0.9999999974 00
26	0.2770E 02	224.0	0.9999999912 00
25	0.3220E 02	223.0	0.9999999892 00
24	0.3750E 02	222.0	0.9999999866 00
23	0.4370E 02	220.0	0.9999999835 00
22	0.5100E 02	219.0	0.9999999797 00
21	0.5950E 02	218.0	0.9999999753 00
20	0.6950E 02	217.0	0.9999999713 00
19	0.8120E 02	216.0	0.9999999649 00
18	0.9500E 02	216.0	0.9999999588 00
17	0.1110E 03	216.0	0.9999999521 00
16	0.1300E 03	216.0	0.9999999441 00
15	0.1530E 03	215.0	0.9999999341 00
14	0.1790E 03	216.0	0.9999999222 00
13	0.2090E 03	222.0	0.9999999069 00
12	0.2430E 03	229.0	0.9999998360 00
11	0.2810E 03	235.0	0.9999998576 00
10	0.3240E 03	242.0	0.9999998181 00
9	0.3720E 03	248.0	0.9999997641 00
8	0.4260E 03	255.0	0.9999996898 00
7	0.4870E 03	261.0	0.9999995877 00
6	0.5540E 03	267.0	0.9999994530 00
5	0.6280E 03	273.0	0.9999992753 00
4	0.7100E 03	279.0	0.9999990412 00
3	0.8020E 03	285.0	0.9999987302 00
2	0.9020E 03	290.0	0.9999983342 00
1	0.1013E 04	294.0	0.9999978275 00

CHANNEL NUMBER 6
 BEGINNING WAVENUMBER OF 715.400 AND ENDING WAVENUMBER OF 750.600

LEVEL	PRESSURE	TEMPERATURE	AVERAGED TRANSMITTANCE
33	0.3000E-03	210.0	0.1000000000 01
32	0.6710E-01	219.0	0.1000000000 01
31	0.9510E 00	276.0	0.1000000000 01
30	0.1760E 01	270.0	0.1000000000 01
29	0.3330E 01	259.0	0.9999999990 00
28	0.6520E 01	245.0	0.9999999970 00
27	0.1320E 02	234.0	0.9999999970 00
26	0.2770E 02	224.0	0.99999999610 00
25	0.3220E 02	223.0	0.99999999490 00
24	0.3760E 02	222.0	0.99999999320 00
23	0.4370E 02	220.0	0.99999999110 00
22	0.5100E 02	219.0	0.99999998820 00
21	0.5950E 02	218.0	0.99999998140 00
20	0.6950E 02	217.0	0.99999997920 00
19	0.8120E 02	216.0	0.99999997240 00
18	0.9500E 02	216.0	0.99999996300 00
17	0.1110E 03	216.0	0.99999995040 00
16	0.1300E 03	216.0	0.99999993290 00
15	0.1530E 03	216.0	0.99999990810 00
14	0.1790E 03	216.0	0.99999987540 00
13	0.2090E 03	222.0	0.99999982990 00
12	0.2430E 03	229.0	0.99999976130 00
11	0.2310E 03	235.0	0.99999966530 00
10	0.3240E 03	242.0	0.99999953280 00
9	0.3720E 03	248.0	0.99999933950 00
8	0.4260E 03	255.0	0.99999917720 00
7	0.4870E 03	261.0	0.99999871380 00
6	0.5540E 03	267.0	0.99999823380 00
5	0.6290E 03	273.0	0.99999761220 00
4	0.7100E 03	279.0	0.99999679400 00
3	0.8020E 03	285.0	0.99999572140 00
2	0.9020E 03	290.0	0.99999437800 00
1	0.1013E 04	294.0	0.99999269020 00

CHANNEL NUMBER 7
 BEGINNING WAVENUMBER OF 730.600 AND ENDING WAVENUMBER OF 767.400

LEVEL	PRESSURE	TEMPERATURE	AVERAGED TRANSMITTANCE
33	0.3300E-03	210.0	0.1000000000 01
32	0.6710E-01	218.0	0.1000000000 01
31	0.9510E 00	276.0	0.1000000000 01
30	0.1760E 01	270.0	0.1000000000 01
29	0.3330E 01	258.0	0.1000000000 01
28	0.6520E 01	245.0	0.9999999790 00
27	0.1320E 02	234.0	0.9999999940 00
26	0.2770E 02	224.0	0.9999999830 00
25	0.3220E 02	223.0	0.9999999790 00
24	0.3760E 02	222.0	0.9999999750 00
23	0.4370E 02	220.0	0.9999999700 00
22	0.5100E 02	219.0	0.9999999650 00
21	0.5950E 02	218.0	0.9999999590 00
20	0.6950E 02	217.0	0.9999999520 00
19	0.8120E 02	216.0	0.9999999460 00
18	0.9500E 02	216.0	0.9999999390 00
17	0.1110E 03	216.0	0.9999999320 00
16	0.1300E 03	216.0	0.9999999250 00
15	0.1530E 03	216.0	0.9999999160 00
14	0.1790E 03	216.0	0.9999999050 00
13	0.2090E 03	222.0	0.9999998920 00
12	0.2430E 03	229.0	0.9999998720 00
11	0.2810E 03	235.0	0.9999998430 00
10	0.3240E 03	242.0	0.9999998000 00
9	0.3720E 03	248.0	0.9999997370 00
8	0.4260E 03	255.0	0.9999996450 00
7	0.4870E 03	261.0	0.9999995110 00
6	0.5540E 03	267.0	0.9999993230 00
5	0.6280E 03	273.0	0.9999990620 00
4	0.7100E 03	279.0	0.9999987010 00
3	0.8020E 03	285.0	0.9999981970 00
2	0.9020E 03	290.0	0.9999975260 00
1	0.1013E 04	294.0	0.9999966400 00

APPENDIX H

AVERAGED TRANSMITTANCE

The result of the averaged transmittance for the first HIRS channel is listed. Ten monochromatic transmittances were averaged over the band. Each separate transmission calculation included only lines that were within a distance of 5 wavenumbers of the transmission frequency.

CHANNEL NUMBER 1
 BEGINNING WAVENUMBER OF 665.200 AND ENDING WAVENUMBER OF 670.200

LEVEL	PRESSURE	TEMPERATURE	AVERAGED TRANSMITTANCE
33	0.3000E-03	210.0	0.1000000000 01
32	0.6710E-01	218.0	0.99997066290 00
31	0.9510E 00	276.0	0.99981046010 00
30	0.1760E 01	270.0	0.99959258300 00
29	0.3330E 01	250.0	0.99913498210 00
28	0.6520E 01	245.0	0.99815199390 00
27	0.1320E 02	234.0	0.99600677000 00
26	0.2770 02	224.0	0.99245518310 00
25	0.3220E 02	223.0	0.99160184130 00
24	0.3760E 02	222.0	0.99067096790 00
23	0.4370E 02	220.0	0.98978478630 00
22	0.5100E 02	219.0	0.98883592240 00
21	0.5950E 02	218.0	0.98787382350 00
20	0.6950E 02	217.0	0.98689231730 00
19	0.8120E 02	216.0	0.98589980590 00
18	0.9500E 02	216.0	0.98489809950 00
17	0.1110E 03	216.0	0.98387236020 00
16	0.1300E 03	216.0	0.98282744230 00
15	0.1530E 03	216.0	0.98173400160 00
14	0.1790E 03	216.0	0.98065383480 00
13	0.2090E 03	222.0	0.97956054910 00
12	0.2430E 03	229.0	0.97843233430 00
11	0.2910E 03	235.0	0.97727991800 00
10	0.3240E 03	242.0	0.97607857000 00
9	0.3720E 03	248.0	0.97483234300 00
8	0.4260E 03	255.0	0.97351818490 00
7	0.4870E 03	261.0	0.97211465280 00
6	0.5540E 03	267.0	0.97064580510 00
5	0.6280E 03	273.0	0.96908607380 00
4	0.7100E 03	279.0	0.96741175970 00
3	0.8020E 03	285.0	0.96553074430 00
2	0.9020E 03	290.0	0.96363157010 00
1	0.1013E 04	294.0	0.96150542660 00

REFERENCES

1. Abramowitz, M. and I. A. Stegun (Eds), Handbook of Mathematical Functions with Formulas, Graphs, and Mathematical Tables, Dover Publications, Inc., New York, 1972.
2. Anding, D. "Band Model Methods for Computing Atmospheric Molecular Absorption", Willow Run Labs, Univ. of Michigan, Ann Arbor, Report 7142-21, Feb. 1957.
3. Armstrong, B. H., "Spectrum Line Profiles: The Voigt Function", Journal of Quantitative Spectroscopy and Radiative Transfer, Vol. 7, pg. 61, 1967.
4. Breene, R. G., Jr., The Shift and Shape of Spectral Lines, Pergamon Press, New York, 1961.
5. Britton, J. R. et al., University Mathematics, W. H. Freeman and Co., San Francisco, 1965.
6. Brugel, W., An Introduction to Infrared Spectroscopy, John Wiley and Sons, Inc., New York, 1962.
7. Burr, E. W., Applied Statistical Methods, Academic Press, New York, 1974.
8. Carnahan, B., H. A. Luther, and J. O. Wilkes, Applied Numerical Methods, John Wiley and Sons, Inc., New York, 1969.
9. Chebyshev, P. L., Complete Collected Works, (Polnae sobranie sochenenii), Vol. 2, Pergamon Press, New York, 1947.
10. Dawson, H. G., London Mathematical Society Proceedings Selections, Vol. 29, pg. 519, 1898.
11. Drayson S. R., "Rapid Computation of the Voigt Profile", Journal of Quantitative Spectroscopy and Radiative Transfer, Vol. 16, pg. 611, 1976.
12. Faddeyeva, V. N., and N. M. Terent'ev, N. M., Tables of the Probability Integral for Complex Argument, Pergamon Press, New York, 1961.
13. Fried, B. D., and S. D. Conte, The Plasma Dispersion Function, Academic Press, New York, 1961.
14. Gibson, Glenn A., "An Efficient Method for Calculating a Transmittance Profile", Scientific Series Agreement Report, DAAG29-79-D-0100, Nov. 76.

References:

15. Goody, R. M., Atmospheric Radiation I, Theoretical Basis, Oxford University Press, Oxford, 1964.
16. Hertzberg, G., Molecular Spectra and Molecular Structure, Vol. I, Spectra of Diatomic Molecules, D. Van Nostrand Co., Inc., New York, 1950.
17. Holtsmark, J., Phys. Z., Vol. 20, pg. 162, 1919.
18. Huson, R. D., Jr., Infrared System Engineering, John Wiley and Sons, Inc., New York, 1969.
19. Hummer, D. G., Mathematics of Computation, Vol. 18, pg. 317, 1964.
20. IBM System/360 Basic FORTRAN IV Language, GC28-6629-2, International Business Machines Corp., New York, 1969.
21. IBM System/360 and System/370 FORTRAN IV Language, GC28-6515-10, International Business Machines Corp., New York, 1974.
22. Jamieson, J. A. et al., Infrared Physics and Engineering, McGraw Hill Book Co., New York, 1963.
23. Kaplan, L. D., "Inference of Atmospheric Structure from Remote Radiation Measurements", Journal of the Optical Society of America, Vol. 49, #10, pg. 1004, 1959.
24. Kielkopf, J. F., "New Approximation to the Voigt Function with Applications to Spectral-Line Profile Analysis", Journal of the Optical Society of America, Vol. 63, pg. 987, 1973.
25. Kroto, H. W., Molecular Rotational Spectra, John Wiley and Sons, Inc., New York, 1975.
26. Kuhn, H. G., Atomic Spectra, Academic Press, New York, 1962.
27. Laidlaw, W. G., Introduction to Quantum Concepts in Spectroscopy, McGraw Hill Book Co., New York, 1970.
28. La Rocca, A. J. and R. E. Turner, "Atmospheric Transmittance and Radiance: Methods of Calculation", AD-A017459, Research Institute of Michigan, Ann Arbor, Michigan, 1975.
29. Lorentz, H. A., "Proceedings of the Academie of Amsterdam", Vol. 18, pg. 134, 1915.
30. L'Vov, B. V., Atomic Absorption Spectrochemical Analysis, Adam Hilges, LTD, London, 1970.

References:

31. McClatchey, R. A. et al., "AFCRL Atmospheric Absorption Line Parameters Compilation", AFCRL-TR-73-0096, Air Force Cambridge Research Laboratories, Bedford, Mass., 1973.
32. McClatchey, R. A. et al., "Optical Properties of the Atmosphere," Third Edition, Report # AFCRL-72-0497, Air Force Cambridge Research Laboratories, Bedford, Mass., 1972.
33. McClatchey, R. A., "Transmittance Functions for Satellite Temperature Sounding", Report # AFCRL-72-0494, Air Force Cambridge Research Laboratories, Bedford, Mass., 1972.
34. McEwan, M. J. and L. F. Phillips, Chemistry of the Atmosphere, John Wiley and Sons, Inc., New York, 1975.
35. Miller, A., R. L. Armstrong, C. W. Welch, "High Resolution Atmospheric IR Transmittance Prediction", Contract DAAD07-73-C-0134, U. S. Army Electronics Command, Atmospheric Science Laboratory, White Sands Missile Range, New Mexico, 1974.
36. Nelson, Controlled Test Atmospheres, Ann Arbor Science Publishers, Ann Arbor, Michigan, 1971.
37. Orchin, M. and H. H. Jaffe, The Importance of Antibending Orbitals, Houghton Mifflin Co., Boston, 1964.
38. Penner, S. S., Quantitative Molecular Spectroscopy and Gas Emissivities, Addison-Wesley Publishing Co., Inc., Reading, Mass., 1959.
39. Posse, K. A., Sur Quelques Applications des Fractions Continues Algebriques, St. Petersburg Academie of Science, 1886.
40. Potter, M. T., "An Efficient Computational Approximation to the Lorentz Line Molecular Absorption Coefficient", M. S. Thesis, University of Texas at El Paso, El Paso, 1977.
41. Rodgers, C. D., "Approximate Methods of Calculating Transmission by Bands of Spectral Lines", NCAR Technical Note 116 + 1A, National Center for Atmospheric Research, Boulder, Colorado, March, 1976.
42. Salzer, H. E., "Formulas for Calculating the Error Function of a Complex Variable", Mathematics of Computation, Vol. 5, pg. 67, 1951.

References:

43. Sissala, J. E. (Ed.), Nimbus 6. User's Guide, Goddard Space Flight Center, Greenbelt, Maryland, 1975.
44. Spiegel, M. R., Advanced Mathematics for Engineers and Scientists, Schaum's Outline Series, McGraw Hill Book Co., New York, 1971.
45. U. S. Standard Atmosphere Supplements, 1966, U. S. Government Printing Office, Washington, D. C., 1966.
46. Van de Hulst, H. C. and J. J. M. Reesnick, Astrophysics Journal, Vol. 106, pg. 121, 1947.
47. Voigt, W., "Annaler de Physique, Lapaz", Vol. 42, pg. 210, 1913.
48. Voigt, W., "Sitzungsberichte der Akademie, Muchen", pg. 62, 1912.
49. Weast, R. C., (Ed.), Handbook of Chemistry and Physics, 56th Edition, CRC Press, Cleveland, Ohio, 1975.
50. Weidner, R-T., and R. L. Sells, Elementary Modern Physics, Allyn and Bacon, Inc., Boston, 1964.
51. Whiffen, D. H., Spectroscopy, John Wiley and Sons, Inc., New York, 1966.
52. Whitten, R. C., and I. G. Poppoff, Fundamentals of Aeronomy, John Wiley and Sons, Inc., New York, 1971.
53. Young, C., "Calculation of Absorption Coefficients for lines with Combined Doppler-Lorentz Broadening", Journal of Quantitative Spectroscopy and Radiative Transfer, Vol. 5, pg. 549, 1965.
54. Zuev, V. Y., "Propagation of visible and Infrared Waves in the Atmosphere", NASA TTF-707, July 1972.